Advances in Polymer Technology

WILEY

REVIEW ARTICLE OPEN ACCESS

A Review on Vehicle Tire Elastomers and Tire Wear Particles: Composition, Degradation Mechanisms, Analytical Methods, and Predictive Multiscale Computational Modeling

Roman Tangalychev[1] | Vasilii Korotenko[2] | Valentin Ivanov[1]

[1]The Faculty of Computer Science and Automation, Smart Vehicle Systems Group, Technische Universität Ilmenau, Robert-Bosch-Ring 1, Ilmenau 98693, Germany | [2]Thermal Separation Processes, Technische Universität Hamburg (TUHH), Eißendorfer Str. 38, Hamburg 21073, Germany

Correspondence: Roman Tangalychev (roman.tangalychev@tu-ilmenau.de) | Vasilii Korotenko (vasilii.korotenko@tuhh.de)

Received: 28 April 2025 | **Revised:** 27 May 2026 | **Accepted:** 5 June 2026

Academic Editor: Srijoni Sengupta

Keywords: analytical strategies | degradation of tire rubber | elastomer chemistry | environmental impact | molecular dynamic simulation | multiscale computational modeling | nonexhaust emission | quantum mechanical simulation | tire wear particles

ABSTRACT

The study of the properties, chemical composition, and degradation patterns of rubber materials used in vehicle tires remains a complex and interdisciplinary task. Rubber for tires—more precisely, complex mixtures of elastomers containing fillers, plasticizers, binders, and other additives—is a condensed chemically active material, the composition and microstructure of which crucially determine the performance characteristics of tires, their durability, and the formation of tire wear particles (TWPs). These particles contribute to environmental pollution and therefore require a detailed understanding of their formation mechanisms, chemical structure, and identification methods. This review provides a comprehensive description of current knowledge about the chemical nature of elastomeric tire systems and the effects of external and operational factors on aging and structural degradation, as well as key physicochemical parameters that determine both performance and environmental impact. We briefly describe the chemical reactions that occur during operation, including oxidation, crosslinking, chain breaking, and the processes of filler–polymer interaction (vulcanization and silica embedding), as well as their role in mechanical stress and long-term

Abbreviations: m/z, mass-to-charge ratio; tan δ, loss tangent; ν, Poisson's ratio; 6PPD, para-phenylenediamine; ATR–FTIR, attenuated total reflectance Fourier transform infrared spectroscopy; BR, butadiene rubber; CB, carbon black; CBS, N-cyclohexyl-2-benzothiazolesulfenamide; CGMD, coarse-grained molecular dynamics; CNT, carbon nanotube; CTP, N-(cyclohexylthio)phthalimide; DAE, distillate aromatic extract oil; DBA, dibenzylamine; DFT, density functional theory; DMA, dynamic mechanical analysis; DPG, 1,3-diphenylguanidine; E, Young's modulus; Ea, activation energy; ENR, epoxidized natural rubber; FEM, finite element modeling; FTIR, Fourier transform infrared spectroscopy; G, shear modulus; G', storage modulus; G", loss modulus; GC–MS, gas chromatography–mass spectrometry; GROMACS, GROningen MAchine for Chemical Simulations; HPLC, high-performance liquid chromatography; K, bulk modulus; LC–MS/MS, liquid chromatography–tandem mass spectrometry; LOD, limit of detection; MBS, 2-(4-morpholinylthio)benzothiazole; MBT, 2-mercaptobenzothiazole; MBTS, dibenzothiazyl disulfide; NBR, nitrile butadiene rubber; NR, natural rubber; PAHs, polycyclic aromatic hydrocarbons; PM2.5, particulate matter with aerodynamic diameter <; 2.5 μm; PM10, particulate matter with aerodynamic diameter <; 10 μm; PMB, polymer-modified bitumen; POPs, persistent organic pollutants; Py–GC–MS, pyrolysis gas chromatography–mass spectrometry; RDF, radial distribution function; ReaxFF, reactive force field; RRC, rolling resistance coefficient; SBR, styrene–butadiene rubber; SDGs, sustainable development goals; SEM-EDX, scanning electron microscopy with energy dispersive X-ray spectroscopy; SLS, standard linear solid model; TAC, tire-associated chemicals; TBBS, N-tert-butyl-2-benzothiazolesulfenamide; TD-GC/MS, thermal desorption gas chromatography–mass spectrometry; TDAE, treated distillate aromatic extract oil; TEM, transmission electron microscopy; TESPD, bis(3-triethoxysilylpropyl) disulfide; TESPT, bis(3-triethoxysilylpropyl) tetrasulfide; TGA, thermogravimetric analysis; TMQ, trimethylquinoline antioxidant; TPP, triphenyl phosphite; TRWP, tire and road wear particles; TTS, time-temperature superposition; TWP/TWPs, tire wear particle(s); UHPLC–HRMS, ultra-high-performance liquid chromatography–high-resolution mass spectrometry; WGI, wet grip index.

stability of the material. In addition, the article discusses modern analytical approaches to the collection, identification, and quantification of TWP, including laboratory methods for determining morphological, chemical, and molecular characteristics. The central part of this review is devoted to multiscale chemical computer modeling as a tool for predicting the behavior and properties of materials, as well as ways of their decomposition and further behavior in nature. We summarize the research results using methods of quantum mechanics (QMs), polyatomic molecular dynamics (MDs), and coarse-grained (CG) modeling, highlighting how these approaches provide a concrete understanding of key structural and property relationships in elastomeric mixtures. Promising areas of future research include combining QM–MD–CG workflows with experimental verification and developing standardized predictive models linking rubber composition to mechanical moduli and environmental emissions.

1 | Introduction

The widespread use of vehicles of all types implies a focus on the processes and consequences associated with their operation and environmental and economic impacts. In view of the fact that the number of vehicle units is steadily increasing and, moreover, we have already entered the era of electric vehicles, the understanding of the complex impact of this factor on our surrounding world has continued to expand and revise in recent decades. It is well known that electric cars, due to their technical and design features, have an increased mass compared to similar models with internal combustion engines. This is caused by the presence of a certain number of accumulator batteries and leads to increased abrasion of wheel rubber (elastomers), which is the largest indicator in the concept of nonexhaust emission (along with brake pad emission).

In 2020, ~28 million tons of rubber were produced globally, with 13.7 million tons of natural rubber (NR) and 15.1 million tons of synthetic rubber. Rubber demand decreased in 2021 due to the pandemic but surged again in 2022. Moreover, in 2023, the global tire industry produced around 2.3 billion units, driven mostly by demand from passenger vehicles, which account for a significant amount of the market due to frequent tire replacements [1]. This high volume includes demand in fast-growing regions such as Asia-Pacific, where countries like China produce more than 900 million tires per year. The needs continue to climb as automotive production and sales increase worldwide, with a notably strong market for replacement tires in areas with a high density of passenger vehicles and aging vehicle fleets. For 2024 and 2025, predictions indicate continuous growth, aided by investments from major tire firms, which are investing billions of dollars to enhance manufacturing capacity to satisfy global demand. While the total numbers for 2024 have yet to be determined, the overall trend indicates that the tire industry will have another robust year, particularly as sustainability measures and innovative tire technologies evolve in response to consumer demand. The tire business consumes 60%–80% of the worldwide NR supply and 60% of the global synthetic rubber production [2, 3]. The environmental impact of end-of-life tires is mitigated by active recycling strategies that currently allow a potential 100% recovery of spent tires [4]. Tire wear generates particle matter, which has lately been identified as a potential environmental issue.

Environmental issues, including climate change and pollution, are shaping the transportation industry's innovation agenda. In Europe, the "EU Tyre Label" is used to rate commercial tires. This technique considers three factors: rolling resistance, abrasion resistance, and wet grip. The "tire triangle" consists of three main conditions (Figure 1) with standardized methods for calculating tire performance indicators. Usually, tires are ranked (A to E) based on rolling resistance and wet traction. Rolling resistance coefficient (RRC)—determines energy losses (heat) during tire deformation by rolling.

A low RRC means less heat generation in the tire rubber (tread); in turn, it leads to less fuel consumption but often worse grip and comfort. The typical range of RRC values—0.006–0.015, according to ISO 28580. On the other hand, the abrasion resistance (wear index) provides resistance to abrasion under the influence of friction. The higher this indicator is, the slower the rubber wears out. However, grip and elasticity normally decrease. Typical range of Wear Index values are 60–250/300, relative to the standard = 100, according to DIN 53516: ↑Hardness → ↑ Wear Index, ↑Silica (without optimizing the binder) → can ↓ Wear Index. And as will be further presented in this review, the wear of the rubber material is associated with the mechanical dissociation of the molecular chains of elastomers (rubber polymers) and the thermal oxidative degradation of the surface. Also, an equally important indicator is the wet traction (wet grip index [WGI]), which reflects the tire's ability to transmit braking force on wet surfaces. It is determined through the braking distance. Typical values of WGI are in the range of 0.8–1.5 (relative to the standard)—the higher the value, the better the grip, according to ISO 23671. In addition, the EU Tyre Label takes into account the noise levels. It displays both the measured noise level (dB) and the ranking (A–C). All the indicators discussed above are important aspects of improving tire performance depending on individual requirements and applications.

In turn, tire manufacturers prefer an expanded approach to the characteristics of their products, which is why they examine and compare a wider list of performance parameters and indicators. This is due to the high competitiveness in this industry as well as the possibilities of technological analysis and experimental base development. Calculation methods are determined by standardized models and internal regulations, in general. This implies internal tests, according to established regulations (including those described above), where the manufacturer receives test results, normalizes the results relative to the reference (a standardized tire created specifically for tests), and only then creates a representative radar chart. The diagram shown in Figure 2 demonstrates 10 basic performance indicators that play an analytical role in evaluating vehicle tires and, naturally, demonstrate performance (the value of 100 corresponds to the standardized tire). It should be noted that the values in Figure 2 are schematic and are presented solely to illustrate the typical compromises between different tire characteristics. They were not based on

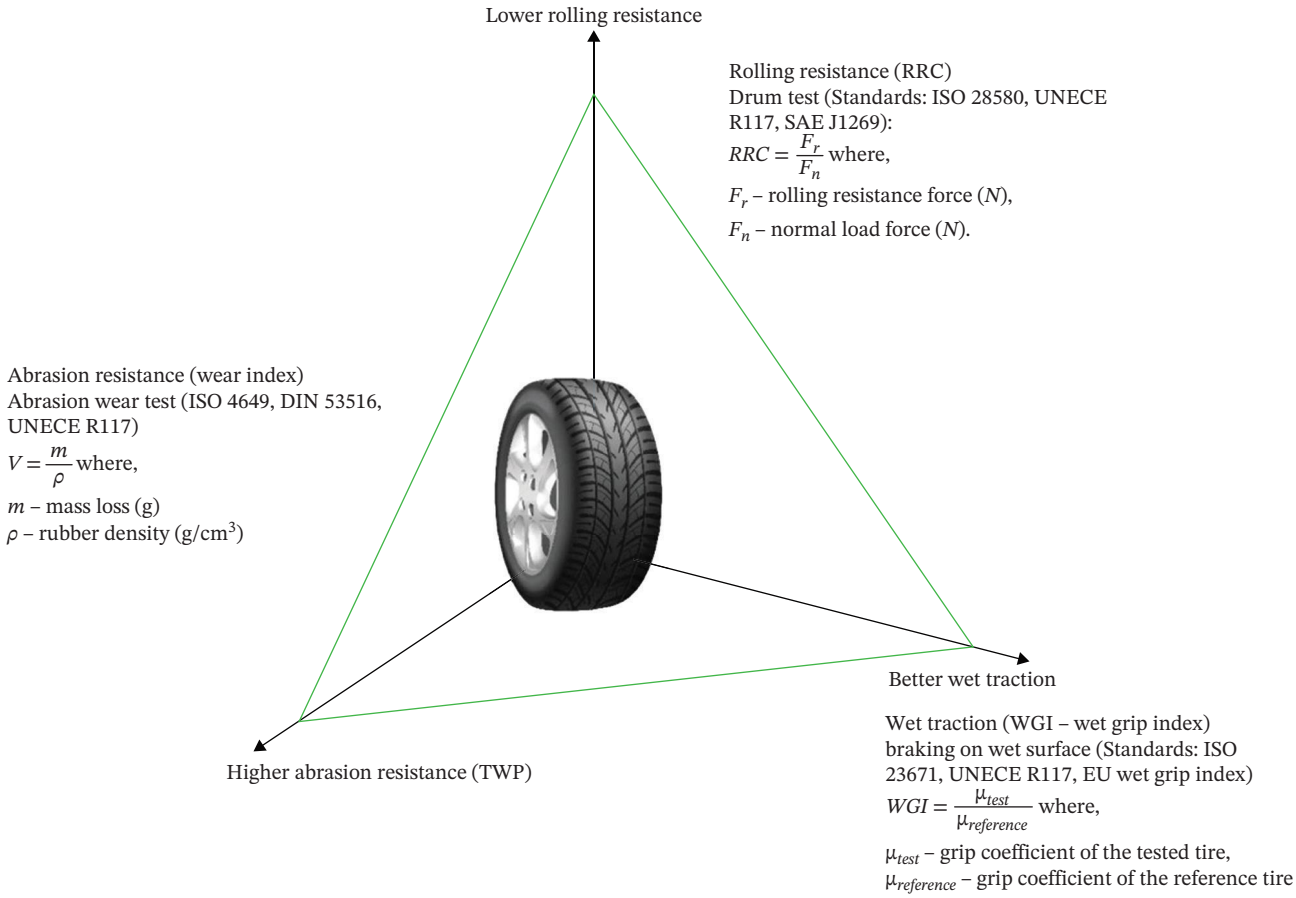

FIGURE 1 | Tire triangle of the most important performance indicators with clarification.

specific measurements, manufacturer data, or the authors' own tests. Modeled on the example of *Tyre Reviews – 2025 AutoBild All-Season Tyre Test*.

The environmental impact of plastics, and microplastics in particular, is well known. Although there is no official ranking and definition of tire wear particles (TWPs) as microplastic, they is still conventionally categorized in this group. According to the results of many relevant studies, it is possible to identify the fact that TWPs and road particle emissions are the highest

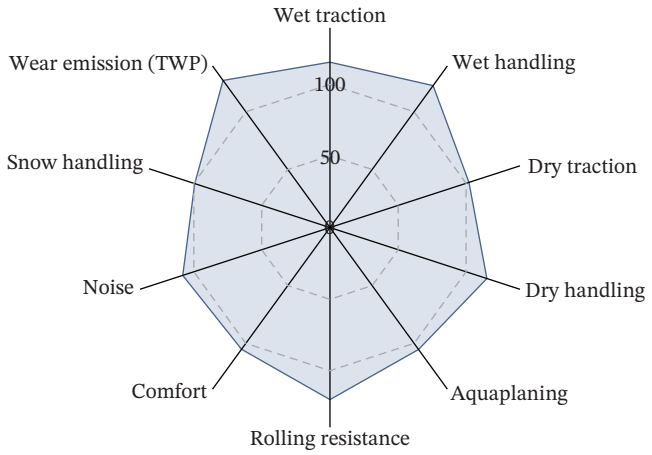

FIGURE 2 | Typical radar chart of a vehicle tire (all-season) with main performance indicators.

environmental pollution factor in this particle size scale ($PM_{2.5}$–PM_{10}),
in particular the elastomer-synthetic polymer wear particle conglomerate—estimated to be up to 42.5%–69.5% of total emissions, what is the private assessment of the authors of the research [5–7]. Several investigations have found their presence on the road [8–11], in air samples [12–14], in rivers [15, 16], soil [17, 18], and marine ecosystems [15]. Wagner et al. [19] estimated that automotive tires are the primary source of synthetic polymers in the environment, with over 1.3 Mt/year in Europe and a slightly lower value in the USA, but it should be noted that the estimate is based on mathematical modeling with a high degree of uncertainty; the initial wear coefficients vary by about two to three times, relative to the number of cars, distance traveled, and speed indicators [20]. However, researchers have questioned whether TWPs can also accumulate in environmental compartments [21, 22]. Recent studies [15, 16, 23] show that tire-associated chemicals (TAC) leak from tires, particles, and rubber granulates into the environment. It has been reported to have significant detrimental consequences on some aquatic [24–26] and terrestrial [27] species, particularly on the antioxidant and antiozonant N-(1,3-dimethylbutyl)-N′-phenyl-p-phenylenediamine (6PPD) and its transformation product 6PPD-quinone (6PPD-Q). Furthermore, tires are a visible source of metal pollution, with detrimental impacts found mostly in aquatic environments [28–30], particularly from zinc (Zn), lead (Pb), copper (Cu), and cadmium (CdSection 3.4). The research community, environmental authorities, and stakeholders have limited understanding of TWPs and TAC in the environment due to the

TABLE 1 | A brief description of the main tire components (as a global average composition), their chemical representation and function of use.

Component	Chemicals composition	Function
Rubber (natural and synthetic)	Natural rubber (NR), styrene–butadiene Rubber (SBR), butadiene rubber (BR)	Provides elasticity, flexibility, and mechanical strength.
Carbon black	N220, N330, N550	Increases strength, wear resistance, and UV protection.
Silica and silica coupling agent	Precipitated silica (Ultrasil VN3, Zeosil 1165MP) / Bis(3-triethoxysilylpropyl) tetrasulfide (Si-69) /	Improves traction, reduces rolling resistance, enhances fuel efficiency/Improves bonding between silica and rubber.
Plasticizers (oils)	Aromatic oils (DAE), Naphthenic oils, TDAE	Increases elasticity, improves processing, and prevents brittleness. 5–80 phr[a]
Antioxidants	6PPD (N-(1,3-dimethylbutyl)-N′-phenyl-p-phenylenediamine), TMQ	Protects against oxidation, ozone degradation, and UV damage. ~ 0.2–15 phr,[a] commonly 0.5–10 phr
Coupling agents (vulcanization)	TESPT, Insoluble sulfur (Crystex HD OT 20)	Forms cross-links during vulcanization, increasing durability. 0.6–6 phr,[a] commonly 1–6 phr, depending on filler
Vulcanization accelerators	CBS, MBTS, and TBBS	Speeds up vulcanization, reducing curing time, and improving properties.
Other additives	Titanium dioxide (TiO_2), stearic acid, zinc stearate, microcrystalline wax	Improves processing, protects against ozone cracking, enhances color.

[a]Information from the patent documentation provided above.

continuous evolution of new types and "refined" tires from various producers. Controlling the danger of TWPs to the environment and human health requires a comprehensive understanding of the variability of these chemicals in commercial tires by means of different approaches and tools [31]. Joint toxicity between multiple chemicals has been evidenced, which could be higher than that of a single chemical alone. In recent years, there has been a growing focus on chemical toxicity and combination. Microplastics (in the form of TWPs) in the environment can carry contaminants such as heavy metals, persistent organic pollutants (POPs), and halogenated organic compounds (HOCs) [32, 33]. This type of microplastic can cause bioaccumulation of other pollutants in exposed organisms [34].

TWPs concentrations in the environment are normally determined through marker concentrations [19, 35]. TWPs' markers are tire composition elements that appear at certain concentrations in tire material. This strategy is constrained by the fact that most accessible marker compounds usually come from various sources as well as fluctuations in marker composition inside the tires. The lack of trustworthy data due to lacking certain analytical methodologies has made it difficult to assign sources of non-exhaust emissions. Tire additives (Table 1) such as vulcanizing agents, activators, organic accelerators, antiscorching agents, plasticizers, and antioxidants improve tire durability and flexibility of the material [36–38]. The surveys have found and revealed that it is difficult to find a difference between TWPs and pavement material [39–41]; therefore, they are frequently evaluated together. As a result, the term TWPs is used in this review to refer to all particles produced by tire abrasion. Also, the impact of TWPs contamination on the environment and human health is still not versatile. Efforts to build official monitoring systems are ongoing [42, 43]. Regardless of the methodologies used, the needs of accurate analytical strategies for qualitative and quantitative TWPs in the environment is universally acknowledged, including computational modeling, are required. Harmonized analytical techniques might considerably enhance the comparability, integration, and shareability of data collected throughout the real world, as well as help to establish control and remediation measures.

In addition to the conventional analytical and experimental methods, whose complexity arises from the rich composition of rubber elastomers used in tires, it is worth emphasizing the prospects of computational chemistry approaches based on cheminformatics. These methods can be effectively applied to predict and evaluate both the current and future states of the chemical system, in this case, the condensed phase of the elastomer. In particular, we are talking about multiscale modeling, starting with the methods of quantum mechanics (QMs)—density functional theory (DFT) and ab initio, where it is possible to obtain the properties of an isolated molecule (or pair of molecules) and information on their interactions (covalent and noncovalent). DFT, a popular method of quantum mechanical modeling for solving chemical problems, is divided into two main categories: (1) the theory of chemical reactivity and its application to solve important chemical problems in the field of DFT and (2) the use of DFT to determine the relationships between structure and properties in catalysis, reactions, and small volumes the molecules. Then, atomistic molecular dynamics (MDs) simulations can be used to describe interactions between molecules in rubber compounds under relevant environmental and operating

conditions. At the next scale, coarse-grained modeling provides a logical step toward larger material volumes and longer time scales within a multiscale modeling workflow.

From the social and political perspective, it is already widely known that the European Commission's Euro7 package includes measures to regulate the emission of TWPs from vehicles by the end of 2024. These laws are projected to be implemented since 2025. While no standardized emission test exists, ongoing on-vehicle and laboratory-based tests indicate that commercial TWP emissions will be regulated to meet emission criteria by testing new tires for abrasion resistance. The requirement for low TWPs emissions, safety, noise reduction, and lower fuel consumption is driving technical improvements in design, raw materials, and chemical additives. It is also possible that this standard will be expanded and modified in terms of specific chemical structures and chemical compositions in general.

The topics covered in this review relate to a number of important areas in scientific and public life and can be classified by means of paragraphs of the Sustainable Development Goals (SDGs) that declare specific concepts and make it possible to understand the classification. The following sections contains these points and a relevant description regarding the field of rubber for vehicle tires, their production, exploitation, and subsequent recycling.

- No 3: Good health and well-being

TWPs contribute to air and water pollution, which can lead to respiratory and cardiovascular diseases. In particular, the review specifically discusses the effect of antioxidants on rubber on certain types of fish that are eaten and may eventually end up in the human body. The influence of TWPs disrupts the delicate biobalance, and it is important to pay attention to this.

- No 4: Quality education

Using modern methods for production and analysis, such as computational chemical multiscale modeling and, in the future, neural networks, the review helps to raise awareness about the corresponding techniques and tools. This contributes to the prospects for the fruitful education of engineers and scientists in the field of sustainable production and analysis of materials.

- No 6: Clean water and sanitation

TWPs can pollute freshwater sources in wastewater, which leads to the leaching of toxic chemicals and, ultimately, has a negative impact on aquatic ecosystems and the quality of drinking water. The review aims to highlight these negative perspectives in terms of particle and chemical morphology [25, 33, 44].

- No 9: Industry, Innovation, and Infrastructure

The review investigates the tools for predicting the properties of rubber for vehicle tires, which in the future will reduce experimental procedures (reducing the financial and environmental workload). This encourages innovation and the development of smarter and more sustainable production processes. In total, it is possible to change the industrial conjuncture and to optimize infrastructure.

- No 11 Sustainable cities and communities

In-depth analysis, along with the appropriate methods and techniques discussed in this review, can help reduce air pollution from various particles as a result of tire wear. This improves the quality of urban air and environmental conditions, increasing the convenience of living in cities and their environmental sustainability [45].

- No 12: Responsible consumption and production

Modern modeling methods, which are presented in this article, will make it possible to develop multistage and multiscale methods for modeling the properties and behavior of a material. This will extend the service life of manufactured products as well as reduce the consumption of raw materials during experimental development and production cycles. There are prospects for reducing waste. All this supports the principles of a closed-loop economy [15].

- No 15: Life on land

TWPs accumulate in soil ecosystems, affecting terrestrial biodiversity and agricultural land. The review presents the impact and consequences of such behavior in the world around us [46, 47].

Among other things, it is possible to add "№7 Affordable and Clean Energy" and "№13 Climate Action" to the goals listed above. These two goals are indirectly related to the topics discussed in this article and may affect, for example, the reduction of carbon dioxide emissions into the atmosphere through the use of tires with reduced rolling resistance (by reducing fuel consumption).

The novelty of this review article consists in a comprehensive and multidisciplinary approach to studying vehicle tire rubber systems, combining chemical, technological, environmental, and computational aspects into a single concept.

The purpose of this review is to present an in-depth analysis of the technological and chemical characteristics of the structure and internal processes in rubber materials used for vehicles, covering elastomer mixes and functional additives. Particular focus is placed on the impact of external degradation factors, including oxidation, ozonation, photodegradation, thermooxidative aging, and biological degradation, as well as the mechanisms of chemical transformations that occur during tire operation.

This article, compared to many other reviews that concentrate either on environmental pollution or the analytical characterization ofTWPs, consolidates multiple traditionally different research domains:

- the chemistry and degradation of tire elastomers,
- analytical methods for TWPs collection, identification, and quantification,
- advanced multiscale computational modeling approaches for predicting material behavior and environmental impact (in terms of nonexhaust emission of TWPs).

The review also discusses the mechanisms of action of functional additives such as antioxidants, vulcanizing agents, and coupling agents, including modern biological and natural substitutes aimed at improving sustainability and reducing toxicity.

The article's focus on multiscale computational chemistry and predictive material modeling is one of its main innovations. Modern

computational techniques based on QMs, MDs, coarse-grained (CG) simulations, and continuum modeling undergo special consideration. These methods are provided as prospective tools for understanding filler-polymer interactions, degradation mechanisms, structure-property correlations, and the future environmental behavior of TWPs. The lack of established methods and conceptual frameworks for using multiscale simulations in tire material science remains insufficiently explored.

The review also contributes novelty by bridging sustainability-oriented tire design with computational prediction strategies. The discussion includes bio-based elastomers, green fillers, natural additives, and environmentally safer alternatives to conventional tire compounds while simultaneously evaluating how computational chemistry can accelerate the development of sustainable rubber formulations. This integrated perspective between sustainable materials and predictive modeling is still insufficiently addressed in the existing literature.

In the area of tire wear and elastomer degradation, the review provides a clear link between the chemical composition of tires, degradation processes, and the production of TWPs, which are often investigated separately in previous studies. The article also shows how multiscale computational techniques can be utilized for predicting structure-property relationships, degradation behavior, and environmental impact. The review also highlights the need for standardized analytical and predictive techniques that can connect tire composition, additive chemistry, and emission characteristics. The paper presents an interdisciplinary framework for subsequent research on sustainable tire materials and environmental assessment by combining experimental, analytical, and computational perspectives.

2 | Part I—Chemical Composition and Degradation Processes

2.1 | Chemical Structures and Processes of a Modern Tire

Modern tires are structurally and compositionally complicated. A contemporary tire consists of three parts: the shell, a metal belt system, and the tire tread [34]. The tread is the part of the tire that contacts the road surface. The chemical structure of automobile tires varies based on their utility type (car, truck vehicles, or summer, winter, all-season) and brand. The automobile tire can include up to 40 compounds, including synthetic and NRs, carbon black (CB), polyesters, nylon, silica, steel, and various organic molecules [48]. The organic polymeric rubber fraction has an average compositional value of 40%–50%, although it's difficult to distinguish between natural and manufactured rubbers. Truck tires are mostly made of NR, whereas automobile tires may contain both natural and synthetic rubber, and the organic component of automobile tires varies by kind rather than brand and producer [23]. Chemical profiles and additives vary significantly depending on the year and country of manufacture, and TWPs composition is impacted by several factors, including driving style, tire type, road surface, and vehicle maintenance. However, there is little information about how TWPs reproduce or replicate the original tire composition. This is due to the processes in the rubber material that occur during the operation and life cycle of the product. Moreover, in the test results of a number of researchers, it was found that both the inclusion of substances from the environment (from the roadway and road infrastructure) and the subsequent transformation of TWPs due to the influence of factors such as humidity, bacteria from the soil, decomposition from ultraviolet (UV) radiation, and oxidation by air [26, 49]. Information about these processes is disclosed in the following sections of this review.

Taking the above into account, the specific composition of the rubber used for a vehicle tire is largely similar between manufacturers (the differences are more likely to be in the use in relation to weather condition, climate, and type of transport) but is ultimately classified as confidential information. This fact complicates the research of scientific groups also because in addition to the exact composition, it is important to consider the production steps and the sequence of synthesis to be able to approximate what transition or final chemical compounds can be formed. It is also important to understand and be able to compare the initial chemical compounds—reagents and their modified forms in the process of production synthesis and exploitation. Nevertheless, currently, there is only an idea of the composition of a vehicle tire, which, in its classical form, in addition to elastomer rubbers, consists of a number of functional additives.

This chapter will demonstrate the basic chemical reactions that occur in a material and lead to destruction through a chain reaction. A number of common functional additives, their analytical properties, and actions that prevent the destruction process will also be considered. Attention is also paid to the percentage and a brief description of the common concept of components in rubber (mixtures of elastomers with additives), as shown in Figure 3 and Table 1. The average composition information is taken from a number of relevant patents (US2821232A, US20240343892A1, US20130030111A1, EP 0 527 396 A1, and CN113999437A) and applies to generalized all types of rubber for vehicle tires.

It is important to note that the components (Figure 4) of modern tires for most vehicles have differences in the composition of the chemicals (or their concentrations) from which they are produced. In particular, tread * compounds typically consist of solution-polymerized NR, styrene–butadiene rubber (SBR), and butadiene rubber (BR) in ratios of about 20–60, 20–50, and 10–40 phr, respectively. Normally, they are reinforced with 40–70 phr of high-structure CB and/or 30–80 phr of precipitated silica, along with 5–12 phr of processing oils and 3–10 phr of bifunctional organosilane coupling agents in relation to the amount of silica [50, 51]. In order to improve fatigue life and ozone resistance, sidewall compounds usually have greater amounts of NR (50–80 phr) and BR (20–40 phr), lower filler loadings of CB (30–50 phr), and higher levels of para-phenylenediamine antidegradants (1–3 phr). On the other hand, to provide long-lasting bonding to textile cords, carcass rubber compounds are primarily composed of NR (70–100 phr) with moderate CB contents of 30–50 phr. They also use resorcinol-formaldehyde-latex adhesion systems, which usually consist of 1–3 phr resorcinol and 2–5 phr methylene donors [52]. To enhance rubber–steel cord adhesion and preserve structural rigidity under cyclic loading, belt, and breaker compounds are made with NR or NR/BR blends reinforced by 50–80 phr of CB and incorporate

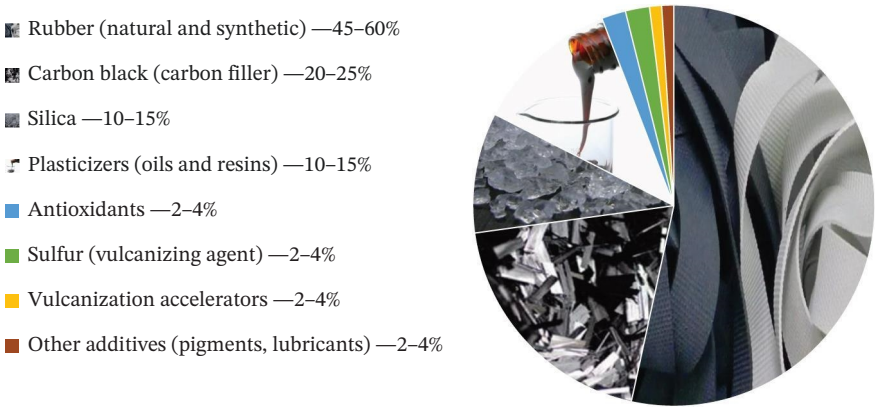

FIGURE 3 | A common concept of the composition for vehicle tires.

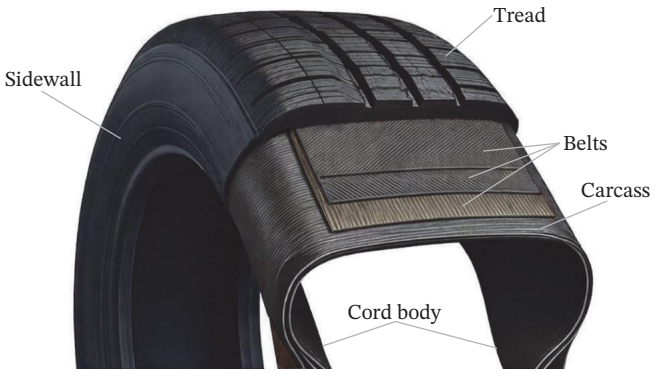

FIGURE 4 | Schematic structure of a tire showing the main structural components, including tread, sidewall, belts, carcass, and cord body.

cobalt-based adhesion boosters at concentrations of 0.2–0.5 phr [53].

*It is noticeable that the thread is presented in general terms in Figure 3 and Table 1, and is usually considered as a general component of vehicle tires, including by other authors of scientific researches, so in this publication it will also be the main part of the analysis. The reason is that this part of the tire directly comes into contact with the road surface (therefore, this rubber composition is subjected to the most extreme conditions of temperature, friction, emission, etc.).

2.2 | NR–Based Tires

Research on natural and bio-based rubber compositions for tires has expanded rapidly over the past decade due to the scale of the tire manufacturing industry for vehicles, the level of technology development, and a clear commitment to environmental management and sustainability. An important area of research is the creation of technologies and techniques for the production and integration of natural additives and biomaterials into rubber. Many research groups are exploring the possibility of replacing the most toxic or most expensive components in the rubber composition for vehicle tires. The study and comparison of the properties of materials based on natural biocomponents as substitutes for classical materials are an interesting and promising field.

The design of tires and tire rubber is moving more and more in the direction of sustainable and green practices as the tire business expands. Epoxidized NR (ENR) has emerged as a viable substitute for SBR in recent years. ENR, which is created by chemically altering NR, provides better air tightness and antiwet skid performance [54]. Better compatibility between ENR and silica results from an open–ring interaction between the epoxy groups in ENR and the silanol groups on the silica surface. ENR is also ideally suited for covering the increasing demands for sustainable development and environmental preservation because it is a bio-based rubber [55]. ENR may react with a variety of functional groups, including amino and carboxyl groups, because of the epoxy groups on its main chain. In order to sustain the elasticity of NR while displaying superior qualities typically associated with synthetic rubbers, such as excellent aging and solvent resistance, ENR's molecular structure can be optimized through crosslinking with a series of carboxylic acids with varying chain lengths and degrees of functionality [56]. Consequently, the application of ENR in tire treads reduces the demand for rubber manufactured from petroleum, which leads to nanocomposites that perform better for specific applications.

Many researchers are creating environmentally friendly, high-performing alternatives to rubber additives used in tire manufacturing as sustainability and environmental concerns gain traction. Utilizing rice husk silica, dandelion rubber, plant fibers, lignin, bio-based oils, and resins in the tire composition is part of the greener strategy implemented by tire producers [57]. A considerable amount of tire additives are fillers, which are substances added to rubber compounds to enhance their properties. Because of its reinforcing qualities, CB is the most often utilized of these. However, the utilization of recovered CB and the creation of new green fillers to replace CB are developing in response to the significant carbon footprint that CB contributes. In addition to achieving benefits like decreased rolling resistance, enhanced durability, and lightweight composites, replacing CB with bio-based fillers has a significant impact on sustainability [58]. Cellulose and its nanostructures are thoroughly studied substitutes. In recent years, there has been increased interest in the potential of nanocellulose as a reinforcing filler for rubber composites [59]. Two important types of nanocellulose, cellulose nanocrystals (CNCs) and cellulose nanofibers (CNFs), are being studied for their potential to reinforce [60].

Among other things, organic acids can be used as a bio substitute for silica. As an example—sorbic acid, often known as chemical-B or SA, is an inexpensive, easily accessible, and environmentally safe natural organic substance. It is widely used as a preservative

and, to a lesser degree, in food items, medications, and cosmetics. Sorbic acid molecules are formed by one carboxyl group and two conjugated double bonds. It is thought that this common structure is utilized as an interfacial modifier for rubbers and fillers. SBR and Halloysite nanotubes (HNTs) were obtained by grafting copolymerization or hydrogen bonding [61]. In addition to enhancing the filler dispersion in the compound, it serves as an environmentally friendly treatment in the tire rubber system.

Based on the subject of the review, it is important to note that computational multiscale modeling as an approach is perfect for defining the structure of new materials and their properties, which will allow us to obtain visible trends at the first stage of analytical research and to amplify experimental procedures. Undoubtedly, knowledge of the processes that take place in the material overtime and during operation is necessary for a complete understanding. Although it is not immediately apparent, a change in the material's structure and chemical composition has a significant impact on the material's, the product's conditions, and general qualities. The problems of material transformation are investigated from several perspectives in this article, allowing readers to comprehend the methods and strategies for the study's subsequent phases.

2.3 | Understanding of Chemical Transformations During Exploitation

As is known, the main mass of a tire is accounted for by several specific elastomers—NR, BR, and SBR—macromolecules of copolymer, in which, as expected, many different functional additives are distributed with a certain degree of uniformity. If we consider the process of transformation, or rather to say, destruction of the polymer chain in macromolecules of copolymers due to complex aging, we can distinguish a number of certain stages. The basic stage of material degradation is the destruction of interatomic bonds in the molecules of substances due to various kinds of impacts, which leads to the formation of a number of specific radicals in the form of polar functional groups, such as hydroxyl (·OH), carbonyl (·C═O), and carboxyl (·COOH). These newly formed radicals enter into subsequent reactions with the copolymer molecules forming the base of the tire and are also modified by the external influence of primary factors. This process can be called a chain radical chemical reaction and in the case of the tested rubber material (composition of elastomers), leads to its degradation and, as a consequence, to cracks on the surface, increased emission of material, and, eventually, the product being taken out of service.

The causes and factors leading to such consequences as material destruction can be categorized into five groups:

2.3.1 | Air Oxidation

On contact with air and, in particular, oxygen, an oxidation process occurs. The oxidation of elastomers is due to the reaction of air and oxygen with the polymer chains of which it is composed. The main chemical processes include the steps of disruption of polymer molecules, formation of oxidized functional groups, and, possibly, cross-linking of newly formed molecules (polymer residues).

The destruction of copolymer macromolecules is due to their structure of a multiatomic chain of carbon and hydrogen particles. Between these elements there are so-called chemical bonds (which are based on the energy interaction between atoms through the overlapping of electron clouds); in the process of oxidation, oxygen from the air attacks the chemical bonds of the molecule, causing their rupture, and thus several new substances and remnants of polymer chains are formed, and oxygen forms free radicals—a reactive particles that are able to start a chain radical chemical reaction with other compounds in the condensed rubber phase. In classical cases, radicals are formed as polar groups such as hydroxyl (·OH), carbonyl (·C═O), and carboxyl (·COOH) groups. These new chemical groups eventually change the physical properties of the material, making it stiffer and less elastic. Crosslinking of molecules also occurs during oxidation, and "crosslinks" can be formed because of covalent bonds between polymer molecules that were formed after the macromolecules of the copolymer were broken. In this case, the material loses its ability to stretch and be flexible, which contributes to the formation of cracks under load and continued destructions.

2.3.2 | Temperature Fluctuations in the Operating Environment

Temperature fluctuations also have a significant effect on rubber material, and this interaction can be attributed to physicochemical processes. First of all, it is important to note such a phenomenon as thermal degradation. High temperatures during operational processes can lead to the breakdown of molecular bonds in the polymer. In particular, automobile and motorcycle tires can be heated to high temperatures in sports racing conditions or at high speeds on autobahns or highways, and tire temperatures can reach 90°C–120°C for conventional cars and up to 200°C for motorcycle racing tires. This leads to the important consequence that free radicals (polar groups) appear more rapidly at high temperatures, leading the polymer material to reduce elasticity, cracking, and eventual destruction. However, under normal mixed cycle operating conditions, such as driving on city roads, tire temperatures typically range between 40 and 60°C [62].

Increasing temperature also accelerates the kinetics of chemical reactions, including, as discussed above, oxidation or hydrolysis and other polymer chain breakdown processes. Temperature fluctuations combined with oxidation result in rapid aging of rubber. The higher the temperature, the faster the oxidation processes proceed, and the faster the polymer chains break down and molecular weight decreases or additional inefficient crosslinking between polymer macromolecules occurs (depending on temperature).

On the other hand, chain scission reduces viscosity, whereas more crosslinking increases stiffness. Both can cause fractures and loss of tensile strength. The modeling evidence indicates that high temperatures increase tire wear rates, while thermomechanical processes produce fine (<2.5 μm) and ultrafine (<100 nm) particles. Moreover, it was found that increasing the temperature from 5 to 25°C led to a 40% increase in the tire wear emission rate [63]. It was also shown that following thermooxidative aging, SBR abrasion rates dropped by no more than 30%,

most likely due to enhanced rubber hardness [64]. Tire aging results indicate that oxygen inside the tire contributes to the aging process. Normally, when a tire is filled with air, the internal oxygen partial pressure is significantly greater than atmospheric pressure. In the case of TWPs, in particular, tires in stock typically have slower oxidation kinetics compared to operational tires [65].

Typically, thermooxidative aging of tires is measured by a change in performance. Mechanical characterization measures tensile strength and abrasion resistance, whereas chemical characterization covers crosslink density and composition, which are analyzed by means of utilized ATR–FTIR analysis to identify changes in surface functioning of SBR composites subjected to temperatures of 70°C [64]. It was discovered that oxidation began at the surface and spread to the interior regions of the material component (permeability of O_2). The content of the antioxidant 6-PPD was shown to drop to only 20% after 21 days of thermooxidative aging [66].

Moreover, it is worth mentioning the possible interaction of tires with various oils, gasoline, diesel, and other substances (in the context of this study,solvents) that occur on the roadway and roadside area. Temperature acts as a catalyst for the processes of interaction between elastomers and solvents, which lead to softening and further accelerated destruction of the material.

Thermal extension and compression are also significant factors in the aging-degradation process of rubber. Elastomers, like other materials, expand when heated and compressed when cooled. Repeated cycles of extension and compression cause microscopic damage at the molecular level, causing small cracks to appear at first, which grow larger overtime. These changes make the material less resistant to mechanical stress. Finally, crystallization at low temperatures should also not be forgotten. Some types of rubber can partially crystallize, losing their elasticity and, as expected, becoming stiffer and more prone to cracking under mechanical stress.

2.3.3 | Ozonolysis

The influence of ozone, as well as oxygen, has a significant effect on the aging process of the tire and the degradation of the material in general. Ground-level ozone is generated from nitrogen oxide NO_x, including NO_2, oxygen, and energy of the sun. The presence of volatile organic chemicals could stimulate their creation. Diesel cars and other sources can release NO_x, which is a significant traffic-related influence. During ozonolysis from atmospheric air, double bonds (characteristic of many polymers) in polymer molecules are attacked, which causes chemical bonds to change to the *Sp* form when the molecule is oxidized. There is also the process of the formation of polar reactive radicals, which continue the chain reaction of the transformation of stable forms of macromolecules of copolymers into other less stable substances with qualitatively different physical properties. In the scale of observation, this leads to the formation of tread microcracks which tend to deepen inwards. With the additional load factor of cyclic compression–hysteresis loading during normal operation, the cracks enlarge until complete failure. Moreover, rubber material in the stretched position (at the appropriate loss tangent $\tan\delta^*$, which is also proportional RRC) is subject to enhanced ozonolysis due to the double interatomic bonds in the molecules in the stretched state. The interaction between ozone and rubber slows when unsaturated double bonds decrease and a saturated external layer becomes amorphous. This layer of ozonated rubber can consist of 10–40 molecular layers. It shields the rubber until it is abraded during driving, allowing ozone to penetrate the underlying unsaturated elastomers and eventually create a new "protective" layer [48].

Like other external substances with high reactivity, ozone exhibits catalytic properties, creating a region at the interface point (one of which is the condensed phase of elastomers) with an appropriate pH value and surface charge, which enhances the effect of the other solvent substances mentioned above. Ozonolysis impact is mainly significant for airborne TWPs (PM_{10}), which are not observed in a majority of the articles. When road runoff transports particles into receiving waters, ozonolysis becomes less effective (inside of fluid phase).

$^*\tan\delta$, technically, it is the ratio of the loss modulus or viscous modulus (the complex shear modulus—G^*—[viscous component], loss modulus, or G'', is the "imaginary" part of the samples the overall complex modulus) over the storage modulus (Young's modulus E), and hence indicates the tendency of a material to dissipate energy (i.e., more viscous-like) or to store energy (i.e., more elastic-like).

$$\tan\delta = \frac{G''}{G'} \text{ or } \tan\delta = \frac{E''}{E'}. \quad (1)$$

As is well known, both of these moduli are related through the Poisson's ratio (ν) by a simple equation and therefore can be expressed in terms of each other (or through Bulk modulus K) as follows:

$$E = 2G(1+\nu) = 3K(1-2\nu), \quad (2)$$

where E is Young's modulus (storage modulus E' and loss modulus E''), G is the shear modulus (storage modulus G' and loss modulus G''), K is the Bulk modulus, and ν is the Poisson's ratio.

2.3.4 | Exposure to UV Rays (UV Radiation)

This is a photochemical process—which occurs due to the interaction of sunlight, which has high enough energy to break chemical bonds in the macromolecules of the rubber copolymer. This leads to the photodegradation effect, where UV radiation breaks chemical bonds (especially double bonds) and leads to the formation of various free radicals. The earth's surface receives UV radiation ranging from 280 to 400 nm. High-energy UV irradiation (UV–C, 100–280 nm) can break typical polymer bonds (CH_3—CH_2—CH_3, H_2C=CH_2, and HC≡CH). Single bonds do not absorb light beyond 190 nm [47]. Most rubber polymers are resistant to direct UV photolysis, but in the 290–400 nm range, chromophores absorb light, forming radicals in the presence of air. This leads to higher elastomer crosslinking and increased molecular weight; therefore, rubber material becomes breakable, which is unsuitable for normal tire operation. In sum, this leads to the photodegradation effect, in which UV radiation breaks chemical bonds and leads to the formation of various free radicals.

The resulting free radicals, in turn, as in the oxidation process, initiate a chain reaction of destruction of elastomer molecular chains. The scientific community is also aware of the phenomenon of photo-oxidation, in which UV rays accelerate the process of chemical oxidation as radicals formed during photodegradation react faster with oxygen, which leads to more intensive destruction of polymer molecules and an increase in the number of crosslinking in the material. All this makes the rubber stiffer—elasticity is lost and mechanical strength is significantly reduced, and then microcracks appear on the surface, which increase with time. It is worth to note that such degradation of the material is surface erosion—UV radiation primarily affects the outer layers of the material, causing their degradation. At first, tiny cracks form on the surface, which overtime deepen and propagate deep into the material, completely changing the structural properties and performance of the material.

2.3.5 | Biological Degradation

Depolymerization and the surface development of low-molecular-weight compounds, frequently with unsaturated bonds and aldehyde groups, are the results of this devulcanization. Consequently, a decrease in crosslinking and an increase in hydrophilicity are typically noted [67]. Rubber's density, crystallinity, molecular weight, functional group type, tactile sensations, structural substituents, and additives—all those properties affect how easily it degrades [68].

Rubber may be destroyed by both bacteria and fungi [69]. It has been demonstrated that two types of bacteria may use rubber as their only carbon source. *Actinoplanes*, *Streptomyces*, and *Micromonospora* are among the first group of bacteria that produce transparent halos and emit enzymes that break down rubber [70]. The second group reacts to rubber particles that are spread out in the liquid phase. *Gordonia*, *Mycobacterium*, and *Nocardia* are among the most powerful microbes known to degrade rubber. With the exception of *Streptomyces* sp., which can thrive at temperatures as high as 50°C, the majority of them are aerobic, mesophilic bacteria [68]. All these microorganisms have been effectively isolated, for instance, from soil. Temperatures between 30 and 40°C accelerate deterioration for mesophilic bacteria.

Because the surface morphology provides favorable microenvironments, fungi that preferentially target rough rubber surfaces may also destroy synthetic rubber, including poly-(cis-1,4-isoprene). ATR-FTIR studies, which revealed the presence of aldehydes at the rubber surface, validated these degradation processes. Additionally, they may reach deeper rubber layers through tiny gaps [69].

During biodegradation, the surface becomes rough and undergoes chemical surface changes correlated with a decrease in crosslinking and an increase in hydrophilicity. Rubber may eventually mineralize as a result of biodegradation when it is fully oxidized to CO_2. A half-life time and a mineralization rate may be computed from the amount of time needed to mineralize the organic components of the TWPs. It is anticipated that SBR and NR would have differing biodegradability due to their dissimilar molecular architectures, with NR being more biodegradable than SBR. Conclusions on the half-life of TWPs in the environment are not yet available according to the current literature observations.

Surely, all of the above factors are not primary, but indirectly influence the natural mechanical destruction and abrasion during operation (in regards to Complex modulus and $\tan\delta$), but their influence is significant in the scope of considering the rubber material from the chemical analysis and thermodynamics side. It is important to note that the right choice of approach to research and analytical aspects will allow us to model the material properties and regulate and understand its behavior overtime, taking into account the different operational influences.

For the specific regulation of well-known processes, there are certain rules for identifying external influences and analytical determination, such as the following:

- Thermooxidation: ASTM D 573-04 (Rubber – Deterioration in an air oven); ISO 188:2011 (Rubber, vulcanized or thermoplastic: accelerated aging and heat-resistance tests); and DIN 53508:2000-03 (Testing of rubber—Accelerated aging).
- Photooxidation: ISO/TS 22687:2018 (E) (Rubber—Framework for assessing the environmental fate of tire and road wear particles [TRWP]).
- Ozonation: ISO 1431-1:2012 (Rubber, vulcanized or thermoplastic—Resistance to ozone cracking—Part 1: Static and dynamic strain testing); ISO 1431-3:2017 (Reference and alternative methods for determining the ozone concentration in laboratory test chambers); and ASTM D1149-18 (Standard Test Methods for Rubber Deterioration Cracking in an Ozone Controlled Environment).

2.4 | Reaction of Radicals Within the Rubber (Elastomer) Phase

For a holistic and deeper understanding of the processes of rubber material degradation due to changes in the macromolecules of the copolymer, this section highlights the chemical chain reaction process of free radicals that are generated by heat, oxygen, ozone, and UV radiation. The presented reaction mechanisms in this and the following subsections are based on a number of studies from the literature [71, 72], as well as on basic chemical knowledge about polymers. The reaction schemes in the following paragraphs and sections are presented in a classical, generalized form to illustrate, enhance perception, and understanding of the basic chemical processes associated with rubber aging rather than to accurately reproduce tire operating conditions.

The formation of radicals and their subsequent reactions within the condensed rubber phase constitute a multistage radical chain process [73]. Figure 5 schematically illustrates the initial steps of this process, highlighting the main pathways of radical generation, propagation, and early-stage transformation in polymeric materials.

Radical initiation in rubber materials may proceed through several parallel mechanisms, depending on environmental conditions, material history, and the presence of impurities or additives (radical initiation mechanisms for rubber oxidation). Primary macroradicals (R·) can be generated by thermal or

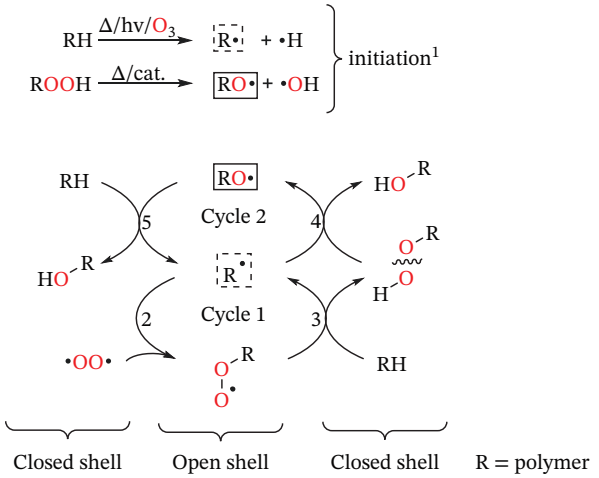

FIGURE 5 | Simplified scheme of the early stages of radical oxidation in polymeric rubber materials, illustrating representative initiation pathways, oxygen uptake, and initial propagation cycles in the condensed phase (R denotes a polymer chain segment).

photochemical homolytic cleavage of C--H bonds [74], as well as through reactions with reactive oxygen species such as ozone [75]. In addition, preexisting hydroperoxides (ROOH), which may form during processing or early stages of aging, can decompose thermally or catalytically in the presence of trace transition metals, yielding alkoxyl (RO·) and hydroxyl (HO·) radicals.

Once formed, carbon-centered macroradicals (R·) rapidly react with molecular oxygen to produce peroxyl radicals (ROO·), which play a central role in the propagation of oxidative degradation. These peroxyl radicals' abstract hydrogen atoms from neighboring polymer chains (RH), forming hydroperoxides (ROOH) and regenerating new macroradicals, thereby sustaining the chain reaction. Alkoxyl radicals generated from hydroperoxide decomposition may also participate in propagation by abstracting hydrogen atoms from the polymer backbone, leading to further radical formation [76].

The scheme shown represents only the early stages of the radical oxidation process. Subsequent reactions involve a complex and highly branched network of secondary transformations, including β-scission of alkoxyl radicals, chain cleavage, crosslinking, formation of carbonyl- and carboxyl-containing groups, and various termination pathways resulting from radical–radical recombination or disproportionation [77]. Owing to the large number of possible reaction routes and their strong dependence on the polymer composition and environmental conditions, a comprehensive description of all downstream reactions is beyond the scope of this section.

2.4.1 | Alkyl Radicals (R·)

Alkyl radicals in the conventional sense are fragments of hydrocarbon chains that are formed predominantly as a result of hydrogen abstraction from C—H bonds (carbon-hydrogen), while direct C—C bond (carbon–carbon) scission typically occurs at later stages of oxidative degradation. In scientific and technical literature, radicals are denoted by the general formula R·, where R represents an alkyl or polymer chain segment. In vehicle tire rubber formed from copolymer macromolecules (NR, BR, and SBR), carbon–carbon double bonds are particularly susceptible to reactions induced by oxidation and UV radiation, leading to the formation of radical sites along the polymer backbone. Subsequent interactions of alkyl radicals with neighboring polymer chains may result in bond scission, causing a reduction in the polymer chain length (degradation) and, consequently, a loss of mechanical strength of the material. Alkyl radicals also readily react with molecular oxygen via radical addition to form peroxyl radicals (ROO·), which play a central role in sustaining and accelerating oxidative chain reactions in elastomeric materials.

2.4.2 | Peroxide Radicals (ROO·)

Peroxide radicals (ROO·) are formed when alkyl radicals react with molecular oxygen, as described above. These radicals represent key reactive intermediates in the oxidative degradation of rubber materials and play a central role in the propagation of radical chain reactions [76]. The formation of peroxyl radicals proceeds via the rapid addition of oxygen to carbon-centered radicals ($R\cdot + O_2 \rightarrow ROO\cdot$). In polymeric systems, peroxyl radicals readily abstract hydrogen atoms from neighboring polymer chains, leading to the formation of hydroperoxides (ROOH) and new alkyl radicals (R·), thereby sustaining the oxidation chain process. Continued repetition of these reactions results in progressive degradation of the polymer backbone and deterioration of mechanical properties. In addition, the thermal or catalytic decomposition of hydroperoxides may generate highly reactive species such as hydroxyl radicals (·OH), which can further accelerate oxidative degradation processes [78].

2.4.3 | Hydroxyl Radicals (·OH) and Alkoxyl Radicals (*RO*·)

Hydroxyl radicals (·OH) and alkoxyl radicals (RO·) are highly reactive oxygen-centered species that play an important role in the oxidative degradation of rubber materials by accelerating radical chain reactions [76]. Although hydroxyl radicals are not abundant due to their extremely short lifetimes and localized formation, their very high reactivity makes them particularly effective in promoting oxidative damage. Their presence in elastomeric systems significantly enhances oxidation rates and contributes to rapid structural deterioration, making their formation a critical factor in the assessment of material stability and antioxidant efficiency. By the way, in humans, they have a similar pattern of action on organic molecules, destroying healthy cells [79].

In rubber materials, these radicals can be generated through several mechanistic pathways. A primary source is the thermal or catalytic decomposition of hydroperoxides (ROOH), which yields alkoxyl and hydroxyl radicals according to the reaction.

$$ROOH \rightarrow RO\cdot + \cdot OH. \quad (3)$$

Under predominantly thermal conditions, this process generally requires elevated temperatures, whereas the presence of trace transition metals such as Fe, Cu, Mn, or Co can substantially lower the activation energy and promote hydroperoxide decomposition at considerably lower temperatures via metal-catalyzed (Fenton-like) pathways [80, 81].

Hydroxyl radicals may also be generated indirectly under UV irradiation through photochemical reactions involving hydroperoxides, peroxides, ozone, or other photoactive species present in the material or its environment [77]. Once formed, hydroxyl and alkoxyl radicals readily attack polymer backbones by abstracting hydrogen atoms or inducing bond scission, leading to the formation of new radical centers. These reactions sustain further propagation of oxidative degradation, ultimately resulting in chain cleavage, loss of mechanical integrity, and the development of cracks in rubber materials.

2.4.4 | Alkoxyl Radicals (RO·)

Alkoxyl radicals (RO·) are formed primarily as a result of thermal, photochemical, or catalytic decomposition of hydroperoxides. These species are highly reactive oxygen-centered radicals capable of inducing polymer chain scission. The formation of alkoxyl radicals proceeds via the mechanism described in Equation (3). Once generated, alkoxyl radicals readily attack hydrocarbon chains within the polymer matrix, promoting bond cleavage and interactions with neighboring polymer segments. As a result, RO· radicals significantly accelerate aging processes and contribute to the propagation of degradation chain reactions in rubber materials.

2.5 | Radical Chain Chemical Reaction

In general terms, the interaction of radicals with copolymer macromolecules proceeds through several key stages, including initiation, chain propagation, branching, and termination of radical reactions. The dominant reaction types leading to bond cleavage or oxidation include hydrogen atom abstraction, radical addition to unsaturated bonds, and oxidative chain processes. A summary of these interactions is provided in Table 2, which is based on established principles of radical chemistry and relevant literature sources [82, 83].

Of course, manufacturers have been using and upgrading rubber compounds (elastomer compounds) for many years by adding additives of various types and functionalities. In addition to a vulcanizing agent and an organic dissolution accelerator, antioxidants always occupy a key place in application. This type of additive serves as protection against oxidation processes, photochemical degradation, and aging of the material in general. A number of the most used and popular additives in tire manufacturering are known, such as N-(1,3-Dimethylbutyl)-N′-phenyl-p-phenylenediamine (6PPD), N-phenyl-2-naphthylamine, and 2,6-Di-tert-butyl-4-methylphenol, which are used in concentrations up to 3% of the weight of the whole product (Table 3).

There are also uncertainties regarding the classification of tires based on their chemical composition and environmental impact; for example, when using the EU tire labeling classifiers, it is indicated that lower rolling resistance is associated with a higher content of synthetic rubbers and 6PPD, but nevertheless, they are classified as "green" (producing an effect of ecological purity) types of rubber. However, due to the reduced concentration of toxic chemical additives, fuel consumption and, as a result, carbon dioxide emissions are reduced. The environmental impact of tires is associated not only with CO_2 emissions or the use of environmentally friendly raw materials but also with microplastic and/or TWPs. Such a gap in formulations deserves attention from the relevant regulatory authorities.

2.6 | Antioxidants and Methods of Decelerating and Terminating Material Degradation

In view of the fact that this review article is mostly concerned with the chemical aspects of this scientific field, the mechanisms of chemical exploitation of the most common types of antioxidants and a description of some of their properties are described next.

To prevent degradation processes of rubber (elastomer blends) at chemical-molecular levels, various methods are used to block free radicals and slow down oxidation and photodegradation of macromolecules of copolymers. The main strategies include the use of various antioxidants (UV inhibitors and ozone stabilizers), as well as optimization of the elastomer blend structure with additives that enhance their resistance to environmental conditions over a wide temperature range.

In general, antioxidants are chemical inhibitors that play a key role in preventing chemical radical chain reactions (described above) during an oxidative reaction. They react with free radicals, converting them into unreactive compounds with an inert nature. This "radical trapping" is primarily aimed at interacting with alkyl (R·), peroxy (ROO·) and hydroxyl (·OH) radicals, converting them into less active products, thus preventing further degradation of the polymer chains in the material. For example, phenolic antioxidants such as para-phenylenediamine 6PPD give up a hydrogen atom (dehydrogenation-deprotonation) to the reactive radical, converting it into a nonpolar and inactive compound.

$$\mathrm{ROO}\cdot + \mathrm{AH} \rightarrow \mathrm{ROOH} + \mathrm{A}\cdot \tag{4}$$

where AH is the antioxidant and A· is the dehydrogenated form of the antioxidant, which can also be considered as a radical, but has a markedly more stable nature and no tendency to destroy the macromolecules of the copolymer and their new, understudied forms remain in the volume of the rubber phase. However, then, through the emission, they also enter the environment. Antioxidants have many radical interaction sites, meaning that they are able to donate a large number of hydrogen atoms, thereby deactivating a significant number of reactive radicals formed during the exploitation process of the material discussed above.

Another important characteristic of some antioxidants is their ability to decompose hydroperoxides (ROOH) by reducing them to stable, nonradical products, thereby preventing the formation of highly reactive alkoxyl and hydroxyl radicals. For example, phosphites and thioesters, such as triphenyl phosphite (TPP), can effectively neutralize hydroperoxides formed during oxidation.

$$\mathrm{ROOH} + \mathrm{P(OC_6H_5)_3} \rightarrow \mathrm{ROH} + \mathrm{P(OC_6H_5)_3O}, \tag{5}$$

where $P(OC_6H_5)_3$ is TPP, ROH is a stable organic alcohol, and $P(OC_6H_5)_3O$ is the oxidized form of the antioxidant.

TABLE 2 | Stages of the chain chemical reaction with chemical equations and description.

Initiation The formation of first free radicals by breaking chemical bonds due to heat, UV radiation or chemicals from the atmosphere such as ozone. For example, UV radiation can break carbon–carbon double bonds in a polymer to form free radicals.	$RH \xrightarrow{\Delta T,\ h\nu} R\cdot + H$where RH is the polymer molecule, R· is the hydrocarbon radical (residue) formed after the dehydrogenation.
Development of a chain reaction (propagation) The radicals (R·) formed react with oxygen molecules (·OO·) from the air to form peroxyl radicals (ROO·), which attack neighboring polymer molecules, continuing to break their carbon–carbon or carbon–hydrogen bonds.	$R\cdot + \cdot OO\cdot \rightarrow ROO\cdot$where ROO· is the peroxyl radical.
It leads to the formation of new radicals that continue the destruction of chains. For example, ROO· peroxyl radicals attack the macromolecules of the copolymer (rubber elastomers), forming new radicals of similar and other types and hydroperoxides, as well as stripping off the hydrogen atom (dehydrogenation).	$ROO\cdot + RH \rightarrow ROOH + R\cdot$where ROOH is a hydroperoxide.
Abstraction of the hydrogen atom A free radical (such as ROO· or ·OH) attacks the polymer by stripping off a hydrogen atom. This leads to the formation of a radical on the polymer chain. The mechanism of the process generally represents a sequence where the radical attacks a rather weak C—H bond by stripping off a hydrogen atom. The most vulnerable are methylene groups (CH_2) and allylic bonds (CH═CH—CH_2—) in polymers such as butadiene rubbers.	$RH + X\cdot \rightarrow R\cdot + HX$where X· is the external radical, such as hydroxyl radical (·OH) or peroxyl radical (ROO·); HX is the by-product, such as water upon interaction with the hydroxyl radical or hydroperoxide upon (ROO·).
Dehydrogenation In the hydrogen abstraction process above, the formation of unsaturated structures may occur from the polymer chain, which changes the structure of the polymer. This reaction occurs in chains with saturated hydrocarbons (single chemical bond). It is important to note that the reaction product—double bond (alkene type) increases the reactivity of the chain section and the tendency to further oxidation. $-CH_2-CH_2- \xrightarrow{t,\ ^\circ C} -CH=CH- + H_2$	
Branching Breaking chemical bonds by oxidation Under the action of radicals, polymer chains may undergo oxidative scission, particularly in regions containing carbon–carbon double bonds. Such processes can occur under conditions of elevated temperature and oxidative stress and lead to the formation of oxygen-containing fragments and new radical centers. This mechanism can be represented schematically as follows: $R-CH=CH-R + nO_2 \rightarrow$ oxidation products (e.g., $R-CHO, R\cdot$)where R—CHO represents an aldehyde functional group formed as one possible product of oxidative chain cleavage.	
One of the reaction products becomes a common hydrocarbon radical (R·), and the second part forms a carbonyl-containing fragment (R═O) with a C═O bond and corresponding properties. The complex representation of the chain reaction in the material leads to the formation of various products such as ketones, aldehydes, alcohols, or acids.	$ROOH \rightarrow RO\cdot + \cdot OH$where RO· is an alkoxyl radical, and ·OH is a hydroxyl radical.
The hydroperoxide decomposes to form an alkoxyl radical (RO·) and a hydroxyl radical (·OH), which continues the chain reaction. The formation of carbonyl-containing compounds (such as ketones or aldehydes) may subsequently occur through secondary oxidation pathways. Carboxylic acids formation is then very likely.	$R-CHO + O_2 \rightarrow R-COOH + \cdot O$ where R—COOH is a carboxylic acid.
Termination The destruction process continues until the two free radicals meet and recombine, forming stable products (R − R, ROOR), which completes the chain reaction. This completes the chemical radical chain reaction on a certain scale. However, this process rarely stops all reactions because there are many active radicals remaining. At this point, the already significantly altered polymer structure can lose elasticity and mechanical strength, resulting in rubber cracking. $R\cdot + R\cdot \rightarrow R-RR\cdot + ROO\cdot \rightarrow ROOR$where R—R is different forms of hydrocarbons, ROOR is an organic peroxide (dialkyl peroxide).	

TABLE 3 | The combined table of the most used different types of organic additives for rubber of vehicle tires (included m/z signal for mass-spectrometry analysis) and limit of detection (LOD) in accordance with the *Compendium of Chemical Terminology* by International Union of Pure and Applied Chemistry (IUPAC).

Name/Abb (CAS)	Structure/sum formula	Class/analytical technique	m/z signals	Ref.
N-(1,3-dimethylbutyl)-N′-phenyl-p-phenylenediamine/ 6PPD (793-24-8)	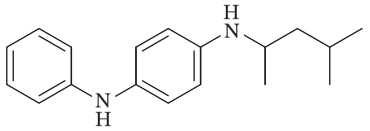 $C_{18}H_{24}N_2$	Antioxidant/ LC–MS/MS; UHPLC–HRMS.	268, 183	[19, 84]
	LOD: 10–20 ng·L^{-1} for aqueous matrices and 0.1–1 ng·g^{-1} for solid extracts;			
1,3-diphenylguanidine/DPG (102-06-7)	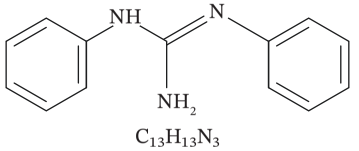 $C_{13}H_{13}N_3$	Vulcanization accelerator/ LC–MS/MS	211, 93	[43]
	LOD: common 0,5–5 ng·L^{-1}			
2-Mercaptobenzothiazole/MBT (149-30-4)	LOD: 0.2–1 ng·L^{-1} 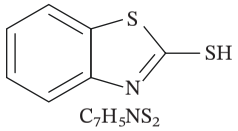 $C_7H_5NS_2$	Vulcanization accelerator/ HPLC–ESIMS; UHPLC–MS; GC–MS	168, 109	[83]
	LOD: for solid matrices 5–43 μg·kg^{-1}; for aqueous extracts 1–10 ng·L^{-1}			
Dibenzylamine/DBA (103-49-1)	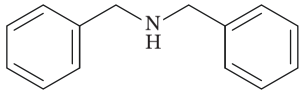 $C_{14}H_{15}N$	Vulcanization activator/GC–MS	106, 91	[65]
	LOD: for solid matrices 1–5 ng·kg^{-1}; for aqueous extracts 1–10 ng·L^{-1}			
N-Cyclohexyl-2-benzothiazolesulfenamide/CBS (95-33-0)	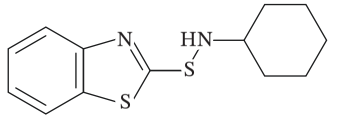 $C_{13}H_{16}N_2S_2$	Vulcanization accelerator/LC–MS	167, 98	[85]
	LOD: common 1–10 ng·L^{-1}			
N, N′-Diphenylurea/(102-07-8)	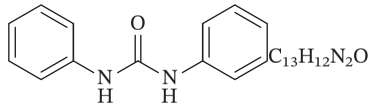 $C_{13}H_{12}N_2O$	Vulcanization retarder/LC–MS	77, 94	[22]
	LOD: common 4–6 ng·L^{-1}			
Tributylamine/(102-82-9)	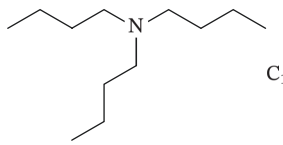 $C_{12}H_{27}N$	Impurity of vulcanization accelerator/GC–MS	186, 184	[83]
	LOD: common 0.1–10 ng·L^{-1}			

(Continues)

TABLE 3 | (Continued)

Name/Abb (CAS)	Structure/sum formula	Class/analytical technique	m/z signals	Ref.
2-(4-Morpholinyl)benzothiazole/24MoBT (4225-26-7)	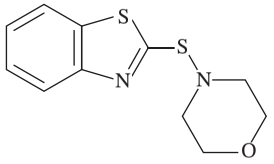 $C_{11}H_{12}N_2OS$	Vulcanization accelerator/LC–MS LOD: common 0.1–1 ng·L^{-1}	220	[86]
N-(Cyclohexylthio)phthalimide/CTP (17796-82-6)	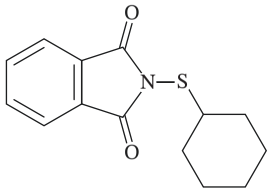 $C_{14}H_{15}NO_2S$	Antiscorching agent/GC–MS LOD: common 0.1–1 ng·L^{-1}	179	[87]
ε-Caprolactam/(105-60-2)	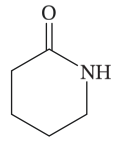 $C_6H_{11}NO$	Decomposition product/GC–MS LOD: common 5–20 ng·L^{-1}	170, 55	[83]
Benzothiazole/(95-16-9)	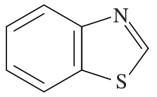 C_7H_5NS	Decomposition product/GC–MS LOD: common <1–10 ng·L^{-1}	135	[22]

Another important part of the fight against material aging and degradation is the use of UV stabilizers (photodegradation inhibitors), which are used to absorb UV rays or dissipate their energy. In this way, UV absorbers convert their energy into harmless heat, preventing the macromolecules of the copolymer from breaking down. Classic examples of such compounds are benzophenones, benzotriazoles, and halogenated UV absorbers. One example is benzotriazoles, which absorb UV radiation in the range of 280–400 nm, thereby reducing the effects of UV radiation on the macromolecules of copolymers. It is also important to consider substances such as "quenchers," which are energy dissipaters and neutralize the excited state of molecules that occurs under UV light. They convert the energy from UV radiation into a safe form—heat—and prevent photochemical degradation. Nickel compounds (e.g., nickel complex compounds) are often used for such purposes [88].

Use of ozone stabilizers (ozonolysis inhibitors). As part of the measures to preserve the material from aging for as long as possible, manufacturers also use special stabilizers that prevent the formation of cracks in the material caused by ozonolysis. One of the popular groups of anti-ozonates are aromatic amines and the already well-known para-phenylenediamine (PPD) and its derivatives. Under standard material conditions, these substances react with ozone earlier than polymer chains, and, importantly, anti-ozonates prevent the formation of cracks on the rubber surface, especially under conditions of stretching and active use. Special paraffin waxes can also be highlighted, which can migrate to the rubber surface and create a physical barrier that prevents ozone from penetrating the polymer matrix. This is particularly effective in protecting rubber in the absence of mechanical stress.

It is also worth mentioning such basic methods of increasing the performance of rubber material as vulcanization. During the vulcanization process, polymer chains are linked together by "sulfide bridges," which create a three-dimensional mesh that increases resistance to thermal, chemical, and mechanical stresses. It also improves the rubber's resistance to oxidation and cracking. The reaction (using the example of intermolecular polymer bonding of individual units of NR—cis-1,4-polyisoprene) can be summarized as follows:

$$n(-CH_2 - C(CH_3) = CH - CH_2-) + nS \xrightarrow{acc,t,^\circ C} n[-CH_2 - CH(CH_3) - S_x - CH(CH_3) - CH_2-] \quad (6)$$

Any elastomer molecule (natural or synthetic) contains double carbon–carbon bonds (—C═C—) which react with sulfur. When heated—the process usually takes place at 140–180°Csulfur reacts with the rubber to form new chemical bonds with sulfur between the different molecules of the polymer. In the absolute majority, in the place of carbon atoms, there were double bonds (after their rupture). The types of new bonds formed in the macromolecules of the copolymer depend on the vulcanization conditions and are divided into mono, di or polysulfide bridges (– S – , – S – S – , – S – S – S – S – , etc.). Vulcanized rubber has a branched mesh structure, as a result of which, compared with nonvulcanized rubber, it has lower elasticity but a higher strength. As the sulfur content increases, the hardness of the resulting material increases. Depending on the sulfur content in vulcanized rubber, soft rubbers (5%–10% sulfur) and hard rubbers (more than 30% sulfur) are distinguished. Graphically, in a two-dimensional formula structure, this reaction can be represented as Figure 6.

What is more to specify is the fact that this process always uses additional additives (Table 3) such as mercaptans, thiurams, and guanidine that accelerate and stimulate the vulcanization reaction. Moreover, at this stage of rubber material production, all other functional additives (antioxidants, antiozonates, and stabilizers) are also added to the composition of the melt under discussion - the condensed phase [89].

Vulcanization has a direct impact on rubber's long-term oxidative stability since the structure of the subsequent mesh influences the material's resistance to oxygen and high temperatures. Long polysulfide bridges are particularly weak and quickly oxidized; they degrade into shorter segments, sulfoxides, and sulfones. In addition to the chemical nature of the bonds, the density of the mesh is important: the higher the degree of crosslinking, the lower the mobility of the chains and the rate of oxygen penetration into the volume of the material, slowing the material's aging process. In practice, this means that NR with typical sulfur vulcanization ages quickly and must be treated with antioxidants [90]. Thus, vulcanization increases rubber's strength and elasticity at the same time, but long-term oxidative stability is limited by the chemical nature of crosslinking: long sulfur polysulfide bridges are a weak point, so a competent manufacturing step (with the formation of mono- or disulfide bridges) is the basis for high stability.

It is important to clarify that Sulfur is embedded into the rubber compound through certain additives such as TESPT and TESPD. In addition to sulfur atoms, these additives also contain silicon atoms, which form new bonds with polymer chains

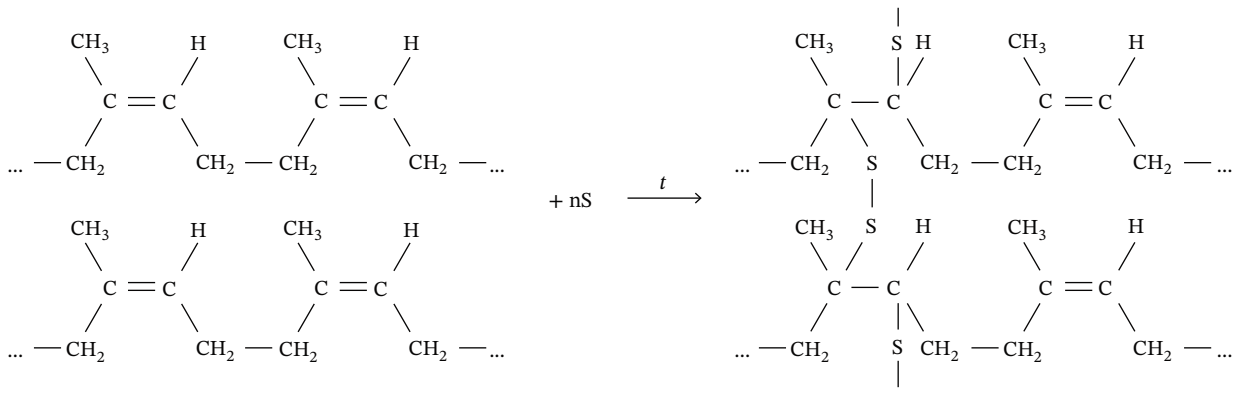

FIGURE 6 | Graphical representation of the vulcanization reaction through structural formulas of natural rubber (cis-1,4-polyisoprene) and sulfur.

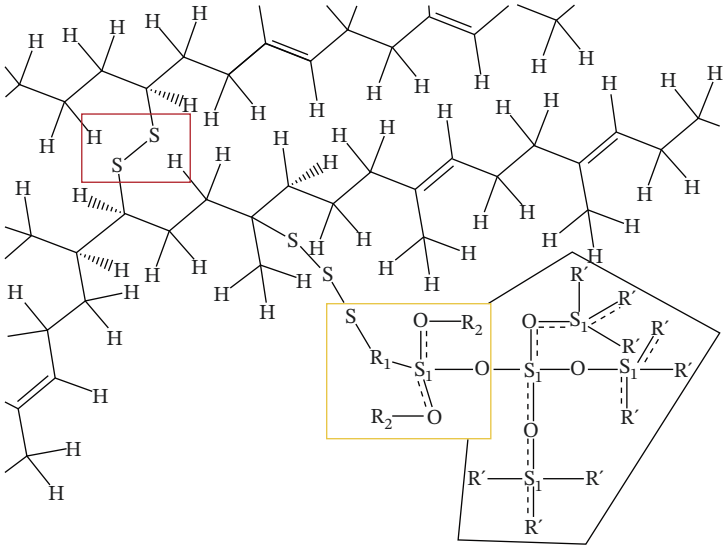

FIGURE 7 | Part of the structural two-dimensional formula of crosslinked polymer chain links with a disulfide bridge and a silane-silica radical. It was created in professional software—ChemDraw based on a general understanding of the molecular structure and literature [91]. R′ – Silica chains (O – Si – O); R_1, R_2 – Alkyl sites.

(polymer–silane–silica) in the rubber material. These silicon additives are known to serve as a reinforcing filler, enhancing the quality properties of the product [91]. The combined chemical formula of this polymer link, after a chain of reactions, can be represented as Polymer – S_n – CH_2 – CH_2 – CH_2 – Si – O – Si – Silica surface.

The molecular structure of these rubber elastomers, which are crosslinked together by using sulfur bridges (in this case, NR and BR), as well as the visual structure of the bonds for silica reinforcement (through silane), is illustrated in Figure 7. The red rectangle shows the disulfide bridge between NR and BR, and the yellow rectangle shows the silane link connecting to the surface of silica particles (gray frame).

Moreover, biologically pure additives derived from waste can also be utilized as components that can increase the properties or protect the rubber material. These supplements can also replace existing functional additives that are toxic and/or costly as well. In the investigation, a wood–polymer nanocomposite was created by extrusion using a polyethylene matrix and a 50% by weight wood flour filler. It was verified using TEM images that cellulose microfiber separation and filler interaction take place. The TGA technique was used to determine the final processed and untreated composites based on the residual mass and beginning temperature. Due to the creation of crosslinks following UV irradiation, all WPCs (wooden–plastic composite) have grown more heat-resistant following exposure to accelerated ambient conditions. The mechanical characteristics of the material functionalized using carbon nanotube (CNT) have significantly improved, according to the DMA results. Composites that are exposed to UV light experience photodegradation, which decreases their modulus of elasticity while they are being stored. Since the functionalized CNT formed hydrogen bonds and reduced mobility between polyethylene and fiber, a composite including WPCs-CNT exhibited the greatest modulus of elasticity and higher transient shift both before and after exposure to the environment. In order to obtain value-added WPC, the researchers propose that the processed fiber be utilized as "solid waste" for filling PE [92].

All these numerous processes, which proceed sequentially and in parallel at a wide temperature and pressure gradient, occur continuously in the volume of the rubber composition. The kinetic component (time dependence) and the thermodynamic component (external conditions and influence of additives) have been discussed in a limited number of studies currently and are valuable for understanding and further application in prediction techniques by means of chemical computational modeling, both for the purpose of material quality improvement (performance indicators) and for the environmental impact of processes (ecological indicators). As stated above, the chemical processes lead to changes in the chemical structure, loss of specified mechanical properties (loss of viscoelasticity and mechanical strength, etc.), aging, and degradation of the material due to polymer degradation. This leads to an increase in TWP emissions and loss of functionality of the entire product, with accompanying environmental pollution. Naturally, even at the early stages of material transformation under external environmental conditions and the resulting degradation of the material structure, deterioration of key tire properties can already be observed, including higher rolling resistance, decreasing wet traction, and lower abrasion resistance. These indicators reflect important points that relate to the performance of tires as well as the environmental aspect.

The control and analysis, and consequently the prevention of such occurrences, can also be realized through chemical computational modeling. In particular, when selecting key reagents and their concentration, imposing values of external parameters such as temperature, pressure, and concentration of oxidizing substances (oxygen, ozone, etc.) All this makes it possible to predict and anticipate the course of chemical steps and the final result depending on the time range. This will facilitate the selection of antioxidants and, at the same time, make it possible to understand which substances will be exposed to the environment as pollutants during operation under real conditions.

Evidently, one of the important stages in creating a modeling methodology is to conduct real-world tests to validate the model and correlate it with real conditions and expand the scope of application, including qualitative and quantitative pollution analysis. This is a laborious process that involves many stages of real chemical analysis using precision equipment and various technologies. When identifying the dependencies between the real results of the analysis and multiscale modeling (from quantum mechanical analysis to coarse-grained analysis), conclusions can be drawn on the effect of the composition of the elastomer mixture (rubber) on its tendency to wear and performance characteristics, according to the laws of viscoelasticity.

3 | Part II—Analytical Methods for TWPs

3.1 | Identification in the Environment and Analytical Methods for TWPs

In order to holistically understand the environmental impact and operational perspective over a specific time period, it is important to understand the original composition of tires in terms of their chemical content. Of course, this is difficult as manufacturers are not interested in disclosing their formulations, making it complicated to further identify contaminants caused by TWPs emissions (not to mention that chemical transformations of the original substances may occur during operation). Nevertheless, there is a number of methods to analytically determine the composition of TWPs by leaching collected particle fractions and agglomerates (e.g., from roadside verges, stormwater runoff, soil, and water bodies near roads). The samples were then analyzed by mass spectrometry of various types, depending on the chemical markers to be searched for and investigated.

Monitoring TWPs in samples from various environmental compartments is problematic due to limited analytical techniques. TWPs analysis methods can be divided into qualitative or quantitative, depending on the desired information. The purpose of a technique determines the issues that must be addressed during optimization. Choosing an appropriate sample approach is essential for every method, irrespective of its purpose. The first stage of the experiment involves obtaining a representative sample and determining the best pretreatment method for subsequent instrumental analysis stages.

Qualitative techniques evaluate the presence of tire-derived chemicals or particulate matter in a sample. Typically, markers with high specificity and stability are chosen based on reference material analysis [93]. There are two types of quantitative approaches for analyzing TWPs: providing the chemical number of particles (number-based quantitation) [94] and those that provide the masses of tire components (mass-based quantitation). Besides, it is possible to note two types of mass-based quantitation methods: those that measure individual components of TWPs [95] and those that calculate their total mass [23]. Quantitative analysis involves measuring the mass or concentration of analytes, which can also serve as markers in qualitative analysis. Analytical procedures in this area of investigation are often quail-quantitative, with both detection and quantification as targets.

Quantitation presents challenges in obtaining the needed information. High sensitivity is required for mass-based methodologies used to measure certain tire-related chemicals. Correlating the analytical method's response to the amount of the analyte in the sample is a challenging task. To accurately quantify the total mass of TWPs in a sample, a reliable response-content relation is also crucial. Analytical difficulties can be characterized by their origin. This evaluation distinguishes between two types of challenges: those related to sample complexity and those related to the approach used. It is difficult to make a clear difference between the two groups since some of the issues can be attributable to a mix of both causes, and the analytical method used is always determined by the sample's characteristics. However, categorizing the obstacles allows for a more linear exposition of the complicated components of TWPs analysis.

3.2 | Existing Collection Strategies in Environment

In this field of investigation, sample collection is critical because of the very inhomogeneous distribution of TWPs, even in small areas. To account for heterogeneity, sampling procedures often compare TWPs accumulation across locations with considerable differences. Choosing the right sampling approach is crucial for research on the distribution and movement of TWPs between environments. Comparing TWPs accumulation outcomes across matrices depends on sampling effectiveness.

There are a number of basic and several specific methods for collecting samples, which vary depending on the environmental conditions and the geographical location of the testing and analysis sites. In the classic case, without the use of special technical means, a sterile brush (moistened), a metal spatula, or a vacuum cleaner-type dust collector is used to collect samples from road dust [8, 13]. In turn, for the study and collection of particles that have fallen into the soil, it is recommended to use metal or polymer (low adhesion) spatulas, trowels, or more specialized tools, such as stainless steel folding shovels and core sampling tools [96, 97]. The use of such techniques is regulated in accordance with ISO/TS 21396:2017.

As for airborne particles, various techniques can be used, such as continuous collection of gas (air) volume from the surrounding atmosphere using a quartz, Teflon, or polycarbonate filter regulated by ISO/TS 20593:2017 [84]. The mass of captured particles is measured by simply comparing the masses (by weighing the filters) before and after the sampling. There are alternative sampling methods, such as a passive sampling system for collecting fine particles along motorways, implemented in Germany [45]. In particular, a special device was developed that splits the flows to reduce turbulence and minimizes the influence of UV radiation, wind, precipitation, and other contaminants. This sampling technique allows particles to be captured on a transparent adhesive surface and then immediately analyzed by external optical inspection and/or X-ray examination of individual particles (primarily the coarse fraction larger than 1 mm). This and similar studies confirm that most of the polluting particles found in the immediate vicinity of roads are particles of tire wear and vehicle brake systems. In addition, it is possible to conduct research using test vehicles equipped with devices that collect particles directly from their tires while in motion (through a tube installed close to the tire) [98].

With regard to the aquatic environment, there is currently no specific regulated standard or generally accepted methodology or technique for collecting TWPs. Various research groups use

a variety of techniques to collect samples from the sea, river surfaces, or, most commonly, from street drains where rainwater from roads flows. Scooping shovels (similar to those used to collect organic pollutants such as hydrocarbons) are used to collect samples from water surfaces, while collectors or manual collection are used for wastewater, and the proportion of the sample volume is then calculated relative to the flow rate (liquid volume consumption per unit of time). One study found that such methods can only collect particles with a density of <1.18 g/cm^3 that remain on the water surface. The remaining (presumably large) part settles at the bottom, where it spreads through the aquatic environment by underwater currents and similar phenomena. In such studies, inorganic and organic fractions of materials are usually analyzed using ICP and TED–GC–MS [95, 99].

3.3 | Leaching

Leaching experiments are frequently carried out as part of tire rubber ecotoxicity testing. Leached zinc and organic substances such as benzothiazoles, antioxidants, PAHs, or phthalates have mostly been linked to ecotoxic consequences [100, 101]. It was only recently shown that tire rubber leachates in urban freshwaters cause occur fish death. According to Tian et al. [24], the impact was associated with 6-PPD-quinone, an oxidation product of 6-PPD. This example indicates that tire constituents as well as their transformation products can be ecotoxicologically relevant. The reverse leaching process is the sorption process of organic molecules on the surface and is another mechanism that might influence the surface characteristics of TWPs and, consequently, their destiny. It might affect TWPs' hydrophobicity and charge of the surface, which would modify how they aggregate [102]. Dissolved organic carbon (DOC) concentrations in road runoff, which is where TWPs are usually found, are in the mg/L range. It is expected that hydrophobic DOC fractions will bind to the TWPs surface in particular. Leaching is predicted to assist in the elimination of antioxidants from tire rubber, which will lead to increased tire rubber chemical and biological deterioration [87]. More thought should be given to the interdependence of leaching and microbial degradation of TWPs (as it was discussed previously).

Other aging processes can also have an impact on leaching. The leaching potential of TWPs is also impacted by any procedure that modifies their chemical composition. Additionally, because of variations in certain particle surfaces, the leaching kinetics will be impacted by changes in the physical state of TWPs. It is well known that photo- and thermooxidation, as well as ozonation, can lower antioxidant concentrations such as 6-PDD and create different derivative compounds that may leak from TWPs [24] (Section 2.6). Because of their enhanced hydrophilicity, the newly produced compounds can have distinct leaching kinetics. When 6-PPD is ozonated, for instance, 6-PPD-quinone is produced, which is more soluble than its "ancestor" molecule, which also will be discussed below. The particle size is reduced by fragmentation. An improved leaching will occur when the particle size decreases. Some investigations [100] corroborate this theory, whereas other studies [103] showed no connection between leaching and particle size.

3.3.1 | The Process of Sample Preparation

As is widely known, sample pretreatment for micropollutants aims to concentrate and separate particles from the environment, minimizing interference and matrix effects caused by both organic matter and inorganic components. Pretreatments vary widely depending on the kind of environmental matrices (air, soil and sediments, dust road, and water), the analysis goal, and the analytical methodologies. Minimal matrix removal is often required for elemental analysis by scanning electron microscopy with Energy Dispersive X-ray spectroscopy (SEM–EDX), while acid digestion is used for elemental analysis by inductively coupled plasma with optical or mass spectrometry detection [39, 104].

The polymeric matrix (elastomers) is often analyzed via solvent extraction or solid-phase purification. It is demonstrated in Table 4, where extraction strategies are provided for recovering molecular markers in TWPs from different environmental matrices. On the other hand, polymer analysis using techniques such as analytical pyrolysis linked to gas chromatography–mass spectrometry (Py–GC–MS) can be followed by sediment extraction and digestion of interfering biogenic components [106]. The next section contains a more in-depth review of molecular and polymeric TWPs indicators. Airborne particles collected using active or passive air filtration do not require sample modification since optical microscopy and SEM–EDX analysis may be performed promptly after these sampling procedures and calibration. A group of researchers analyzed individual particles on the filter surface using SEM–EDX to recognize the difference between exhaust and abrasion particles based on shape and chemical content [108]. Another team examined coarse particles in the air around heavily used roads and motorways [45].

Density separation of soil and sediment samples using NaCl [97, 109], NaI [110], or polytungstate salts [9] removes the inorganic matrix and yields an organic fraction rich in analytes. They mixed the material with 4 L of saltwater and 800 g of NaCl. After stirring and sedimentation, the supernatant was sieved through stainless-steel sieves and treated with 30% H_2O_2 to eliminate biogenic organic remains (debris) before morphological and spectroscopic examination. The authors used biogenic digestion to make sea surface microlayer materials [3, 96]. Heavy metals including Zn, Cr, and Pb as well as organics like PAHs, 1,3-diphenylguanidine (DPG), and benzothiazole derivatives have all been studied in leaching from TPs exposed to water [83, 99].

For various types of microplastic as general and, in particular, tire rubber, it's important to analyze sample pretreatments for their capacity to avoid interferences and provide consistent analyte recovery. Experiments can test this capacity by comparing in-matrix calibration with external calibration. However, such comparisons are not currently accessible for TWPs analysis. To evaluate the repeatability and efficacy of sample purification procedures, genuine matrices can be spiked with standard or reference TWPs or to be observed regarding the checking of the data base in an open source. Quality control methods are expected to be included in future quantitative research studies.

3.4 | Analytical Methods and Markers

Current TWPs quantification approaches, including mass spectrometry, as it widely spread, use chemical markers as analytes.

TABLE 4 | The key components of the rubber–elastomers with analytical information for identification in the TWPs mixture.

Name/Abb (CAS) and structure	Polymeric marker (structure)	Analytical method	m/z signals	Ref.
Styrene–butadiene rubber/SBR (9003-55-8) 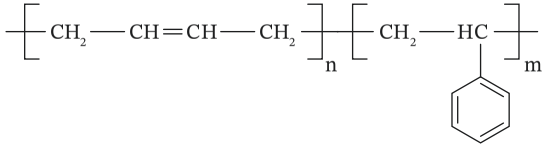 $C_{12}H_{14}$	Cyclohex-3-enylbenzene 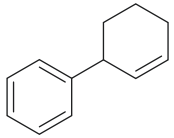	Py–GC–MS	158, 104, 91	[93, 105]
Butadiene rubber/BR (9003-17-2) 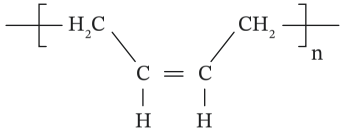 C_4H_6	Vinylcyclohexene 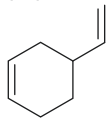	Py–GC–MS	108, 54, 79	[23, 54, 106, 107]
Natural rubber/NR (9003-31-0) 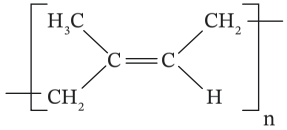 C_5H_8	Dipentene 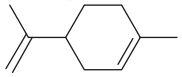	Py–GC–MS	136, 68	[96]

The optimum analytical marker for quantifying TWPs should have specificity, stability against degradation and leaching, be present in all tires independent of the model or brand, and have an acceptable analytical response. Markers are often picked from the tire fraction, while the other fractions are formed via the particle's interaction with the environment during production. Analytical markers used in the literature and modern investigations can be classified as elemental, molecular, or polymeric [19].

3.4.1 | Analysis by Using Elemental Markers

These markers are individual inorganic elements that are used in the production of rubber material for the tires of vehicles. Of course, it is difficult to identify and separate chemical elements that may also be present in the environment or road infrastructure. Research groups are implementing various approaches to address these complexities, and this is discussed below.

Due to the presence of various amounts of CB in the composition (used to increase the strength and durability of rubber), there are limitations to the use of optical and vibrational spectroscopy; therefore, elemental markers in tires are usually determined using classical methods such as SEM–EDX and mass inductively coupled plasma spectrometry (ICP–MS). Undoubtedly, the diverse composition also affects the subsequent analytical detection of molecular and polymeric organic markers. After analyzing the composition of tires and a number of relevant literatures, as well as the works of other scientific groups, it can be concluded that the most common elemental marker of TWPs is zinc, which is used as a vulcanizing agent. It is also important to pay attention to sulfur, which forms the "sulfide bridges" during the reduction of polymer-sulfur compounds and is also used during vulcanization (as described above) [46]. Elementary markers are often more resistant to decomposition than molecular markers, but they are nonspecific because they can come from various sources [48, 111].

On the other hand, there are modern methods that use a chemometric approach to distinguish TWPs from other environmental particles. In particular, the scientists have trained an algorithm that is able to recognize more than 100,000 particles using machine learning (neural networks), SEM/EDX data, and morphological parameters. After that, a check was carried out using a three-fold cross-analysis, with the result that the average forecast accuracy is 98%. This approach made it possible to accurately identify six types of particles, including TWP, metallic particles, and organic particles.

This approach involves doing a qualitative multielement assessment, followed by multivariate data analysis of elemental profiles, to identify particle sources. Adachi and Tainosho [112] analyzed road dust samples using FESEM/EDX single-particle analysis to identify 24 inorganic elements (Mg, Al, Si, P, S, K, Ca, Ti, V, Cr, Mn, Fe, Ni, Cu, Zn, Sr, Y, Zr, Sn, Sb, Ba, La, Ce, and Pb), whose concentration in the samples exceeded the Maximum Permissible Concentration (MPC) standards. For example, the following research ranges are given in the TWPs and road particles literature for roadside soils: $Zn \approx 66–450\ mg{\cdot}kg^{-1}$, $Cu \approx 40–180\ mg{\cdot}kg^{-1}$, $Pb \approx 24–110\ mg{\cdot}kg^{-1}$, and $Cd \approx 0.7–2.5\ mg{\cdot}kg^{-1}$. For the aqueous phase, typical concentrations are more often in the range of $Zn \approx 70–500\ \mu g{\cdot}L^{-1}$, $Cu \approx 8–270\ \mu g{\cdot}L^{-1}$, $Pb \approx 20–100\ \mu g{\cdot}L^{-1}$, and $Cd <\approx 14\ \mu g{\cdot}L^{-1}$; the values strongly depend on the technique (total versus soluble fraction), local sources, and hydrological regime [20, 31]. Apart from that, the scientists used cluster analysis to categorize particles based on their elemental makeup and origin, including tire wear, vehicle brakes, and road paint [94].

In another article, it was found that a group of researchers had successfully obtained new environmentally friendly polymer nanocomposites based on a silicone rubber matrix filled with spent fibers and chromium oxide nanoparticles. At an optimized concentration, which is based on 1 wt.% hybrid filler, it is possible to achieve the highest modulus of elasticity, dielectric constant, and hydrophobicity compared to pure silicone rubber and other composites. The morphology is smooth and clear. The phases of fillers and matrixes even after weathering were without gaps or etching, reflecting improved properties. The recommended nanocomposite improves the physical, surface, and mechanical properties of silicone rubber by wetting the matrix with all distributed fillers, resulting in a homogeneous, stable final composite. Such a nanocomposite can be recommended for lamination and indoor applications [113].

Another research group conducted an experimental study to prove a strategy for eliminating other sources of Zn from the environment. Preprocessing of samples is an important prepreparation procedure. This is aimed at increasing the selectivity of inorganic markers (primarily zinc), which makes them suitable for quantitative purposes. In the study under discussion, it was suggested that separation due to density difference (before ICP–MS analysis) may help separate zinc from heavier inorganic road dust, which is not caused by tire wear. For such separation, a sodium polydentate solution was used, into which certain amounts of road dust were introduced. As a result, heavy, insoluble Zn particles such as ZnO precipitate, while soluble Zn particles such as sulfide, chloride, and sulfate of zinc dissociate in solution. Tire particles with lower density were separated by flotation or coagulation and analyzed for zinc content. The average zinc content is about 8.7%, and an average tire material content of 50% was used for quantitative determination. The sensitivity of the quantitative method is likely to be limited by the background Zn signal in the sample matrix rather than the instrumental sensitivity (0.002 mg/g). The authors then performed three quantitative TWPs analysis methods with different particle size and type distributions. The experimental analysis included the determination of Zn by chemical decomposition followed by the use of ICP–MS; determination of additives (DPG, 6-PPD, and six different benzothiazoles) by extraction with an organic solvent followed by LC–MS; and determination of the polymer fraction by TED–GC–MS. This study proved that elementary, as well as molecular and polymer markers (which will be discussed below), can be used for complex quantitative and qualitative determination of TWPs with proper sample preparation and appropriate analytical strategies [84, 95].

3.4.2 | Analysis by Using Molecular Markers

Among other things, TWPs in environmental samples can also be identified using molecular markers and usually correspond to organic chemical compounds that are used as additives in tires. It is obvious that molecular markers are more specific than elementary ones, due to the structure of organic molecules; they can

also be more sensitive to degradation, dissolution, and leaching. Table 3 provides a list of chemicals commonly used as molecular markers in laboratory and experimental analyses. The presence and quantity of various compounds in tires vary depending on the formulation,the manufacturing process, and the application area of the product, which makes their use as quantitative indicators and analytical responses ambiguous Perhaps it makes sense to regulate a unique and unitary additive for all manufacturers, which will serve as a marker for identifying and detecting TWPs in nature. Indeed, the additive should have low toxicity and resistance, ideally add positive physical properties to the material, and be inexpensive.

Benzothiazoles are low-molecular-weight chemicals that act as vulcanization accelerators in tire manufacturing. The most popular benzothiazole accelerators are 2-(4-morpholinylthio)benzothiazole (MBS) and N-cyclohexyl-2-benzothiazolsulfenamide (CBS) and N-(1,3-benzothiazol-2-ilsulfanyl)cyclohexanamine, which can be determined by HPLC or HCH after Soxhlet extraction or traditional solvent extraction [85, 114].

One can immediately conclude that benzothiazole accelerators are not suitable TWPs indicators due to their high consumption and transformation during vulcanization. Commercially available MBS and CBS may contain impurities such as 2-(4-morpholinyl) benzothiazole (24MoBT), which may be formed as by-products during vulcanization. A number of studies have conducted analytical surveys on road dust, soil, and surface water near heavily used roads. For this, GC and LC methods were used after extraction with toluene, methanol, and dichloromethane. Although 24MoBT and CBS have acceptable analytical characteristics due to their individuality, their use as quantitative markers is limited due to their low environmental resistance (decomposition due to oxidation by air and UV radiation) and the presence of 24MoBT in the antifreeze for automotive radiators. The amount of 24MoBT and CBS in TWPs varies depending on the type and concentration of accelerators used in tire production as well as vulcanization parameters [86, 115]. According to one of the scientific groups conducting research in this field, the use of Benzothiazoles for tires as quantitative markers of TWPs requires an assessment of the influence of external factors (atmospheric exposure, ultra violet, and liquid leaching), as well as an assessment of the quantity and quality of active and extractable additives and by-products in tire formulations (which may react when the imposition of external conditions both with other components of the rubber material and with substances from the outside) [22]. For example, the results of extraction of samples after leaching revealed a chemical interaction between the analyzed substances and the organic (polymer) part of the matrix, which added uncertainty to the formulation of the research strategy.

Another scientific group proposed the use of the analytical technique Py–GC–MS for the selective quantitative determination of target molecules of benzothiazole (and its close derivatives) crosslinked with sulfur (sulfur bridge) in an elastomeric rubber tire material. This method uses benzothiazole as a unitary single marker in the pyrolysis process for all possible benzothiazole accelerators, overcoming the limitations caused by the leaching and dissolution of TWPs molecular markers. Pyrolysis is known to initiate the breaking of N—S and C—S bonds in rubber-bound benzothiazole compounds, which cannot be identified by solvent extraction. However, there is a lack of information on how related benzothiazole derivatives affect the signal and quantitative estimation [116, 117].

In addition to the discussed vulcanization acceleration additive, alternative molecular markers for liquid chromatography after solvent extraction also exist, including the vulcanizing agent 1,3-DPG and the antioxidant N-(1,3-dimethylbutyl)-N0-phenyl-p-phenylenediamine (6-PPD) [84]. 6-PPD is less susceptible to leaching and dissolution than MBS and CBS due to its low hydrophilicity [41]. However, it is prone to the formation of a derivative form,6PPD-quinone, which is less stable than the initial form and also has high leachability due to reduced hydrophobicity [24]. One of the scientific groups analyzed the distribution and concentration of 6-PPD and isothiazoles in TWPs from tunnel dust samples using MeOH extraction and UHPLC–MS/MS spectroscopy. It was found that 6-PPD compounds are more resistant after vulcanization, as well as probably to external influences during operation, than MBS and CBS, which leads to a clearer analysis and experimental results [95, 118].

In addition to the mentioned techniques, it is worth noting the approach using a substance that is used as an emulsifier in tire rubber compositions (in concentrations of about 0.5%). We are talking about a group of hydrogenated resin acids (8-isopimarene-18-oic acid, 8-pimarene-18-oic acid, 13b(H)-abietene-18-oic acid, and 13a(H)-abiet-8-ene-18-oic acid) as another promising molecular marker for quantitative measurement of tire wear in collected road dust samples. The authors propose to qualitatively and quantitatively evaluate TWPs in the samples using known concentrations of tar acid in tire tread rubber compounds provided by manufacturers. It is assumed that rubber materials lose the concentration of target resin acids overtime due to evaporation, leaching, and photochemical reactions. This was seen in tire samples after 24 h of artificial aging [119].

A similar approach was proposed by another scientific group, which uses oleamide as a marker for the quantitative determination of TWPs in road dust by the GC–FID method [55]. This compound is used in the manufacture of tires to enhance their performance and abrasion resistance. Organic extraction from samples of tire particles from the environment was, as usual, isolated and evaluated using the GC–MS method. The choice of Oleamide as a marker was made for reasons of its sufficient concentration and clear identification on chromatograms. The total TWPs in organic concentrates were calculated using GC–FID based on the oleamide content in the collected samples of car and bus TWPs (up to 2% by weight of organic additives) [119].

3.4.3 | Analysis by Using Polymer Markers

Modern research in this field has focused on measuring and analyzing TWPs using polymer markers—elastomer monomer units (Table 4). These indicators can be quite individual in relation to substances in the environment and more stable and reliable than elementary or molecular markers. Py–GC–MS [96, 105, 106, 120] and TD–GC/MS are commonly used to detect elastomers in environmental samples [93].

The characteristics determining the analytical features of rubber samples are focused on the nature of monomers and dimmers, which are the main decomposition products under experimental and real conditions. These include isoprene and dipentene (DP)

for NR, 1,3-butadiene and vinylcyclohexene (VCH) for 1,3-butadiene, and styrene and VCH for SBR. Detection limits in the mg/g range are determined by the Py-GC-MS or -GC/MS methods and their analytical and calibration limits [93]. Pyrolysis products of monomers can also be found in other anthropogenic and natural organic compounds, making them unsuitable as particular markers [121]. Styrene can be produced by the pyrolysis of diesel exhaust particulate matter. Dimers are being used as pyrolysis markers for the tire rubber. Quantifying BR and SBR separately might be hard due to their shared pyrolysis products (Table 4). Dimeric markers were shown to be more selective for rubber polymers than monomers, leading to their adoption in two ISO technical requirements [122, 123].

In addition to the analytical methods listed in Table 5, there are other methods—FTIR/Raman, TD–GC/MS, and GC–FID—used in the field of identification of the composition and quantity of chemical compounds from samples of TWPs. It is possible to identify methods that have a similar physical meaning (relative to gas chromatography) but differ due to the initial stages, in particular, heating samples to a certain temperature.

Regarding analytical and laboratory methods for studying the content of any desired substances, it can be concluded that it is necessary to use a number of different methods for a reasonable analysis of samples. It will allow us to get a complete understanding regarding the forms, composition, and concentrations. It should be noted that preliminary studies using multiscale modeling can provide a forecast regarding the composition of rubber particles, including studies of the diffusion and dispersion of solid substances in the condensed phase of the material.

In addition to these different types of markers, it is possible to identify a number of other compounds that are formed as reaction products of starting reagents used in production cycles and subsequent environmental transformations. Knowledge of the initial substances, especially the most toxic ones, may represent a compromise between the commercial, scientific, and social sectors. The ability to apply chemical multiscale modeling techniques can help to anticipate and predict the reaction products formed during the operation of a material, and the superimposition of external thermodynamic parameters can extend the range of possible variations in the products of chemical transformations under extreme conditions. Under some assumptions, it is possible to find a proportional ratio (under initial conditions) of the composition's masses in rubber and some specific additives and, knowing the degree of distribution of the additive in the volume of the phase, determine the amount of emission of this additive relative to the found weight of TWPs (rubber particles).

Clearly, after the analytical part, through which a number of values and quantities can be obtained relating to the mass and concentration of the substances sought in analytes—collected substances from the environment—it is also important to correctly calculate, find correlations, and convert the data obtained to specific, comparable data and/or existing evaluation standards.

3.5 | Quantitative (Mathematical) Analytical Technique

There are currently no specific established methods or techniques for determining the concentrations and composition of

TABLE 5 | Comparison of analytical techniques and a brief description of their features.

Analytical technique	Measurement objects	Technical specifications	Detection limits	Advantages	Limitations
SEM–EDX	Morphology and particle size, elemental composition (Zn, Si, Fe, etc.), inorganic compounds	Resolution up to 1–5 nm; elemental analysis at 0.1–30 keV energy; element distribution mapping; suitable for particles from ~0.1 μm and above	LOD: ~0.1–1 wt.% for most items; only elements with atomic number $Z > 5$, so not identify organic	High spatial resolution, the only method to understand the form of particles	Limited for organic compounds; requires vacuum and conductive coating; expensive instrumentation
Py–GC–MS	Organic polymer matrix NR/SBR/BR and additives	Pyrolysis temperature: 500–700°C (gas—He or N_2); mass spectra with a mass range of m/z 15–600; sample required 10–100 μg.	ppm-s levels; not for inorganic components; destructive method	The type of rubber and additives can be distinguished;	Destructive method; complex spectra interpretation; relatively high operating costs
ICP–MS	Quantitative analysis of elements (Zn, Al, Fe, etc.)	Dissolution in HNO_3/HF/HCl; ionization in plasma Ar ~6000–8000 K (>90%); 0.1–1 mL solution required.	ppb–ppt levels; not for organic components; destructive method	Very high sensitivity	Requires acid digestion and hazardous reagents, no morphology information; expensive instrumentation

TWPs in advance, and the majority of current approaches rely on the size distribution of wear particles and mathematical concepts of emission rather than the chemical aspect (composition, nature of substances, and their environmental impact). On the one hand, this is reasonable because these assessments are time-consuming, the technique is hard to replicate and standardize, the initial chemical composition of vehicle tires is unpredictable, and there are external, thermodynamic factors. However, given its significant, if not crucial, impact on the system (rubbers–elastomer combinations with additives), it is clear that the chemical component cannot be disregarded.

In the context of this review, it is important to consider more thoroughly the scientific survey of Rødland et al. [23], where the concept of determining the concentration of both TWPs and road surface wear (containing similar polymers from tire composition —polymer-modified bitumen (PMB), which are obtained by incorporating recycled rubber agglomerates into bitumen) is discussed. However, it is possible to analyze TWPs exclusively, thanks to a number of equations and specific parameters used. For these purposes, the value of the tire emission factor (EF) is entered [124]. EFs are representative values that link the quantity of a pollutant to the road activity that causes its emission. Previous studies, for example, have calculated the mass of tire particles (mg) per kilometer driven by a personal car (km) by measuring the tire loss in mass from driving in various settings, such as highway and urban driving. The author's suggested emission parameters were applied to calculate tire wear. The EF for highway driving is 0.104 g/km for personal vehicles (PV) and 0.668 g/km for large vehicles. Urban driving has higher EFs of 0.132 g/km for PV and 0.850 g/km for heavy vehicles (HV). With this information, it is possible to estimate the mass of tire particles produced over a given time at any site by means of Equation (7), which is based on road-specific tread emission. These estimations are used to determine the expected mass of the tire, which then gives the expected ratio between SBR + BR and SBS in a sample.

$$\mathrm{EM}_T = \left(L_r \cdot N_{\{v,r,t\}} \cdot \left(\left(R_{\{\mathrm{PV}\}} \cdot \mathrm{EFT}_{\{\mathrm{PV}\}}\right) + \left(R_{\{\mathrm{HV}\}} \cdot \mathrm{EFT}_{\{\mathrm{HV}\}}\right)\right)\right), \tag{7}$$

where EM_T is estimated mass of tire in a sample (mg); L_r is the length of the particular road stretch r (km); $N_{\{v,r,t\}}$ is the number of vehicles that have traveled the particular road stretch r during the given time period t; $EFT_{\{PV\}}$ is the EF for personal vehicle tires (mg/km); $EFT_{\{HV\}}$ is the EF for heavy vehicle tires (mg/km); $R_{\{PV\}}$ is the ratio of personal vehicles at the sampling location; and $R_{\{HV\}}$ is the ratio of heavy vehicles at the sampling location.

There is also one certain value—the variable *Sc* is utilized when the styrene concentration of calibration curve standards differs from the predicted styrene content in tires. The styrene content distinguishes between different types of tires based on the ratio of SBR to BR, as well as the type of SBR used in each tire. SBR has on average 27.4% styrene, and BR has obviously 0% styrene. The average ratio of SBR to BR is 65%–35%, which means that most tires will have a styrene content of 17.8% ($0.274 \times 0.65 = 0.178$) [3].

If a sample is obtained near a location where polymer additives are not added to the asphalt, it is likely that the styrene–butadiene fraction occurs exclusively as a result of tire emissions [18, 125]. Therefore, the four chosen values will provide the entire mass of SBR + BR in the samples. Once traffic data for the site is received, Equation (8) can be used. If no traffic data is available, Equation (9) should be used. This technique calculates S_c based on the styrene content of the SBR1500 and tires alone.

$$M_T = \frac{M_{\{\mathrm{SB}\}} \cdot S_C}{\left(S_{\{\mathrm{PV}\}} \cdot R_{\{\mathrm{PV}\}}\right) + \left(S_{\{\mathrm{HV}\}} \cdot R_{\{\mathrm{HV}\}}\right)}, \tag{8}$$

$$M_T = \frac{M_{\{\mathrm{SB}\}} \cdot S_C}{S_v}, \tag{9}$$

where M_T is the mass of tire in a sample (mg); $M_{\{SB\}}$ is the mass of SBR + BR in a sample (μg); *Sc* conversion factor for styrene content in standards vs real tires; $S_{\{PV\}}$ is the mass of SBR + BR in personal vehicle tires (μg/mg); $R_{\{PV\}}$ is the ratio of personal vehicles at the sampling location $S_{\{HV\}}$ is the mass of SBR + BR in heavy vehicle tires (μg/mg); $R_{\{HV\}}$ is the ratio of heavy vehicles at the sampling location; and *Sv* is the average mass of SBR + BR in vehicle tires (μg/mg).

The information presented in this Part II demonstrates how time-labor-intensive the processes of working with TWPs in a real environment and laboratories are, as well as the complexity of mathematical assessment and forecasting. Research groups are trying to apply their own analytical approaches that will most accurately reflect the qualitative and quantitative content of the substances under study in the samples. For a multifaceted study, a number of scientists have recently begun to use computational modeling methods that allow them to obtain physicochemical values and parameters that can be further analyzed and correlated for real systems through quantum mechanical analysis (e.g., DFT) and MDs. This will be under observing in the next part.

4 | Part III—Predictive Chemical Computational Methods and Multiscale Analysis of Material Properties

4.1 | Multiscale Computational Approaches for Rubber Materials: Motivation, Framework, and Challenges

The previous section shows that both the chemical processes taking place in rubber and the analytical methods used to study them are time-consuming and costly because of their complexity. Environmental aspects, including the impact on ecosystems and aquatic life, have been considered only in a limited way by few researchers. At the same time, the influence of these processes on performance indicators is still not fully understood and requires new approaches and tools. This situation makes the use of chemoinformatics especially attractive as it can help optimize production, guide the choice of components, and provide a clearer picture of how a given material will behave overtime under external conditions. The question of the environmental footprint of rubber and its additives also remains open. Which compounds persist, transform, or accumulate and how strongly they affect the environment are issues that cannot be ignored.

An increasing number of research groups now apply computational multiscale modeling of chemical processes, including reactions and interactions. These approaches integrate quantum

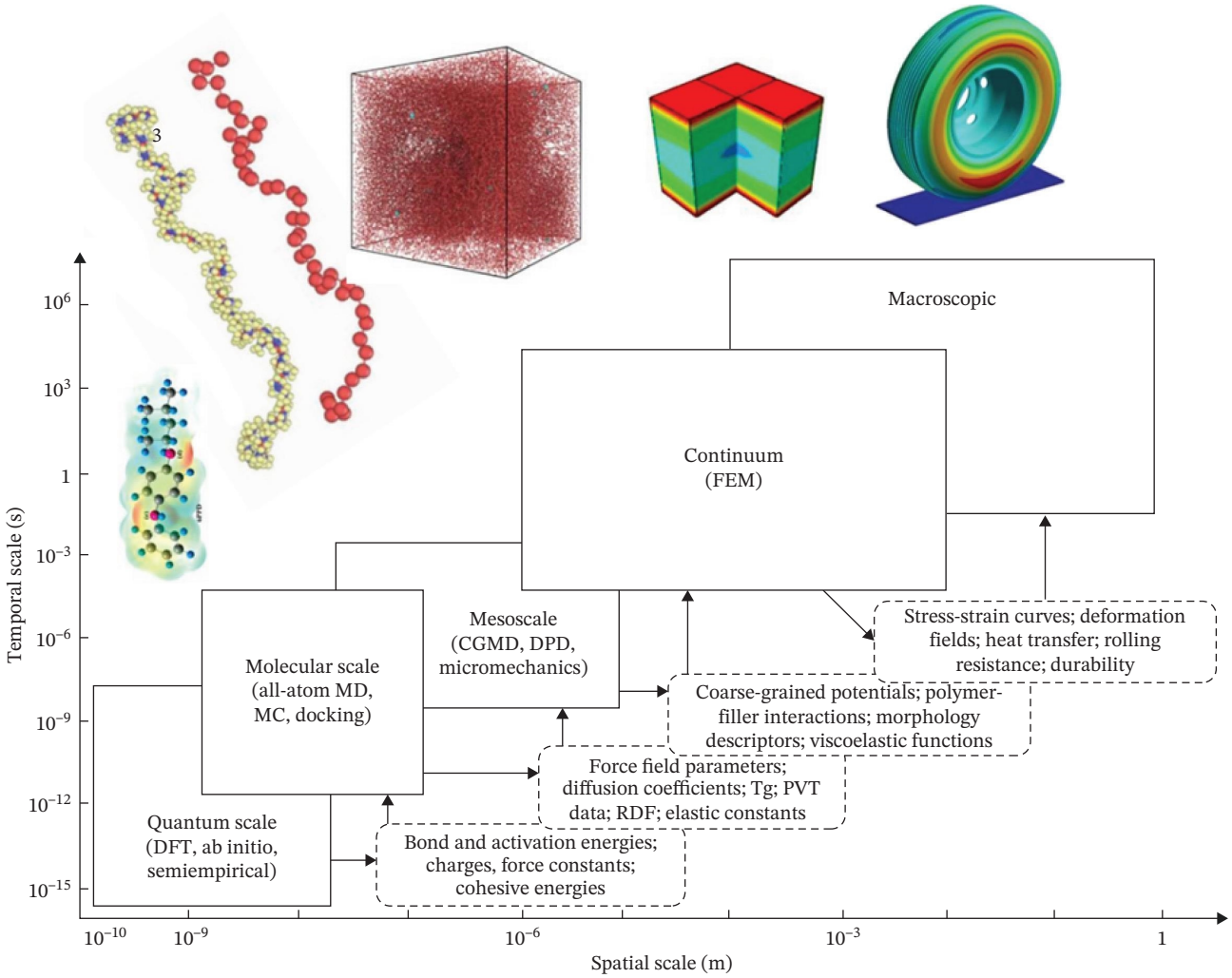

FIGURE 8 | Multiscale modeling workflow linking quantum, molecular, mesoscale, and continuum simulations.

calculations (DFT, ab initio) for reaction energetics, MDs for diffusion and mechanical constants, mesoscale CG simulations for morphology and viscoelasticity, and continuum finite element modeling (FEM) for stress–strain response and durability. The hierarchical transfer of parameters between scales is illustrated in Figure 8. At the same time, results from each level require experimental validation: QM against spectroscopy (IR, UV–Vis, Raman, and XPS), MD against Tg, PVT, diffusion, and tensile tests, mesoscale against DMA and rheology, and FEM against tire macrotests of load, deformation, and durability. This integrated workflow allows computation and experiment to reinforce each other, ensuring predictive power across length and time scales.

Despite this structured hierarchy, multiscale modeling of rubber materials remains technically challenging for several fundamental reasons. Rubber compounds are chemically complex mixtures of polymers, fillers, crosslinkers, plasticizers, and numerous additives, and capturing their interactions consistently across scales is nontrivial. Elastomers exhibit highly flexible, amorphous molecular structures with strong entanglements and strain-induced crystallization, which complicate the development of transferable force fields and coarse-graining schemes. Moreover, the relevant processes span extreme temporal and spatial ranges: electronic rearrangements and bond breaking occur on the femtosecond–nanometer scale, whereas viscoelastic relaxation, filler network dynamics, and macroscopic deformation extend to milliseconds and centimeters. No single modeling technique can cover this range; transferring parameters between DFT, MD, CG, and FEM introduces systematic uncertainties. Filler–polymer and filler–filler interactions are also sensitive to surface chemistry and morphology, which are difficult to represent accurately in simulations. Environmental aging, oxidation, and fatigue involve long-term chemical and structural changes that remain challenging to model explicitly. Together, these factors explain why a fully predictive multiscale framework for rubber materials remains an open scientific problem.

Each modeling level therefore operates within characteristic spatial and temporal regimes and passes information to the next stage. At the quantum level, DFT provides the most accurate data on electronic structure, energy barriers, binding energies, and optimized geometries; however, the computational cost restricts these calculations to relatively small systems. These results feed into atomistic MD, where external force fields allow simulation of thermodynamic parameters, structural metrics such as RDFs, relaxation times, diffusion coefficients, viscosity, and elastic moduli under service-relevant conditions. CG simulations further reduce computational cost by mapping groups of atoms into effective beads with parameters derived from MD, enabling mesoscale morphology, viscoelastic response, and

long-timescale relaxation. Finally, FEM incorporates constitutive models informed by lower-scale simulations to predict stress, strain, heat transfer, curing, and macroscopic tire behavior.

A concise comparison highlights the differing accuracy, computational cost, and applicability of these methods. DFT achieves the highest accuracy for reaction energetics and electronic structure but is computationally expensive and limited to small molecular systems. Atomistic MD offers moderate accuracy at a much lower cost and is suitable for nanostructure–property relationships, though dependent on force field quality and accessible trajectory length. CG simulations further reduce computational cost by mapping groups of atoms into effective beads with properties determined from MD, enabling mesoscale morphogenesis, viscoelastic response, and long-timescale relaxation. Finally, FEM combines constitutive models informed by lower-scale simulations to predict stress, strain, heat transport, curing, and macroscopic tire behavior. A quick comparison points out the varied accuracy, computational cost, and application of these approaches. Although DFT is computationally costly and restricted to tiny-molecule systems, it delivers the best precision for electronic structure and reaction energetics. Atomistic MD is appropriate for and provides reasonable accuracy at a significantly reduced cost.

This workflow has been verified based on experimental studies [126–128], which are also presented in this chapter.

4.2 | Quantum Mechanical Modeling of Additives, Reactions, and Environmental Impact

Antioxidants and antidegradants have been studied with computational tools, which not only map their protective action but also expose their hidden risks. A striking illustration comes from the extensive study of Li et al. [129] They dissected the entire cocktail of tire additives, from antioxidants and vulcanizing agents to plasticizers and accelerators, and then asked a sharp question: how do these molecules behave once released into the environment and what do they do to living organisms such as coho salmon? Using multiscale computational analysis, they explored BR, SBR, and NR, enhanced with vulcanizing agents (DTDM and DTDC), activators (stearic acid and ZBS), accelerators (MBT and sulfonamides), antiscorching agents (CTP and MTP), and antiaging blends (coumarone resin and 1,1-bis(2-methylbutan-2-ylperoxy)cyclohexane). At the center of this complex formulation stood the most controversial antioxidant, 6PPD, scrutinized not only for its role in protecting rubber but also for its biological consequences.

In particular, the researchers performed a series of simulations to evaluate both the technical role of 6PPD as an antioxidant and its environmental impact. They modeled how the compound is released into the environment during use and how strongly it interacts with the coho salmon growth hormone receptor P10607, a protein already known to cause harmful effects when inhibited [44, 130]. The strength of this interaction was expressed as binding affinity, the energy required for 6PPD to attach to the protein. To make the comparison systematic, six classes of tire additives were selected and combined in a complete factorial experiment using the Minitab software. This design generated 96 distinct additive formulations. Each formulation was assessed by molecular docking and MDs simulations. Using Discovery Studio 2020, the additives were docked to the P10607–rubber complex, and binding energies were then computed with GROMACS. The individual results for the most common additives are summarized in Table 6 [131, 132]. The findings were clear: many additives showed a negative impact on the hormone, and the magnitude of inhibition depended on both the type and concentration of the compound. The more negative the binding energy, the stronger the inhibition. In this respect, 6PPD raised particular concerns: its binding values were among the strongest observed, and its widespread use makes this result especially alarming. However, docking and short MD simulations cannot fully capture protein flexibility, solvent effects, or long-term metabolic processes. The strong binding values reported here should therefore be interpreted as indicative trends rather than definitive toxicity metrics.

TABLE 6 | The binding energy of individual tire additives with protein (P10607).

Tire additives	Binding energy (kJ/mol)
Antioxidant	
6PPD	−68.600
D	−30.945
BHT	−31.208
Organic accelerator	
CZ	−28.485
MBT	−51.358
Vulcanizing agent	
DTDM	−35.068
DTDC	−49.879
Vulcanizing activator	
ZBS	−40.936
SA	−89.258
Antiscorching agent	
CTP	−8.899
MTP	−30.212
Plasticizer	
CM	−42.041
BC	−71.703

The evaluation of antioxidant efficiency and structural modification of 6PPD derivatives was a central part of the study by Li et al. [129]. The guiding question was simple but ambitious: can one keep the shield while dulling the sword? In other words, can 6PPD be modified to retain its protective power yet lose some of its toxicity? As an amine antioxidant widely used in tire production, 6PPD protects rubber by scavenging alkoxy radicals that appear under frictional heating and UV light, acting as a molecular fire extinguisher against thermooxidation [133]. Its efficiency depends on the ability to split N—H and C—H bonds after capturing radicals such as ROO· and RO· [81], a property measured through dissociation enthalpy ΔH [134, 135]. The N—H bond in A—N—H is especially critical, since its rupture leads to

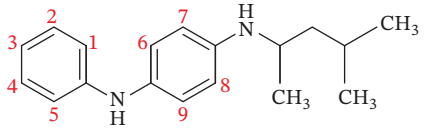

FIGURE 9 | The accessible modification sites and molecular structure of 6PPD.

the formation of 6PPD derivatives after radical absorption [136, 137]. With this logic, nine candidate sites for modification were mapped on the 6PPD molecule, as shown in Figure 9. Hydroxyl groups were chosen as substituents because hydroxylation can make or break antioxidant strength [138]. Through exhaustive computational modeling, the team created families of new molecules: singly, doubly, and triply hydroxylated derivatives, each a potential successor to the parent 6PPD.

The dissociation enthalpy ΔH was calculated with the Gaussian09 package on the Compute Canada platform using geometry optimization at the B3LYP/6-31G(d) level. Lower dissociation enthalpy corresponds to a higher antioxidant activity. The results showed a clear downward trend for 88% of the tested 6PPD derivatives, with decreases ranging from 0.15% to 26.48%. For 20 of the new molecules, the dissociation enthalpy was reduced by more than 15%. Among the groups, mono-substituted derivatives showed the largest reduction of 16.47%, followed by di-substituted derivatives with 20.74% and tri substituted derivatives with 26.48%. These findings confirmed that the degree of hydroxylation directly influences the radical-scavenging ability of the antioxidants. Yet, dissociation enthalpy values depend heavily on the chosen functional and basis sets, and the neglect of entropic effects may limit quantitative accuracy. The observed trends are robust, but the absolute numbers should be treated with caution.

Docking and MDs modeling were then used to examine the binding affinity and potential reduction of toxicity in the modified derivatives. Those with lower dissociation enthalpy were chosen for further testing, and their interaction with the coho salmon growth hormone receptor P10607 was quantified through binding energy calculations. Since a lower absolute binding energy indicates weaker affinity [139], this metric was used as a marker of reduced toxicity. Fifteen derivatives with promising functional properties were analyzed, and docking combined with MD simulations produced their binding energies with P10607. Eleven of them showed lower toxicity than unmodified 6PPD, which had a binding energy of −68.6 kJ/mol, with reductions ranging from 0.04% to 68.73%. The top five derivatives decreased toxicity by more than 30% (32.95%–68.73%), the middle group by 0.37%–54.58%, while the last group showed only small improvements or even increased toxicity. Based on these results, three candidates, 6PPD 106, 6PPD 108, and 6PPD 91, were identified as the most promising from an environmental perspective (Figure 10).

In the final step, the oxidation products of these three derivatives were also studied. Their binding affinities to P10607 were evaluated again, and the analysis revealed that 6PPD 106 and its oxidized forms had the weakest binding to the hormone receptor. This contrasted with unmodified 6PPD and its quinone, both of which showed strong inhibition. The outcome positioned 6PPD 106 as the leading candidate for further development as a safer alternative in tire formulations.

Energy barriers of ozonation reactions and quinone formation from 6PPD derivatives were investigated through computational chemical modeling. The focus was on calculating the activation energy (*Ea*) for the ozonation of 6PPD derivatives [138]. Since the activation barrier defines the minimum energy required for a chemical reaction to proceed, lower values correspond to faster reaction rates and thus provide mechanistic insights into the pathways that lead to quinone formation. Reaction energy barriers were computed using Gaussian09. According to the simulations, O_3 can attack the active sites at C6 or C8 by activating the vicinal carbon atom, consistent with the known reactivity of ozone toward electron-rich aromatic systems [140].

The ozonation pathway generates phenol intermediates and singlet oxygen ($^1O_2$) as the main products, while the final outcome is the formation of quinones together with H_2O_2. For the derivative 6PPD 106, the computed energy barrier was 86.97 kJ/mol, which is about 13% higher than the lowest barrier calculated for other 6PPD molecules. By comparison, the barrier for unmodified 6PPD was 77.01 kJ/mol. These results indicate that the probability of quinone formation is higher for unmodified 6PPD, whereas substitution in 6PPD 106 increases the barrier and reduces the likelihood of this pathway (Figure 8).

The research results demonstrated a clear relationship between the molecular structure of antioxidants and their activity. Variables such as the number of unsaturated bonds, the extent of conjugation, the degree of hydroxylation, and the position of

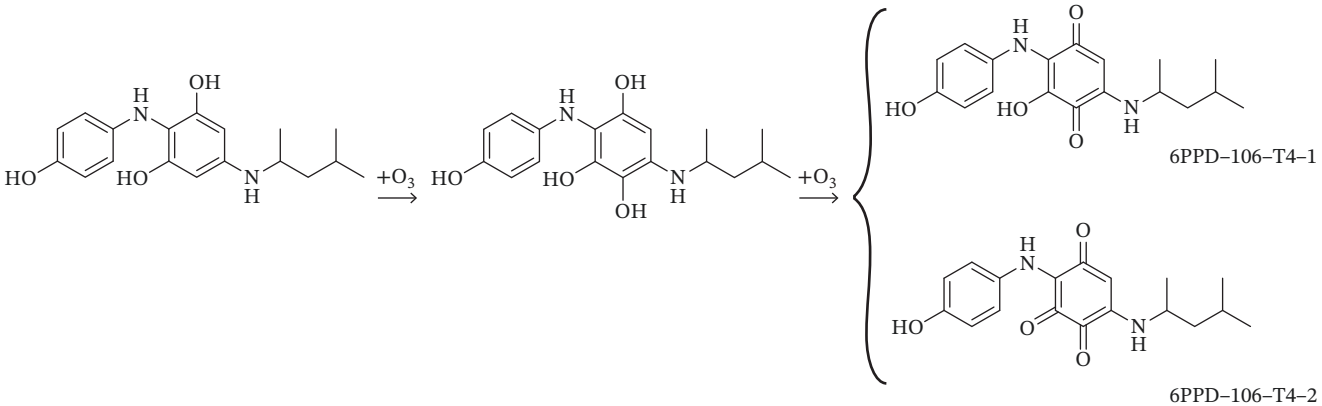

FIGURE 10 | Ozonation path of 6PPD-106 with two derivatives products.

hydroxyl groups all strongly influence the ability to neutralize free radicals. This study also illustrates the power of computational chemoinformatics. Each stage of the investigation was addressed with a dedicated method: dissociation enthalpy was determined through quantum chemical calculations, biochemical interactions were probed by molecular docking, and the energy barriers of oxidation and ozonation were evaluated with MDs. Nevertheless, the integration of methods remains constrained by computational cost and by the challenge of linking atomistic predictions to complex mixtures and long-term degradation in real materials. This gap highlights the need for more multiscale validation strategies.

A different example of such integration [141e investigated functionalized SBR–silica interactions and dynamic mechanical performance using a combined DFT and DMA (dynamic mechanical analysis) approach. Adsorption energies between end-chain-functionalized polybutadienes and a silica surface were calculated with DFT, while DMA provided experimental validation. Since no standard quantitative method exists to assess the interaction between fx-SBR and silica, this study highlights the importance of coupling theory and experiment and underlines the need for further methodological development to guide the design of improved materials.

In recent research, efforts have been directed at improving the balance between rolling resistance, traction, and abrasion resistance of tire tread compounds. For this purpose, both nonfunctional styrene butadiene copolymers with an optimized structure (SBR) and functionalized styrene–butadiene copolymers (fx-SBR) have been developed. Functionalization improves filler dispersion, strengthens polymer–filler interactions, and helps reduce hysteresis losses in tire tread compounds.

To decrease rolling resistance without sacrificing wet or icy traction, several innovations have been introduced. Modified fillers such as silica and CB, modified polymers including SBR and BR, and filler–polymer masterbatches based on silica or CB have been prepared [142]. Since raw polymers are hydrophobic, while silica is hydrophilic, surface modification of silica is required to achieve uniform mixing. This difficulty arises from the hydroxyl groups on the silica surface, which hinder dispersion in the polymeric matrix. Reports indicate that fx-SBR can simultaneously improve rolling resistance, wet traction, and wear performance [143].

The molecular basis of these improvements has been probed using DFT simulations of adsorption energies between functionalized butadiene oligomers and silica. In particular, adsorption on the α-quartz (001) surface at 160°C was examined. Various functionalized oligomers were modeled with Gaussian09 using all electron calculations and the B3LYP functional in combination with the cc-pVTZ and cc-pVQZ basis sets. The resulting adsorption energies provide a quantitative framework linking molecular-level interactions with the macroscopic performance of vulcanized rubber compounds. The following actions were performed for the molecular simulations: optimization of the clean surfaces; preoptimization of the interfaces; refining the optimization of the interfaces to obtain total energies and adsorption energies; and calculation of the adsorption energies between the oligomer and silica surface.

The following formula has been used to compute the interaction/adsorption energy per molecule of the end-chain-functionalized butadiene oligomers on the α-quartz (001) surface:

$$E_{\mathrm{int/ads}} = E^{\mathrm{tot}}\left(\frac{\mathrm{oligomer}}{\mathrm{surface}}\right) - [E^{\mathrm{tot}}(\mathrm{oligomer}) + E^{\mathrm{tot}}(\mathrm{surface})], \tag{10}$$

where $E^{\mathrm{tot}}(\frac{\mathrm{oligomer}}{\mathrm{surface}})$ is the total energy of the optimized interface, $E^{\mathrm{tot}}(\mathrm{oligomer})$ is the total energy of the optimized gas-phase oligomer, and $E^{\mathrm{tot}}(\mathrm{surface})$ is the total energy of the optimized clean surface.

The researchers then modeled and selected the most efficient polymeric compounds for rubber synthesis. For evaluation, they used a standard passenger car radial tire tread silica-based compound recipe [144]. Model SBRs with end-chain functionalization identical to the oligomers employed in the DFT calculations were synthesized in the laboratory [145]. These model polymers had comparable micro and macrostructure, with the main difference among the four SBR samples being the type of functionalization. The model SBRs were incorporated into silica compounds, and their dynamic mechanical properties were measured. Rheological characterization included two types of tests: a temperature sweep at high frequency and a deformation sweep at 60°C.

The adsorption energy between functionalized butadiene oligomers and the silica surface was calculated in the same study using DFT simulations. End-chain functionalization was selected because higher adsorption energies indicate stronger oligomer–silica interactions, which favor improved performance. The experimental results showed that Payne effect values obtained for compounds synthesized with fx-SBR of different functionalities were consistent with the DFT-calculated adsorption energies. This confirmed a strong correlation between adsorption strength and macroscopic performance of silica-filled vulcanized compounds. Strong fx-SBR–silica interactions enhance silica dispersion and reduce rolling resistance, thereby improving the overall tire performance.

In summary, the development of DFT-based molecular simulation protocols to determine adsorption energies of functionalized butadiene oligomers, combined with the synthesis of model fx-SBRs carrying selected functional groups, is a sound approach. The close agreement between computational predictions and experimental validation underlines the high potential of this strategy.

Polymer–asphalt interactions and functionalization of rubbers have been investigated using DFT modeling. Youn et al. [13] modeled SBS with representative asphalt molecules and quantified binding through computed interaction energies and charge-transfer numbers. The results indicate strong affinity to aromatics and saturates and poor compatibility with asphaltenes, which rationalizes both reinforcement and phase separation in SBS-modified asphalt. This is a vivid example of how quantum calculations can lift the veil on what otherwise looks like a messy black mixture.

In parallel, there was highlighted that targeted functionalization of SSBR can increase adsorption on silica surfaces and thereby improve filler dispersion, reduce hysteresis, and support low rolling resistance compounds. The study demonstrates a practical screening route where DFT adsorption energies inform the experimental selection of functional groups [146]. It is almost

like using theory as a compass to navigate a sea of chemical possibilities.

Vulcanization and crosslinking agents were examined through quantum chemical modeling. Shi et al. [147] established a full Zn(II)-activated sulfur vulcanization mechanism for SBR with zinc dithiocarbamate accelerators. Calculated free-energy barriers identified the preferred initiation, precursor formation, and crosslinking steps and explained the high efficiency of dithiocarbamates relative to self-crosslinking routes.

Complementarily, Nanthanasit et al. [146] used DFT to design electron beam-compatible crosslinking agents for NR and validated them experimentally. The combined approach shows that specific diacrylates lower crosslinking barriers and reduce required irradiation dose, enabling cleaner and lower-temperature curing [26]. This is a neat demonstration of how computation can directly inspire greener processing routes.

Recycling and depolymerization have been investigated through a combination of reactive MD and DFT. Yan et al. [148] showed how supercritical water promotes sulfur migration during depolymerization of scrap tires. Hydroxyl radicals lower the barrier for C—S cleavage and drive sulfur into the aqueous phase mainly as stable oxyanions. This provides a mechanistic basis for cleaner oil and gas fractions and suggests process levers such as higher temperature or aqueous-phase recycling. In other words, even waste tires can be coaxed into more useful products if we understand the invisible choreography of atoms.

4.3 | Atomistic MDs Simulations of Structure–Property Relationships

Friction, wear, and surface interactions are effectively captured by MD, which directly connects the molecular structure with the mechanisms of reinforcement in rubbers. Shear models of rubber confined between mineral layers reveal that both polymer chemistry and aggregate type strongly influence the tribological response [61]. SBR exhibits the highest coefficients due to its aromatic structure, while natural and polybutadiene rubbers are weaker. Among aggregates, microcline produces the strongest friction and calcite the weakest, reflecting differences in interfacial electrostatics. The dependence on sliding speed is nonmonotonic, with friction first increasing and then decreasing as longitudinal stress changes, and temperature effects are also distinct, with SBR showing a complex rise–fall–rise pattern, while natural and polybutadiene rubbers remain almost unchanged. These atomistic insights explain how the tread composition, mineralogy of aggregates, and environmental conditions govern skid resistance at the tire–pavement contact.

Reinforcement can also be achieved through blending. Adding *Eucommia ulmoides* gum (EUG) to NR tunes free volume, stiffness, and tribological properties [149]. The optimal 30–70 composition raises Young's modulus by a third compared to pure NR, increases friction for improved braking, and lowers chain mobility that suppresses wear. At the rubber–silica interface, van der Waals forces dominate, and moderate EUG content reduces adhesion energy and shear damage risk. The drawback is higher heat accumulation during sliding, suggesting that additional fillers with good thermal conductivity may be required. Overall, this blend achieves the best balance of strength, frictional performance, and durability, making it a promising formulation for aircraft tires. Here, molecular design meets practical engineering, and the result is a material that is tuned as finely as a musical instrument.

CNTs offer another powerful route for reinforcement. Simulations show that CNTs reduce chain mobility and increase bulk, shear, and Young's modulus by up to 27% at 15% loading while also raising the coefficient of friction from 1.03 to 1.16 [150]. Yet, more is not always better: excessive CNT content causes agglomeration, stress localization, and weaker interfacial binding, which limit their effectiveness. The reinforcement mechanism follows three characteristic stages described as attraction, superposition, and competition. Defect engineering provides an additional leverage. Stone–Wales CNTs in nitrile butadiene rubber (NBR) stabilize antioxidants, suppress chain motion, and reduce free volume [151]. As a result, the mechanical moduli increase by up to 12%, while the friction coefficient and wear rate fall by 28% and 21%, respectively. These findings demonstrate that both the CNT concentration and defect structure can be tuned like knobs on an instrument to optimize durability and frictional stability.

Other nanofillers provide comparable or even greater benefits. Nano SiO_2 reinforces NBR through hydrogen bonding with polymer chains, which reduces free volume from 20.7% to 15.5%, generates about 30 hydrogen bonds, and increases the shear modulus by 25% [152]. Under sliding against copper, friction stress decreased by 34%, and temperature spikes vanished, confirming that hydrogen bonding can effectively restrict chain motion, lower interfacial heating, and enhance wear resistance. Graphene offers still stronger reinforcement in swollen NBR compared with CNTs [153]. At equal loading, it improved both elastic modulus and tensile strength more efficiently, thanks to its larger surface area and stronger chain adsorption. With two graphene sheets, the modulus increased by 47%, tensile strength by 31%, and solvent diffusion decreased by 11.6%. These results underline the promise of nanofillers for improving both strength and tribological stability, with graphene emerging as the champion additive for swollen NBR.

Rubber–asphalt interactions and asphalt modification have been clarified by experiments and MD simulations, which explain why crumb rubber improves road performance. Multiscale analyses show the strongest affinity to aromatics, followed by saturates and resins, with asphaltenes showing the weakest interactions [154]. Rubber absorbs light fractions, swells, and transfers its mechanical response to the binder, thereby improving rutting resistance. Microscopy reveals a two-phase structure where rubber particles grow as they absorb light components, while FTIR analysis shows that the modification is primarily physical and dominated by van der Waals forces. These observations connect macroscopic improvements in rutting resistance with molecular-level binding energies and selective absorption.

Further simulations quantified how controlled desulfurization and mild depolymerization enhance compatibility [155]. Both processes reduce solubility parameter differences and increase binding energies, while excessive chain scission undermines the interfacial strength. Diffusion coefficients rise with degradation at elevated temperatures, confirming higher molecular mobility. In simple terms, careful processing strengthens stability, but overprocessing can ruin it.

Compatibility also depends strongly on asphalt origin and composition [156]. Smaller solubility parameter gaps and higher contents of light fractions produce stronger interactions, as shown by Esso asphalt with $\Delta\delta = 3.24$ and the largest interaction energy of −3369.9 kJ/mol, whereas Karamay asphalt exhibited weaker compatibility. RDF analysis confirmed that van der Waals forces dominate, with peaks between 3.1 and 5.0 Å indicating better blending in asphalts rich in aromatics and saturates. These findings, validated by softening point tests, provide a rational basis for selecting raw materials for durable rubber-modified asphalts.

At mineral interfaces, crumb rubber enhances adhesion and moisture resistance [157]. Simulations with silica surfaces revealed stronger adhesion energies and less moisture damage when rubber was added, with CR molecules clustering closer to the surface than the polar asphalt components. Although severe degradation can weaken these advantages, adhesion tests confirmed that rubber improves bonding and water resistance at the asphalt–aggregate interface.

Chemical treatments offer another means of boosting interfacial bonding [158]. Introducing oxygen-containing groups onto rubber surfaces increased calculated interaction energies and was validated experimentally by a higher tensile strength ratio and reduced abrasion loss in pavements. Hydroxyl groups improved NR–polyurethane bonding by 59%, while carbonyl groups enhanced SBR–polyurethane adhesion by 20%. Laboratory NaOH treatment confirmed the functionalization and improved durability. Together, these results provide a clear molecular explanation for the stronger bonding observed in polyurethane-bonded rubberized pavements.

Structural and mechanical properties of elastomers can be uncovered by combining MDs with experiments, which together reveal how the molecular architecture controls macroscopic performance. For SBR, three formulations with different styrene contents were compared to connect chain scale metrics with tread properties [159]. A higher styrene content reduced free volume and chain mobility, raised T_g (glass transition temperature), and increased hardness and wear resistance, but it also elevated rolling resistance. Lower styrene content produced the opposite effect: more flexibility, lower T_g, improved energy dissipation, but reduced durability. To bridge atomistic and macroscopic scales, the authors introduced a simple MD-derived parameter, $\mathrm{Fsim} = \mathrm{CED} \times (Ds \times T)$, which correlated almost perfectly with experimental $\tan\delta$ ($R^2 = 0.99$). This is an elegant example of how a single compact formula can capture the essence of rolling resistance and skid resistance.

NR was investigated using a combined CG MD and machine learning framework [160]. Simulations of cis-1,4-polyisoprene with phospholipids and proteins showed that nonrubber components and hydrogen bonds dominate reinforcement by adsorbing chain ends, restricting mobility, and triggering strain-induced crystallization. Machine learning analysis ranked hydrogen bond strength as the most decisive factor (information gain 93), ahead of nonrubber content (56) and nonhydrogen interactions (15). This highlights how subtle physical crosslinks created by nonrubber components orchestrate chain orientation and crystallization under strain, explaining the remarkable strength of NR and pointing toward the biomimetic design of new rubbers.

In NBR, small-molecule modifiers such as hindered phenols form reversible hydrogen bonds with nitrile units, tuning damping and stiffness [161]. Simulations showed that crosslinking raised the elastic and shear modulus by 20%–24%, while excessive crosslinking reduced elasticity. The optimal A/B ratio of 30/30 phr maximized hydrogen bond number (≈16 per cell), binding energy (~1811 kcal/mol), and damping capacity (η), with T_g around 281 K. These results demonstrate the delicate balance where reversible hydrogen bonds stabilize energy dissipation and provide excellent damping, but only if crosslink density is kept in check.

All-atom MD extended across wide pressure–temperature ranges mapped P–V–T behavior, T_g shifts, and reinforcement by fillers and crosslinks [162]. In NR, BR, and SBR, T_g increased by 2.3 K per 100 atm in pure rubbers and by up to 3.3 K per 100 atm in crosslinked forms. Thermal expansion coefficients were higher in the rubbery state but decreased under pressure. The addition of nanoparticles or crosslinking further suppressed chain mobility. Tensile tests showed that stress decreased with temperature but increased with pressure, with NR being the strongest and BR being the weakest. The agreement with the experiment within 6% error underscores how MD can provide quantitative guidelines for elastomer design under extreme service conditions.

Recycling and pyrolysis were analyzed through reactive MD, offering atomistic insight into decomposition pathways of waste tires and clarifying why sulfur persists in the products [163]. Simulations of mixed rubbers (NR, SBR, and butyl) with ReaxFF at 1800–3000 K revealed four stages: structural adjustment, chain scission yielding oils and gases, decomposition of heavy oils into lighter fractions, and secondary cracking into gases. Product distributions depended strongly on temperature: light oils reached nearly 80% at 2000 K, while gases dominated at 3000 K with about 60% yield. Radical chemistry drove the process. Methyl radicals and methane promoted both gas formation and CB growth, while ethylene, acetylene, and butadiene reflected sulfur crosslink breakdown. The key advance was sulfur tracking: most sulfur remained in condensed products as sulfides or elemental S, while less than 5% appeared as H_2S gas. At 3000 K, about 64% of sulfur was present as free S, explaining the high sulfur content of oils and chars. These insights identify temperature and sulfur pathways as practical levers to tune product distributions, pointing the way toward cleaner tire pyrolysis technologies. However, ReaxFF predictions remain highly parameter dependent, and the extreme conditions simulated may not fully capture the complexity of industrial pyrolysis environments.

4.4 | Coarse-Grained Simulations and Mesoscale Modeling of Reinforced Elastomers

Reinforcement by carbon nanostructures has been illuminated by coarse-grained MD (CGMD), which shows how nanofillers influence dispersion, chain orientation, and stress transfer in vulcanized rubbers. In CNT-filled NR, tensile strength increased from 20.2 to 27.3 MPa as tube length grew, corresponding to a 35% reinforcing efficiency [164]. Intertube crosslinking boosted strength even further by more than 80% at only 3% crosslinking, while polymer grafting enhanced load transfer for short CNTs, raising the tensile strength by more than 12%. These improvements were traced to better dispersion, stronger interfacial contact, chain wrapping, and the formation of mechanically interlocked networks. The message is clear: CNTs can knit the

polymer into a stronger fabric, provided their content and connections are carefully tuned.

CB nanoparticles also reinforce NR, with the particle size controlling the balance between alignment and aggregation [165]. Medium-sized particles (~20 Å) optimized chain orientation and strain-induced crystallization, producing the best mechanical response. At 40 phr loading, Young's modulus increased by up to 55% and tensile strength by 117% compared with neat NR. Moderate grafting density further improved modulus by 118% and strength by 93%, while excessive grafting wrapped chains too tightly and limited reinforcement.

Fullerene C60, even at very low loading, restricts chain mobility, suppresses pore formation, and improves thermal transport [166]. At 0.2 phr, Young's modulus, yield strength, and tensile strength rose by about 24%, 23%, and 52%, respectively, while thermal conductivity increased by up to 17% at 0.1 phr. The strongest effect appeared at a uniform dispersion of ~20 particles, whereas aggregation at higher concentrations diminished efficiency. A small number of perfectly dispersed fullerenes thus act like tiny keystones, locking the structure together.

Hybrid systems of CB and CNTs display a clear synergy [167]. Replacing part of the CB with CNTs increased Young's modulus and tensile strength by more than 50% and 80%, respectively. CNTs promoted chain orientation, crystallization, and stronger interfacial adsorption, while cyclic shear tests revealed an enhanced Payne effect, linked to nanoparticle network breakup and interfacial separation at large strains. These results provide molecular-level guidance for designing nanofilled rubbers that combine static strength with dynamic damping.

Graphene requires careful model parameterization. A calibrated CG force field was developed for graphene/NBR (GNS/NBR) nanocomposites, enabling mesoscale simulations that capture both interfacial and bulk mechanics [168]. All atom trajectories were mapped to coarse beads, bonded terms fitted with iterative Boltzmann inversion, and nonbonded parameters tuned against interfacial pull-out tests. The optimized model reproduced NBR density with less than 0.2% error and tensile stress within a 4.9% deviation from all atom benchmarks. At the graphene–NBR interface, shear stress from pull-out simulations matched closely (140.7 MPa in CG vs. 138.8 MPa in AA). This transferable force field offers a reliable framework for mesoscale studies of graphene-reinforced NBR, providing predictive power for rational nanocomposite design.

Silica-based systems have also been examined with CGMD, revealing how nanoparticle aggregation and interfacial chemistry govern reinforcement in rubber [169]. In NR, early aggregation stiffened the material at small strain by forming rigid particle networks but reduced tensile strength at large strain due to premature network failure and chain desorption. Longer chains encapsulated particles and reduced aggregation, while a higher crosslink density promoted clustering and accelerated interfacial failure. These findings identify chain length and crosslink density as practical levers to manage aggregation and optimize silica-filled NR composites.

Under extreme uniaxial tension, smooth silica weakened polyisoprene because of weak interfaces and reduced entanglements [170]. In contrast, grafted silica and sulfur crosslinks restored stress transfer, strengthened nanoparticle network dynamics, and suppressed microvoid growth, enhancing strain hardening and delaying failure. This work shows how CG simulations with IBI-derived potentials can quantitatively link nanoparticle surface chemistry and crosslinking to either reinforcement or deterioration mechanisms, offering molecular-level guidance for the design of durable silica-filled elastomers.

4.5 | Continuum Finite Element Modeling of Tire Mechanics and Manufacturing Processes

An overview and current directions position the finite element method (FEM) as the foundation of modern tire research, replacing costly test-only approaches with predictive simulations of structure, mechanics, heat transfer, and vibration [171]. With careful meshing, realistic constitutive rubber models, boundary conditions, and algorithms for tire–road contact, FEM enables static, dynamic, and modal analyses across passenger, truck, and aircraft tires, as well as new generations of nonpneumatic and smart designs. Case studies such as the Firestone/Ford Explorer failures and even the Concorde crash reveal that critical stress concentrations could, in principle, have been foreseen. The benefits are clear: reduced prototyping, multiphysics integration, and systematic optimization of rolling resistance, durability, noise, and safety. Looking forward, the most promising directions include multiscale coupling with material models, integration of smart materials and environmental impact assessments, and the use of real-time sensing for proactive safety monitoring. FEM is no longer just a numerical tool but a design philosophy. At the same time, FEM outcomes remain highly dependent on constitutive models and boundary condition choices, and small deviations in parameterization can lead to large differences in the predicted stresses.

Contact interaction and service conditions have been clarified by FEM simulations validated against experiments, showing how inflation pressure reshapes tire–rail contact mechanics [172]. An ANSYS model with Mooney–Rivlin rubber and an elastic–plastic rim reproduced a deformation of about 34 mm under a 9810 N load. Rim Von Mises stress increased from 130.5 to 166.4 MPa as pressure rose, while peak contact pressure reached 4 MPa, with frictional stresses concentrated at patch corners. These results demonstrate in a very direct way that inflation pressure governs stress distribution and contact patch evolution, providing practical guidance for road–rail vehicle design.

Manufacturing processes are also accessible to FEM. A coupled thermomechanical framework in ABAQUS has been developed to link heat transfer, cure kinetics, and modulus evolution during rubber vulcanization [173]. Using custom UMATHT and UMAT subroutines, the model captured nonlinear heat conduction with exothermic crosslinking and continuously updated material properties as functions of temperature and degree of cure. Simulations reproduced experimental temperature profiles with deviations below 2.6°C and predicted nonuniform cure and press force near 250 N, while constant-property models significantly underestimated these effects. Such validated tools make it possible to optimize vulcanization cycles and mold forces in tire and large-rubber product manufacturing. Yet, such frameworks still simplify cure chemistry and may not fully capture the heterogeneities present in industrial-scale vulcanization.

Dynamics and new architectures are being explored with high-fidelity FEM models in Abaqus/Explicit, which capture the response of nonpneumatic tires and enable the optimization of spoke networks [174]. After validation against static stiffness tests with errors below 1%, simulations showed that moderate mesh refinement reduces force fluctuations efficiently, while higher obstacle height and speed strongly amplify vibration. An optimized bionic spoke design reduced vibration amplitudes by about 18% vertically and 30% longitudinally at 30 km/h by stabilizing the grounding pressure distribution. These results highlight how validated FE models can quantify comfort and durability improvements and provide guidance for the design of advanced nonpneumatic tire architectures.

Taken together, the base of computational research on rubber and tires demonstrates how modern theory has moved far beyond illustrative models to become an indispensable partner of experiments and design. From DFT and docking studies that clarify additive reactivity and toxicity, through multiscale MD that links nanofillers, interfaces, and friction to macroscopic properties, to FEM frameworks that optimize tire architecture and manufacturing, these methods reveal the invisible mechanics and chemistry that shape the performance and sustainability. At the same time, each approach carries limitations–dependence on parameterization, simplified environments, or high computational cost–which underline the need for continued validation and integration across scales. The overall picture is one of rapid convergence: computation is no longer an auxiliary tool but a central pillar guiding the safer, greener, and more efficient design of next-generation elastomers and tires.

5 | Conclusion

According to this review, the synthesis (including production steps), formation, behavior in nature, and subsequent distribution of chemicals derived from rubber particles are still not fully understood. It is worth noting that the reason for the uncertainty is the high complexity and diversity of processes and chemical systems, which consist of a number of components that are subject to changes in time and due to external parameters. Research teams, which consider environmental aspects, are primarily tasked with correctly identifying and analyzing the chemical components that enter the environment in order to further identify the harmful effects and consequences. In turn, for manufacturers seeking to improve performance and other efficiency indicators, it is important to understand and predict the properties of the material, which change overtime, and modify existing chemical systems-mixtures of polymer macromolecules to improve the quality characteristics of the material.

When discussing sustainable development and green vehicle use options, the environmental impact of direct exposure to TWPs and their chemical additives on a different scale should also be taken into account. In future studies, the chemical composition of various types of tires and the analysis of emission increases should be continued. It is important to organize and conduct specific procedures simulating both abiotic stress factors (such as temperature, UV radiation, and mechanical impact) and biotic stress factors (such as pollution and microbiological degradation) within controlled scenarios.

The understanding of the effects of material aging affects both fields of research (ecology and performance) and is considered throughout the life of the tire material, from creation in production cycles to distribution in nature or during processing into subsequent products. By comparing the effects of aging, it can be concluded how these processes of destruction and degradation occur and which materials are more vulnerable to a particular test system, as well as how the properties of the tested material differ under specific aging conditions.

Changes in the composition of TWPs should be considered as well as be accompanied by a thorough characterization of the particles before and after the aging test, including analysis of particle size, density, shape, and composition. It is necessary to apply techniques that will quantify the changes in TWPs characteristics and correlate these changes with environmental factors. This is crucial if the results obtained are about the properties of the material (performance) and the degree of abrasion (emission) and can be applied in regions with different climates, taking into account seasonality.

To solve the abovementioned challenges, as well as to reduce the complexity of many other types of production and analysis, it seems logical and expedient to use computational chemical modeling methods known as cheminformatics. Currently, in many areas of scientific research (materials science, biochemistry, electrochemistry, etc.), chemical modeling is used on the scale of quantum mechanical calculations analysis (including DFT, ab initio, and semiempirical methods) that describe electronic interactions, MDs and CG simulations that capture collective molecular behavior, and finally continuum finite element models that reproduce macroscopic mechanical response within condensed phases.

The research on these methods presented in this review is focused on both environmental and industrial topics. In particular, we looked at the effects of the antioxidant additive 6PPD, its derivatives, and the products of oxidative reactions. When extending the analysis of the material using CG modeling methods, the entire spectrum of actions can be considered for multiscale computational modeling. Given the diversity of rubber compounds for tires, there is a clear interest in continuing research in this area and studying the chemical properties of various components, both individually and in combination with other components in the condensed rubber phase. In addition, it is important to consider the factors of the production stages, during which a series of syntheses and chemical changes of raw materials occur (which have not yet been fully disclosed in the literature). During use and after exposure to the environment, TWPs chemicals are also subject to changes under the influence of intense parameters (T, P, UV, etc.), leading to obvious deterioration of material properties, degradation, and decomposition.

In the application of computational chemical modeling of rubber materials, there are certain values and characteristics (such as Young's modulus (E) and shear modulus (G), bulk modulus (K) (as well as their dynamic variants), Poisson's ratio, permeability to oxygen molecules, ozone, etc.) that determine the properties of the material and its behavior during operation. On the other hand, tan δ values can be obtained experimentally, which determine the viscoelastic parameters of the material, including

hysteresis (Equation 1 and Equation 2) and all it serves as a tool for validation. By comparing the simulation data with the experimental data, it is possible to calibrate the created model and extrapolate the data to a wide range of values using specific viscoelastic models (standard linear solid [SLS] model and generalized Maxwell model). It is also possible to compare the simulation results at different temperatures and the results obtained using TTS (time and temperature superposition).

All these stages—from industrial transformations to oxidation and leaching in the environment—can be investigated using multiscale chemical computational analysis, which avoids the laborious processes of experimental identification. Moreover, with a well-constructed model (based on the values of concentrations or proportions of system components), it is possible to predict the properties of the material, the temporal stages of aging—the degradation of the material, and its behavior in the environment. As for application in the production cycle, the properties and characteristics (reduced rolling resistance and wet grip) of the compound can be predicted based on the substances added to the system. This will help reduce the costs of production development, chemical design, repeated experiments, and so on.

5.1 | Challenges and Future Research Directions

Future research should focus on building practical bridges between individual modeling scales and experimentally measurable properties. A first milestone is the integration of QM-derived reaction barriers, charge distributions, and optimized geometries directly into all-atom MD force fields for specific elastomer formulations, enabling consistent prediction of crosslinking kinetics and oxidation pathways. A second milestone is the development of CG models in which coarse-graining parameters are systematically derived from MD trajectories rather than fitted empirically; this would allow mesoscale morphology, filler–polymer interactions, and viscoelastic behavior to be reproduced with controlled accuracy. A third near-term goal is coordinated validation experiments in which spectroscopic measurements (IR, Raman, XPS), mechanical tests (DMA, tensile, fatigue), and diffusion studies are performed on the same materials used in simulations to evaluate the transferability of parameters across scales. In the medium term, progress is expected from automated workflows combining QM, MD, CG, and FEM within a single pipeline, enabling uncertainty quantification at each step and establishing traceable links between molecular mechanisms and tire-level performance metrics such as rolling resistance, wear rate, and durability. Long-term goals include incorporating aging, oxidative degradation, and environmental exposure into multiscale models through reactive MD and hybrid QM/MM schemes, as well as creating benchmark datasets that allow the community to compare multiscale predictions under standardized conditions.

Evidently, this is a nontrivial task, but based on the current situation in the scientific area, it is a highly promising direction. It is important to put forward a mature and well-founded hypothesis, carry out computational modeling and obtain results, derive specific rheological values, and then use existing or create new physical materials to conduct laboratory and real-life trials for specific viscoelastic parameters. This will allow us to compare indicators for rubber with model predictions. Systematic research in these areas will allow us to fine-tune a multiscale model and develop a methodological approach to basic investigation and evaluation of prediction of tire characteristics. This activity may also improve the fundamental understanding of condensed matter physics for multicomponent elastomeric (rubber) compounds, leading to the generation of modern and valuable knowledge.

Author Contributions

Roman Tangalychev: conceptualization, formal analysis, methodology, writing – original draft preparation. **Vasilii Korotenko**: conceptualization, methodology, software – original draft preparation. **Valentin Ivanov**: data curation, formal analysis, writing – review and editing.

Acknowledgments

We acknowledge support for the publication costs from the Open Access Publication Fund of the Technische Universität Ilmenau. The authors only used artificial intelligence (AI) tools for grammatical correction. AI did not generate any scientific content, data analysis, interpretation, or conclusions.

Funding

This research received no external funding. Open Access funding enabled and organized by Projekt DEAL.

Disclosure

All authors have read and agreed to the published version of the manuscript.

Conflicts of Interest

The authors declare no conflicts of interest.

Data Availability Statement

Data will be available upon request.

References

1. B. Baensch-Baltruschat, B. Kocher, C. Kochleus, F. Stock, and G. Reifferscheid, "Tyre and Road Wear Particles—A Calculation of Generation, Transport and Release to Water and Soil With Special Regard to German Roads," *Science of the Total Environment* 752 (2021): 141939.

2. R. Sieber, D. Kawecki, and B. Nowack, "Dynamic Probabilistic Material Flow Analysis of Rubber Release From Tires Into the Environment," *Environmental Pollution* 258 (2020): 113573.

3. K. M. Unice, M. L. Kreider, and J. M. Panko, "Use of a Deuterated Internal Standard With Pyrolysis-GC/MS Dimeric Marker Analysis to Quantify Tire Tread Particles in the Environment," *International Journal of Environmental Research and Public Health* 9, no. 11 (2012): 4033–4055.

4. Bridgestone, "Long-Term Environmental Vision (2050 and Beyond): Towards 100% Sustainable Materials," (2024).

5. E. Chae, U. Jung, and S.-S. Choi, "Quantification of Tire Tread Wear Particles in Microparticles Produced on the Road Using Oleamide as a Novel Marker," *Environmental Pollution* 288 (2021): 117811.

6. J. M. Panko, K. M. Hitchcock, G. W. Fuller, and D. Green, "Evaluation of Tire Wear Contribution to PM2.5 in Urban Environments," *Atmosphere* 10, no. 2 (2019): 99.

7. B. Giechaskiel, T. Grigoratos, M. Mathissen, et al., "Contribution of Road Vehicle Tyre Wear to Microplastics and Ambient Air Pollution," *Sustainability* 16, no. 2 (2024): 522.

8. I. Järlskog, D. Jaramillo-Vogel, J. Rausch, et al., "Differentiating and Quantifying Carbonaceous (Tire, Bitumen, and Road Marking Wear) and Non-Carbonaceous (Metals, Minerals, and Glass Beads) Non-Exhaust Particles in Road Dust Samples From a Traffic Environment," *Water, Air, & Soil Pollution* 233, no. 9 (2022).

9. M. Kovochich, J. A. Parker, S. C. Oh, et al., "Characterization of Individual Tire and Road Wear Particles in Environmental Road Dust, Tunnel Dust, and Sediment," *Environmental Science & Technology Letters* 8, no. 12 (2021): 1057–1064.

10. P. Klöckner, T. Reemtsma, and S. Wagner, "The Diverse Metal Composition of Plastic Items and Its Implications," *Science of the Total Environment* 764 (2021): 142870.

11. D. Mengistu, A. Heistad, and C. Coutris, "Tire Wear Particles Concentrations in Gully Pot Sediments," *Science of the Total Environment* 769 (2021): 144785.

12. E. S. Rødland, O. C. Lind, M. J. Reid, et al., "Occurrence of Tire and Road Wear Particles in Urban and Peri-Urban Snowbanks, and Their Potential Environmental Implications," *Science of the Total Environment* 824 (2022): 153785.

13. J.-S. Youn, Y.-M. Kim, M. Z. Siddiqui, et al., "Quantification of Tire Wear Particles in Road Dust From Industrial and Residential Areas in Seoul, Korea," *Science of the Total Environment* 784 (2021): 147177.

14. Z. Gao, J. V. Cizdziel, K. Wontor, et al., "On Airborne Tire Wear Particles Along Roads With Different Traffic Characteristics Using Passive Sampling and Optical Microscopy, Single Particle SEM/EDX, and μ-ATR-FTIR Analyses," *Frontiers in Environmental Science* 10 (2022): 1022697.

15. C. Rauert, S. Vardy, B. Daniell, N. Charlton, and K. V. Thomas, "Tyre Additive Chemicals, Tyre Road Wear Particles and High Production Polymers in Surface Water at 5 Urban Centres in Queensland, Australia," *Science of the Total Environment* 852 (2022): 158468.

16. T. R. Barber, S. Claes, F. Ribeiro, et al., "Abundance and Distribution of Tire and Road Wear Particles in the Seine River, France," *Science of the Total Environment* 913 (2024): 169633.

17. A. Müller, B. Kocher, K. Altmann, and U. Braun, "Determination of Tire Wear Markers in Soil Samples and Their Distribution in a Roadside Soil," *Chemosphere* 294 (2022): 133653.

18. E. S. Rødland, M. Gustafsson, D. Jaramillo-Vogel, et al., "Analytical Challenges and Possibilities for the Quantification of Tire-Road Wear Particles," *TrAC Trends in Analytical Chemistry* 165 (2023): 117121.

19. S. Wagner, T. Hüffer, P. Klöckner, M. Wehrhahn, T. Hofmann, and T. Reemtsma, "Tire Wear Particles in the Aquatic Environment—A Review on Generation, Analysis, Occurrence, Fate and Effects," *Water Research* 139 (2018): 83–100.

20. J. Kang, X. Liu, B. Dai, et al., "Tyre Wear Particles in the Environment: Sources, Toxicity, and Remediation Approaches," *Sustainability* 17, no. 12 (2025): 5433.

21. P. Klöckner, B. Seiwert, S. Wagner, and T. Reemtsma, "Organic Markers of Tire and Road Wear Particles in Sediments and Soils: Transformation Products of Major Antiozonants as Promising Candidates," *Environmental Science & Technology* 55, no. 17 (2021): 11723–11732.

22. K. M. Unice, J. L. Bare, M. L. Kreider, and J. M. Panko, "Experimental Methodology for Assessing the Environmental Fate of Organic Chemicals in Polymer Matrices Using Column Leaching Studies and OECD. 308 Water/Sediment Systems: Application to Tire and Road Wear Particles," *Science of the Total Environment* 533 (2015): 476–487.

23. E. S. Rødland, S. Samanipour, C. Rauert, et al., "A Novel Method for the Quantification of Tire and Polymer-Modified Bitumen Particles in Environmental Samples by Pyrolysis Gas Chromatography Mass Spectroscopy," *Journal of Hazardous Materials* 423 (2022): 127092.

24. Z. Tian, H. Zhao, K. T. Peter, et al., "A Ubiquitous Tire Rubber-Derived Chemical Induces Acute Mortality in Coho Salmon," *Science* 371, no. 6525 (2021): 185–189.

25. K. Hiki, K. Asahina, K. Kato, et al., "Acute Toxicity of a Tire Rubber-Derived Chemical, 6PPD Quinone, to Freshwater Fish and Crustacean Species," *Environmental Science & Technology Letters* 8, no. 9 (2021): 779–784.

26. M. Brinkmann, D. Montgomery, S. Selinger, et al., "Acute Toxicity of the Tire Rubber-Derived Chemical 6PPD-Quinone to Four Fishes of Commercial, Cultural, and Ecological Importance," *Environmental Science & Technology Letters* 9, no. 4 (2022): 333–338.

27. J. Ding, M. Lv, Q. Wang, et al., "Brandspecific Toxicity of Tire Tread Particles Helps Identify the Determinants of Toxicity," *Environmental Science & Technology* 57, no. 30 (2023): 11267–11278.

28. K. H. Vardhan, P. S. Kumar, and R. C. Panda, "A Review on Heavy Metal Pollution, Toxicity and Remedial Measures: Current Trends and Future Perspectives," *Journal of Molecular Liquids* 290 (2019): 111197.

29. U. Mahrosh, M. Kleiven, S. Meland, B. O. Rosseland, B. Salbu, and H.-C. Teien, "Toxicity of Road Deicing Salt (NaCl) and Copper (Cu) to Fertilization and Early Developmental Stages of Atlantic Salmon (*Salmo salar*)," *Journal of Hazardous Materials* 280 (2014): 331–339.

30. S. Meland, R. Borgstrøm, L. S. Heier, B. O. Rosseland, O. Lindholm, and B. Salbu, "Chemical and Ecological Effects of Contaminated Tunnel Wash Water Runoff to a Small Norwegian Stream," *Science of the Total Environment* 408, no. 19 (2010): 4107–4117.

31. E. Rødland and Y. Lin, "Actions Are Needed to Deal With the High Uncertainties in Tire Wear Particle Analyses," *Environmental Science & Technology* 57, no. 23 (2023): 8461-8462.

32. Michelin, *Sustainable Tires: Michelin Makes Yet More Progress!* (Michelin Group, 2024).

33. Q. T. Birch, P. M. Potter, P. X. Pinto, D. D. Dionysiou, and S. R. Al-Abed, "Sources, Transport, Measurement and Impact of Nano and Microplastics in Urban Watersheds," *Reviews in Environmental Science and Bio/Technology* 19, no. 2 (2020): 275–336.

34. Bridgestone, *Plant to Produce Rubber Grown in Arid Zones - Guayule: Development of a New Source of Natural Rubber* (Bridgestone Corporation, 2022).

35. A. Wik and G. Dave, "Occurrence and Effects of Tire Wear Particles in the Environment—A Critical Review and an Initial Risk Assessment," *Environmental Pollution* 157, no. 1 (2009): 1–11.

36. N. Hamrahjou, S. N. Sadat-Mansouri, S. Taghvaei-Ganjali, and R. Zadmard, "Calix[4]arene Phosphonato Derivative as a Novel and Capable Processing Aid Agent for Improving Dynamic, Mechanical, and Thermal Behavior of Tire Tread Rubber Compounds," *Iranian Polymer Journal* 31, no. 6 (2022): 729–740.

37. G. H. LeFevre, A. C. Portmann, C. E. Müller, E. S. Sattely, and R. G. Luthy, "Plant Assimilation Kinetics and Metabolism of 2-Mercaptobenzothiazole Tire Rubber Vulcanizers by *Arabidopsis*," *Environmental Science & Technology* 50, no. 13 (2016): 6762–6771.

38. M. A. López-Manchado, M. Arroyo, B. Herrero, and J. Biagiotti, "Vulcanization Kinetics of Natural Rubber–Organoclay Nanocomposites," *Journal of Applied Polymer Science* 89, no. 1 (2003): 1–15.

39. F. Amato, F. R. Cassee, H. A. C. D. van der Gon, et al., "Urban Air Quality: The Challenge of Traffic Non-Exhaust Emissions," *Journal of Hazardous Materials* 275 (2014): 31–36.

40. C. Tang, Y. Zhu, R. Zheng, et al., "Nontarget Analysis and Characterization of p-Phenylenediamine-Quinones and -Phenols in Tire Rubbers by LC-HRMS and Chemical Species-Specific Algorithm," *Analytica Chimica Acta* 1326 (2024): 343123.

41. K. Müller, D. Hübner, S. Huppertsberg, T. P. Knepper, and D. Zahn, "Probing the Chemical Complexity of Tires: Identification of Potential

Tire-Borne Water Contaminants With High-Resolution Mass Spectrometry," *Science of the Total Environment* 802 (2022): 149799.

42. J. Chang, M. Jiao, Z. Zhang, et al., "Mechanistic Insight Into the Adverse Outcome of Tire Wear and Road Particle Leachate Exposure in Zebrafish (*Danio rerio*) Larvae," *Environment International* 178 (2023): 108053.

43. C. Johannessen, P. Helm, B. Lashuk, V. Yargeau, and C. D. Metcalfe, "The Tire Wear Compounds 6PPD-Quinone and 1,3-Diphenylguanidine in an Urban Watershed," *Archives of Environmental Contamination and Toxicology* 82, no. 2 (2022): 171–179.

44. H. E. Bergan-Roller and M. A. Sheridan, "The Growth Hormone Signaling System: Insights Into Coordinating the Anabolic and Catabolic Actions of Growth Hormone," *General and Comparative Endocrinology* 258 (2018): 119–133.

45. F. Sommer, V. Dietze, A. Baum, et al., "Tire Abrasion as a Major Source of Microplastics in the Environment," *Aerosol and Air Quality Research* 18, no. 8 (2018): 2014–2028.

46. P. J. Kole, A. J. Löhr, F. Van Belleghem, and A. Ragas, "Wear and Tear of Tyres: A Stealthy Source of Microplastics in the Environment," *International Journal of Environmental Research and Public Health* 14, no. 10 (2017): 1265.

47. J. Zhang, X. Zhang, L. Wu, et al., "Occurrence of Benzothiazole and Its Derivates in Tire Wear, Road Dust, and Roadside Soil," *Chemosphere* 201 (2018): 310–317.

48. M. Mattonai, T. Nacci, and F. Modugno, "Analytical Strategies for the Quali-Quantitation of Tire and Road Wear Particles – A Critical Review," *Trends in Analytical Chemistry* 154 (2022): 116650.

49. Q. Guo, Z. Men, Z. Liu, et al., "Chemical Characteristics of Fine Tire Wear Particles Generated on a Tire Simulator," *Environmental Pollution* 336 (2023): 122399.

50. B. Rodgers, *Rubber Compounding: Chemistry and Applications*, 2nd ed. (CRC Press, 2015).

51. G. Wypych, *Handbook of Fillers*, Fourth ed., (2016): 1–922.

52. S. K. Enganati, "Multiscale Characterization of Interfacial Region in Flexible Rubber Composites: Initial Structure and Evolution Upon Thermal Treatment," *ACS Applied Polymer Materials* 3 (2021): 4587–4598.

53. G. Buytaert and Y. Luo, "Study of Cu–Zn–Co Ternary Alloy-Coated Steel Cord in Cobalt-Free Skim Compound," *Journal of Adhesion Science and Technology* 28, no. 16 (2014): 222–1555.

54. Z. Wang, Y. Li, W. Song, X. Wu, and L. Zhang, "Performance Enhancement of Bio-Based Rubber Composites Using Epoxidized Natural Rubber for Silica Without Carbon Emissions and Volatile Organic Compounds," *Journal of Applied Polymer Science* 139, no. 30 (2022): e52682.

55. W. Song, Z. Wang, Y. Xing, et al., "Green and Catalyst-Free Cross-Linking of Bio-Based Elastomers Toward Robust, Reprocessable Abilities and Improved Thermal Aging Resistance Enabled by β-Hydroxyl Esters," *ACS Sustainable Chemistry & Engineering* 11, no. 7 (2023): 2784–2796.

56. L. Cao, J. Huang, and Y. Chen, "Dual Cross-Linked Epoxidized Natural Rubber Reinforced by Tunicate Cellulose Nanocrystals With Improved Strength and Extensibility," *ACS Sustainable Chemistry & Engineering* 6, no. 11 (2018): 14802–14811.

57. P. Bernal-Ortega, F. van Elburg, J. Araujo-Morera, H. Gojzewski, and A. Blume, "Heading Towards a Fully Sustainable Tire Tread Compound: Use of Bio-Based Resins," *Polymer Testing* 133 (2024): 108406.

58. B. P. Chang, A. Gupta, R. Muthuraj, and T. H. Mekonnen, "Bioresourced Fillers for Rubber Composite Sustainability: Current Development and Future Opportunities," *Green Chemistry* 23, no. 15 (2021): 5337–5378.

59. M. Tom, S. Thomas, B. Seantier, et al., "Approaching Sustainability: Nanocellulose Reinforced Elastomers—A Review," *Rubber Chemistry and Technology* 95, no. 4 (2022): 515–549.

60. A. Barkane, E. Kampe, O. Platnieks, and S. Gaidukovs, "Cellulose Nanocrystals vs. Cellulose Nanofibers: A Comparative Study of Reinforcing Effects in UV-Cured Vegetable Oil Nanocomposites," *Nanomaterials* 11, no. 7 (2021): 1791.

61. B. Guo, F. Chen, Y. Lei, X. Liu, J. Wan, and D. Jia, "Styrene-Butadiene Rubber/Halloysite Nanotubes Nanocomposites Modified by Sorbic Acid," *Applied Surface Science* 255, no. 16 (2009): 7329–7336.

62. A. Sakhnevych and A. Genovese, "Tyre Wear Model: A Fusion of Rubber Viscoelasticity, Road Roughness, and Thermodynamic State," *Wear* 542-543 (2024): 205291.

63. Y. Li, S. Zuo, L. Lei, X. Yang, and X. Wu, "Analysis of Impact Factors of Tire Wear," *Journal of Vibration and Control* 18, no. 6 (2012): 833–840.

64. L. N. Carli, O. Bianchi, R. S. Mauler, J. S. Crespo, and F. Cataldo, "Accelerated Aging of Elastomeric Composites With Vulcanized Ground Scraps," *Journal of Applied Polymer Science* 123, no. 1 (2012): 280–285.

65. J. M. Baldwin and D. R. Bauer, "Rubber Oxidation and Tire Aging—A Review," *Rubber Chemistry and Technology* 81, no. 2 (2008): 338–358.

66. F. Grasland, L. Chazeau, J.-M. Chenal, and R. Schach, "About Thermo-Oxidative Ageing at Moderate Temperature of Conventionally Vulcanized Natural Rubber," *Polymer Degradation and Stability* 161 (2019): 74–84.

67. M. G. Aboelkheir, P. B. Bedor, S. G. Leite, K. Pal, R. D. Toledo Filho, and F. Gomes de Souza Jr., "Biodegradation of Vulcanized SBR: A Comparison between *Bacillus subtilis*, *Pseudomonas aeruginosa* and Streptomyces Sp," *Scientific Reports* 9, no. 1 (2019): 1–12.

68. A. A. Shah, F. Hasan, Z. Shah, N. Kanwal, and S. Zeb, "Biodegradation of Natural and Synthetic Rubbers: A Review," *International Biodeterioration & Biodegradation* 83 (2013): 145–157.

69. B. Sarkar and S. Mandal, "Microbial Degradation of Natural and Synthetic Rubbers," in *Microbial Bioremediation & Biodegradation*, (Springer Nature Singapore, 2020): 527–550.

70. S. Imai, K. Ichikawa, Y. Muramatsu, D. Kasai, E. Masai, and M. Fukuda, "Isolation and Characterization of Streptomyces, Actinoplanes, and Methylibium Strains that Are Involved in Degradation of Natural Rubber and Synthetic Poly(cis-1,4-Isoprene)," *Enzyme and Microbial Technology* 49, no. 6-7 (2011): 526–531.

71. M. C. Celina, "Review of Polymer Oxidation and Its Relationship With Materials Performance and Lifetime Prediction," *Polymer Degradation and Stability* 98, no. 12 (2013): 2419–2429.

72. G.-Y. Li and J. L. Koenig, "A Review of Rubber Oxidation," *Rubber Chemistry and Technology* 78, no. 2 (2005): 355–390.

73. L. M. Smith, H. M. Aitken, and M. L. Coote, "The Fate of the Peroxyl Radical in Autoxidation: How Does Polymer Degradation Really Occur?" *Accounts of Chemical Research* 51, no. 9 (2018): 2006–2013.

74. F. Gugumus, "Re-Examination of the Thermal Oxidation Reactions of Polymers 2. Thermal Oxidation of Polyethylene," *Polymer Degradation and Stability* 76, no. 2 (2002): 329–340.

75. T. Zheng, X. Zheng, S. Zhan, J. Zhou, and S. Liao, "Study on the Ozone Aging Mechanism of Natural Rubber," *Polymer Degradation and Stability* 186 (2021): 109514.

76. V. Korotenko and H. Zipse, "The Stability of Oxygen-Centered Radicals and Its Response to Hydrogen Bonding Interactions," *Journal of Computational Chemistry* 45, no. 2 (2024): 101–114.

77. C. von Sonntag, "Free-Radical-Induced Chain Scission and Cross-Linking of Polymers in Aqueous Solution—An Overview," *Radiation Physics and Chemistry* 67, no. 3-4 (2003): 353–359.

78. W. Zhao, J. He, P. Yu, X. Jiang, and L. Zhang, "Recent Progress in the Rubber Antioxidants: A Review," *Polymer Degradation and Stability* 207 (2023): 110223.

79. V. Korotenko, P. Langrzyk, and H. Zipse, "Computational Prediction of One-Electron Oxidation Potentials for Cytosine and Uracil Epigenetic Derivatives," *The Journal of Physical Chemistry A* 129, no. 20 (2025): 4339–4356.

80. C. Johannessen, P. Helm, and C. D. Metcalfe, "Detection of Selected Tire Wear Compounds in Urban Receiving Waters," *Environmental Pollution* 287 (2021): 117659.

81. R. Tangalychev, V. Korotenko, I. Efimov, and O. N. Efimov, "Properties of AlCl3 Guanidine Deep Eutectic Solvent With Addition of Polyethylene Oxide of Different Molecular Weights Supported by Quantum-Chemical Calculation," *Journal of Energy Storage* 96 (2024): 112665.

82. E. T. Denisov and I. B. Afanas'ev, *Oxidation and Antioxidants in Organic Chemistry and Biology* (CRC Press (an imprint of Taylor & Francis Group), 2005).

83. B. Seiwert, P. Klöckner, S. Wagner, and T. Reemtsma, "Source-Related Smart Suspect Screening in the Aqueous Environment: Search for Tire-Derived Persistent and Mobile Trace Organic Contaminants in Surface Waters," *Analytical and Bioanalytical Chemistry* 412, no. 20 (2020): 4909–4919.

84. P. Klöckner, B. Seiwert, S. Weyrauch, B. I. Escher, T. Reemtsma, and S. Wagner, "Comprehensive Characterization of Tire and Road Wear Particles in Highway Tunnel Road Dust by Use of Size and Density Fractionation," *Chemosphere* 279 (2021): 130530.

85. R. Avagyan, I. Sadiktsis, G. Thorsén, C. Östman, and R. Westerholm, "Determination of Benzothiazole and Benzotriazole Derivates in Tire and Clothing Textile Samples by High Performance Liquid Chromatography–Electrospray Ionization Tandem Mass Spectrometry," *Journal of Chromatography A* 1307 (2013): 119–125.

86. S. Pan, Y. Sun, G. Zhang, J. Li, Q. Xie, and P. Chakraborty, "Assessment of 2-(4-Morpholinyl) Benzothiazole (24MoBT) and N-Cyclohexyl-2-Benzothiazolamine (NCBA) as Traffic Tracers in Metropolitan Cities of China and India," *Atmospheric Environment* 56 (2012): 246–249.

87. X. Fan, R. Gan, J. Liu, et al., "Adsorption and Desorption Behaviors of Antibiotics by Tire Wear Particles and Polyethylene Microplastics With or Without Aging Processes," *Science of the Total Environment* 771 (2021): 145451.

88. P. A. M. Chagas, R. Schneider, D. M. dos Santos, A. J. G. Otuka, C. R. Mendonça, and D. S. Correa, "Bilayered Electrospun Membranes Composed of Poly(lactic-Acid)/Natural Rubber: A Strategy Against Curcumin Photodegradation for Wound Dressing Application," *Reactive and Functional Polymers* 163 (2021): 104889.

89. P. Fan and C. Lu, "A Study on Functionalization of Waste Tire Rubber Powder Through Ozonization," *Journal of Polymers and the Environment* 19, no. 4 (2011): 943–949.

90. H. Peidayesh, Z. Nógellová, and I. Chodák, "Effects of Peroxide and Sulfur Curing Systems on Physical and Mechanical Properties of Nitrile Rubber Composites: A Comparative Study," *Materials* 17 (2024): 71.

91. J. Neethirajan, A. R. Parathodika, G.-H. Hu, and K. Naskar, "Functional Rubber Composites Based on Silica-Silane Reinforcement for Green Tire Application: The State of the Art," *Functional Composite Materials* 3, no. 1 (2022): 7.

92. H. M. Naguib, E. O. Taha, M. A. Ahmed, and U. F. Kandil, "Enhanced Wooden Polymer Composites Based on Polyethylene and Nano-Modified Wooden Flour," *Egyptian Journal of Petroleum* 31, no. 4 (2022): 39–45.

93. P. Eisentraut, E. Dümichen, A. S. Ruhl, et al., "Two Birds With One Stone—Fast and Simultaneous Analysis of Microplastics: Microparticles Derived From Thermoplastics and Tire Wear," *Environmental Science & Technology Letters* 5, no. 10 (2018): 608–613.

94. J. Rausch, D. Jaramillo-Vogel, S. Perseguers, N. Schnidrig, B. Grobéty, and P. Yajan, "Automated Identification and Quantification of Tire Wear Particles (TWP) in Airborne Dust: SEM/EDX Single Particle Analysis Coupled to a Machine Learning Classifier," *Science of the Total Environment* 803 (2022): 149832.

95. P. Klöckner, B. Seiwert, P. Eisentraut, U. Braun, T. Reemtsma, and S. Wagner, "Characterization of Tire and Road Wear Particles From Road Runoff Indicates Highly Dynamic Particle Properties," *Water Research* 185 (2020): 116262.

96. K. M. Unice, M. L. Kreider, and J. M. Panko, "Comparison of Tire and Road Wear Particle Concentrations in Sediment for Watersheds in France, Japan, and the United States by Quantitative Pyrolysis GC/MS Analysis," *Environmental Science & Technology* 47, no. 15 (2013): 8138–8147.

97. A. D. Gray, H. Wertz, R. R. Leads, and J. E. Weinstein, "Microplastic in Two South Carolina Estuaries: Occurrence, Distribution, and Composition," *Marine Pollution Bulletin* 128 (2018): 223–233.

98. D. Hesse, T. Feißel, M. Kunze, E. Bachmann, T. Bachmann, and S. Gramstat, "Comparison of Methods for Sampling Particulate Emissions From Tires Under Different Test Environments," *Atmosphere* 13, no. 8 (2022): 1262.

99. D. Zahn, P. Mucha, V. Zilles, et al., "Identification of Potentially Mobile and Persistent Transformation Products of REACH-Registered Chemicals and Their Occurrence in Surface Waters," *Water Research* 150 (2019): 86–96.

100. C. Halsband, L. Sørensen, A. M. Booth, and D. Herzke, "Car Tire Crumb Rubber: Does Leaching Produce a Toxic Chemical Cocktail in Coastal Marine Systems?" *Frontiers in Environmental Science* 8 (2020): 1–15.

101. M. Koski, J. Søndergaard, A. M. Christensen, and T. G. Nielsen, "Effect of Environmentally Relevant Concentrations of Potentially Toxic Microplastic on Coastal Copepods," *Aquatic Toxicology* 230 (2021): 105713.

102. T. Hüffer, S. Wagner, T. Reemtsma, and T. Hofmann, "Sorption of Organic Substances to Tire Wear Materials: Similarities and Differences With Other Types of Microplastic," *TrAC Trends in Analytical Chemistry* 113 (2019): 392–401.

103. F. S. Degaffe and A. Turner, "Leaching of Zinc From Tire Wear Particles Under Simulated Estuarine Conditions," *Chemosphere* 85, no. 5 (2011): 738–743.

104. M. L. Kreider, J. M. Panko, B. L. McAtee, L. I. Sweet, and B. L. Finley, "Physical and Chemical Characterization of Tire-Related Particles: Comparison of Particles Generated Using Different Methodologies," *Science of the Total Environment* 408, no. 3 (2010): 652–659.

105. C. Rauert, E. S. Rødland, E. D. Okoffo, M. J. Reid, S. Meland, and K. V. Thomas, "Challenges With Quantifying Tire Road Wear Particles: Recognizing the Need for Further Refinement of the ISO Technical Specification," *Environmental Science & Technology Letters* 8, no. 3 (2021): 231–236.

106. I. Goßmann, M. Halbach, and B. M. Scholz-Böttcher, "Car and Truck Tire Wear Particles in Complex Environmental Samples – A Quantitative Comparison With "Traditional" Microplastic Polymer Mass Loads," *Science of the Total Environment* 773 (2021): 145667.

107. D. Cespi, F. Passarini, I. Vassura, and F. Cavani, "Butadiene From Biomass, a Lifecycle Perspective to Address Sustainability in the Chemical Industry," *Green Chemistry* 18, no. 6 (2016): 1625–1638.

108. S. Weinbruch, A. Worringen, M. Ebert, et al., "A Quantitative Estimation of the Exhaust, Abrasion and Resuspension Components of

Particulate Traffic Emissions Using Electron Microscopy," *Atmospheric Environment* 99 (2014): 175–182.

109. R. R. Leads and J. E. Weinstein, "Occurrence of Tire Wear Particles and Other Microplastics Within the Tributaries of the Charleston Harbor Estuary, South Carolina, USA," *Marine Pollution Bulletin* 145 (2019): 569–582.

110. I. Järlskog, A.-M. Strömvall, K. Magnusson, et al., "Occurrence of Tire and Bitumen Wear Microplastics on Urban Streets and in Sweepsand and Washwater," *Science of the Total Environment* 729 (2020): 138950.

111. F. Lu, Y. Su, Y. Ji, and R. Ji, "Release of Zinc and Polycyclic Aromatic Hydrocarbons From Tire Crumb Rubber and Toxicity of Leachate to Daphnia Magna: Effects of Tire Source and Photoaging," *Bulletin of Environmental Contamination and Toxicology* 107, no. 4 (2021): 651–656.

112. K. Adachi and Y. Tainosho, "Characterization of Heavy Metal Particles Embedded in Tire Dust," *Environment International* 30, no. 8 (2004): 1009–1017.

113. H. Naguib, E. Taha, and M. Ahmed, "Boosting Poly(vinyl Chloride) With Waste-Based Plasticizer and Green Nanofiller," *Egyptian Journal of Chemistry* 68 (2025): 15–26.

114. D. P. O'Loughlin, M. J. Haugen, J. Day, et al., "Multi-Element Analysis of Tyre Rubber for Metal Tracers," *Environment International* 178 (2023): 108047.

115. L. J. Knight, F. N. F. Parker-Jurd, M. Al-Sid-Cheikh, and R. C. Thompson, "Tyre Wear Particles: An Abundant Yet Widely Unreported Microplastic?" *Environmental Science and Pollution Research* 27, no. 15 (2020): 18345–18354.

116. F. N. F. Parker-Jurd, I. E. Napper, G. D. Abbott, S. Hann, and R. C. Thompson, "Quantifying the Release of Tyre Wear Particles to the Marine Environment via Multiple Pathways," *Marine Pollution Bulletin* 172 (2021): 112897.

117. M. Celeiro, T. Dagnac, and M. Llompart, "Determination of Priority and Other Hazardous Substances in Football Fields of Synthetic Turf by Gas Chromatography-Mass Spectrometry: A Health and Environmental Concern," *Chemosphere* 195 (2018): 201–211.

118. S. Wagner, P. Klöckner, and T. Reemtsma, "Aging of Tire and Road Wear Particles in Terrestrial and Freshwater Environments – A Review on Processes, Testing, Analysis and Impact," *Chemosphere* 288 (2022): 132467.

119. H. Kumata, M. Mori, S. Takahashi, et al., "Evaluation of Hydrogenated Resin Acids as Molecular Markers for Tire-Wear Debris in Urban Environments," *Environmental Science & Technology* 45, no. 23 (2011): 9990–9997.

120. L. Gueissaz and G. Massonnet, "Study on the Discrimination of Tires Using Chemical Profiles Obtained by Py-GC/MS," *Journal of Analytical and Applied Pyrolysis* 124 (2017): 704–718.

121. Y. Kitamura, C. Kuroiwa, M. Harada, and N. Kato, "Analysis of Rubber Fraction in Suspended Particulate Matter (SPM) on Road," in *Proceedings of the Fall 172nd Technical Meeting of the Rubber Division of the American Chemical Society*., (2007)

122. M. Ghanadi, M. Kah, R. S. Kookana, and L. P. Padhye, "Formation of Disinfection By-Products From Microplastics, Tire Wear Particles, and Other Polymer-Based Materials," *Water Research* 220 (2022).

123. Frontier Laboratories, "Analysis of Additives in Butadiene Rubber Using Thermal Desorption (TD)-GC/MS," n.d.

124. J. Klein, H. Molnár-in 't Veld, G. Geilenkirchen, et al., "Methods for Calculating Transport Emissions in the Netherlands 2017," PBL Netherlands Environmental Assessment Agency (2017).

125. K. Waldschläger and H. Schüttrumpf, "Effects of Particle Properties on the Settling and Rise Velocities of Microplastics in Freshwater Under Laboratory Conditions," *Environmental Science & Technology* 53, no. 4 (2019): 1958–1966.

126. W. Zhao, Y. Jain, F. Müller-Plathe, P. Steinmann, and S. Pfaller, "Investigating Fracture Mechanisms in Glassy Polymers Using Coupled Particle-Continuum Simulations," *Journal of the Mechanics and Physics of Solids* 193 (2024): 105884.

127. W. Zhao, P. Steinmann, and S. Pfaller, "A Particle-Continuum Coupling Method for Multiscale Simulations of Viscoelastic–Viscoplastic Amorphous Glassy Polymers," *International Journal for Numerical Methods in Engineering* 122, no. 24 (2021): 7431–7451.

128. J. Wang and G. Li, "Full-Scale Modelling of Chemical Experiments," *Smart Molecules* 2, no. 1 (2024): e20230010.

129. X. Li, X. Chen, B. Chen, W. Zhang, Z. Zhu, and B. Zhang, "Tire Additives: Evaluation of Joint Toxicity, Design of New Derivatives and Mechanism Analysis of Free Radical Oxidation," *Journal of Hazardous Materials* 465 (2024): 133220.

130. B. Du, Z. Tian, K. T. Peter, E. P. Kolodziej, and C. S. Wong, "Developing Unique Nontarget High-Resolution Mass Spectrometry Signatures to Track Contaminant Sources in Urban Waters," *Environmental Science & Technology Letters* 7, no. 12 (2020): 923–930.

131. X. Chen, X. Li, and Y. Li, "Toxicity Inhibition Strategy of Microplastics to Aquatic Organisms Through Molecular Docking, Molecular Dynamics Simulation and Molecular Modification," *Ecotoxicology and Environmental Safety* 226 (2021): 112870.

132. X. Li, Y. Zhao, B. Chen, et al., "Inhalation and Ingestion of Synthetic Musks in Pregnant Women: In Silico Spontaneous Abortion Risk Evaluation and Control," *Environment International* 158 (2022): 106911.

133. A. G. Ferradino, "Antioxidant Selection for Peroxide Cure Elastomer Applications," *Rubber Chemistry and Technology* 76, no. 3 (2003): 694–718.

134. Y. Ma, Y. Feng, T. Diao, W. Zeng, and Y. Zuo, "Experimental and Theoretical Study on Antioxidant Activity of the Four Anthocyanins," *Journal of Molecular Structure* 1204 (2020): 127509.

135. N. Grasse, B. Seiwert, R. Massei, S. Scholz, Q. Fu, and T. Reemtsma, "Uptake and Biotransformation of the Tire Rubber-Derived Contaminants 6-PPD and 6-PPD Quinone in the Zebrafish Embryo (*Danio rerio*)," *Environmental Science & Technology* 57, no. 41 (2023): 15598–15607.

136. G. Y. Wang, X. M. Lei, G. F. Shi, F. Y. Li, and T. C. Guo, "Simulation Study the Effect of Natural Antioxidants on Atmospheric Free Radical," *Oxidation Communications* 39 (2016): 2904–2912.

137. X. Li, W. Gu, B. Chen, Z. Zhu, and B. Zhang, "Functional Modification of HHCB: Strategy for Obtaining Environmentally Friendly Derivatives," *Journal of Hazardous Materials* 416 (2021): 126116.

138. X.-L. Liao, Z.-F. Chen, Q.-Y. Liu, et al., "Tissue Accumulation and Biotransformation of 6PPD-Quinone in Adult Zebrafish and Its Effects on the Intestinal Microbial Community," *Environmental Science & Technology* 58, no. 23 (2024): 10275–10286.

139. W. Zheng, Y. Wu, W. Yang, Z. Zhang, L. Zhang, and S. Wu, "A Combined Experimental and Molecular Simulation Study of Factors Influencing the Selection of Antioxidants in Butadiene Rubber," *The Journal of Physical Chemistry B* 121, no. 6 (2017): 1413–1425.

140. E. Mvula, S. Naumov, and C. von Sonntag, "Ozonolysis of Lignin Models in Aqueous Solution: Anisole, 1,2-Dimethoxybenzene, 1,4-Dimethoxybenzene, and 1,3,5-Trimethoxybenzene," *Environmental Science & Technology* 43, no. 16 (2009): 6275–6282.

141. L. Rodríguez-Guadarrama, J. Kounavis, J. Maldonado, et al., "Functionalization: A Key Differential Factor in the Design of SSBRs for High Performance Tires," *Rubber World* 260 (2019): 41.

142. F. Zietzschmann, J. Müller, A. Sperlich, et al., "Rapid Small-Scale Column Testing of Granular Activated Carbon for Organic Micro-

Pollutant Removal in Treated Domestic Wastewater," *Water Science and Technology* 70, no. 7 (2014): 1271–1278.

143. R. Yang, Y. Song, and Q. Zheng, "Payne Effect of Silica-Filled Styrene-Butadiene Rubber," *Polymer* 116 (2017): 304–313.

144. R. Hentschke, "The Payne Effect Revisited," *Express Polymer Letters* 11, no. 4 (2017): 278–292.

145. F. Yong, Y. Caihua, H. Kui, C. Yujing, L. Yu, and Z. Taoli, "A Study of the Microscopic Interaction Mechanism of Styrene–Butadiene-Styrene Modified Asphalt Based on Density Functional Theory," *Molecular Simulation* 49, no. 12 (2023): 1203–1214.

146. P. Nanthanasit, P. Nimmanpipug, C. Thongbai, and S. Rimjaem, "Effective Natural Rubber Vulcanization Using Electron Beam Irradiation and DFT Driven Cross-Linking Agents," *Radiation Physics and Chemistry* 228 (2025): 112390.

147. F. Shi, X. Li, Y. Bai, et al., "Mechanism of the Zinc Dithiocarbamate-Activated Rubber Vulcanization Process: A Density Functional Theory Study," *ACS Applied Polymer Materials* 3, no. 10 (2021): 5188–5196.

148. S. Yan, D. Xia, and X. Liu, "Beneficial Migration of Sulfur Element During Scrap Tire Depolymerization With Supercritical Water: A Molecular Dynamics and DFT Study," *Science of the Total Environment* 776 (2021): 145835.

149. J. Wu, F. Teng, B. Su, and Y. Wang, "Molecular Dynamics Study on Tribological Properties of EUG/NR Composites," *Computational Materials Science* 199 (2021): 110732.

150. F. Teng, J. Wu, B. Su, and Y. Wang, "Enhanced Tribological Properties of Vulcanized Natural Rubber Composites by Applications of Carbon Nanotube: A Molecular Dynamics Study," *Nanomaterials* 11, no. 9 (2021): 2464.

151. M. Wang, Y. Li, C. Qian, J. Zhao, and S. Wang, "Molecular Dynamics Simulations of Defective Carbon Nanotubes on the Aging and Friction Properties of Nitrile Butadiene Rubber Composites," *Polymer Composites* 44, no. 2 (2023): 1228–1239.

152. X. Liu, X. Zhou, F. Kuang, H. Zuo, and J. Huang, "Mechanical and Tribological Properties of Nitrile Rubber Reinforced by Nano-SiO2: Molecular Dynamics Simulation," *Tribology Letters* 69, no. 2 (2021): 54.

153. B. Yang, S. Wang, Z. Song, L. Liu, H. Li, and Y. Li, "Molecular Dynamics Study on the Reinforcing Effect of Incorporation of Graphene/Carbon Nanotubes on the Mechanical Properties of Swelling Rubber," *Polymer Testing* 102 (2021): 107337.

154. K. Hu, C. Yu, Y. Chen, W. Li, D. Wang, and W. Zhang, "Multiscale Mechanisms of Asphalt Performance Enhancement by Crumbed Waste Tire Rubber: Insight From Molecular Dynamics Simulation," *Journal of Molecular Modeling* 27, no. 6 (2021): 170.

155. B. Jiao, B. Pan, F. Liu, P. Yin, and Z. Li, "Evaluating the Interfacial Properties Between Crumb Rubber Modified Asphalt and Aggregates Using Molecular Dynamics Simulation Methods," *Construction and Building Materials* 400 (2023): 132809.

156. M. Gao, Y. Chen, C. Fan, and M. Li, "Molecular Dynamics Study on the Compatibility of Asphalt and Rubber Powder With Different Component Contents," *ACS Omega* 7, no. 41 (2022): 36157–36164.

157. B. Jiao, B. Pan, and T. Che, "Evaluating Impacts of Desulfurization and Depolymerization on Thermodynamics Properties of Crumb Rubber Modified Asphalt Through Molecular Dynamics Simulation," *Construction and Building Materials* 323 (2022): 126360.

158. G. Liao, X. Fang, H. Wang, J. Tang, P. Szary, and J. Chen, "Durability Improvement of Poroelastic Road Surface With Treated Rubber: Molecular Dynamics Simulation and Experimental Observations," *Journal of Cleaner Production* 369 (2022): 133334.

159. Y. Li, Y. Wu, Y. Luo, T. W. Chan, L. Zhang, and S. Wu, "A Combined Experimental and Molecular Dynamics Simulation Study on the Structures and Properties of Three Types of Styrene Butadiene Rubber," *Materials Today Communications* 4 (2015): 35–41.

160. Q. Chen, Z. Zhang, Y. Huang, et al., "Structure–Mechanics Relation of Natural Rubber: Insights From Molecular Dynamics Simulations," *ACS Applied Polymer Materials* 4, no. 5 (2022): 3575–3586.

161. Q. He, Z. Xu, Y. Xu, et al., "Mechanical and Damping Properties Analyses of Small Molecular Modifiers/Nitrile-Butadiene Rubber Composite: Molecular Dynamics Simulation," *Macromolecular Theory and Simulations* 32, no. 1 (2023): 2200051.

162. S. Li, H. Zhao, T. Yue, L. Zhang, Y. Chen, and J. Liu, "All-Atom Molecular Dynamics Simulation of Structure, Dynamics and Mechanics of Elastomeric Polymer Materials in a Wide Range of Pressure and Temperature," *Molecular Systems Design & Engineering* 9, no. 3 (2024): 264–277.

163. J. Qi, Y. Wang, P. Xu, et al., "Molecular Dynamics Study of Waste Tire Pyrolysis: Focus on Intermediate Product Evolution and Sulfur Migration Law," *Journal of Environmental Chemical Engineering* 12, no. 6 (2024): 114633.

164. J. Cui, F. Zeng, and Y. Wang, "A Coarse-Grained Molecular Dynamics Study on the Mechanical Behavior of Carbon Nanotubes Reinforced Vulcanized Natural Rubber Composites," *Polymer Composites* 44, no. 11 (2023): 7752–7767.

165. T. Zhang, H. Guo, Q. Li, and F. Zeng, "A Coarse-Grained Molecular Dynamics Study on the Mechanical Behavior of Carbon Black Reinforced Natural Rubber Composites," *Computational Materials Science* 259 (2025): 114167.

166. Q. Li, F. Zeng, J. Cui, and H. Guo, "A Coarse-Grained Molecular Dynamics Simulation on the Mechanical and Thermal Properties of Natural Rubber Composites Reinforced by Fullerene Nanoparticles," *Journal of Molecular Modeling* 31, no. 2 (2025): 56.

167. J. Cui, F. Zeng, D. Wei, and Y. Wang, "Analysis of Static and Dynamic Mechanical Properties of Carbon Black/Carbon Nanotubes Hybrid Filled Natural Rubber Nanocomposites Using Coarse-Grained Molecular Dynamics," *Polymer Composites* 45, no. 6 (2024): 5148–5163.

168. B. Yang, Y. Li, S. Wang, R. Nie, and L. Chen, "The Acquisition and Calibration of Coarse-Grained Force Field Parameters for Graphene/Nitrile Rubber Nanocomposites," *Materials Today Communications* 40 (2024): 109891.

169. H. Guo, F. Zeng, J. Cui, and Q. Li, "Investigation on the Aggregation Behavior and Mechanical Properties of Silica-Filled Natural Rubber Composites: A Coarse-Grained Molecular Dynamics Study," *Computational Materials Science* 252 (2025): 113815.

170. B. Yuan, F. Zeng, C. Peng, and Y. Wang, "Coarse-Grained Molecular Dynamics Simulation of Cis-1, 4-Polyisoprene With Silica Nanoparticles Under Extreme Uniaxial Tension," *Modelling and Simulation in Materials Science and Engineering* 29, no. 5 (2021): 055013.

171. P. Koul, "Advancements in Finite Element Analysis for Tire Performance: A Comprehensive Review," *International Journal of Multidisciplinary Research in Arts, Science and Technology* 2, no. 12 (2024): 1–17.

172. A. Gupta, S. K. Pradhan, L. Bajpai, and V. Jain, "Numerical Analysis of Rubber Tire/Rail Contact Behavior in Road Cum Rail Vehicle Under Different Inflation Pressure Values Using Finite Element Method," *Materials Today: Proceedings* 47 (2021): 6628–6635.

173. S. Limrungruengrat, A. Chaikittiratana, S. Pornpeerakeat, and T. Chantrasmi, "Thermo-Mechanical Finite Element Simulation and Validation of Rubber Curing Process," *Journal of Mechanical Science and Technology* 36, no. 6 (2022): 3039–3046.

174. H. Li, H. Zhou, J. Yang, J. Ge, G. Wang, and T. Xu, "Study of the Dynamic Performance of Rolling Non-Pneumatic Tires Using Finite Element Method," *Journal of the Brazilian Society of Mechanical Sciences and Engineering* 44, no. 7 (2022): 289.